

Study on Metal Oxide Supported Palladium Catalyzed Oxidative Reactions using Molecular Oxygen as the Oxidant

張, 振中

<https://doi.org/10.15017/1500499>

出版情報：九州大学, 2014, 博士（理学）, 課程博士
バージョン：
権利関係：全文ファイル公表済

**Study on Metal Oxide Supported Palladium
Catalyzed Oxidative Reactions using Molecular
Oxygen as the Oxidant**

Zhenzhong Zhang

2015

Contents

Chapter 1. General introduction

1.1 General introduction	3
1.2 References	13

Chapter 2. Intramolecular double C-H bond functionalization for synthesis of dibenzofurans over supported palladium hydroxide catalysts

2.1 Introduction	18
2.2 Results and discussion	20
2.3 Conclusion	27
2.4 Experimental section	27
2.5 References	32

Chapter 3. Aerobic oxidation of cyclohexanones to cyclic enones, phenols and phenyl ethers over supported palladium catalysts

3.1 Introduction	35
3.2 Results and discussion	37
3.3 Conclusion	54
3.4 Experimental section	55
3.5 References	67

Chapter 4. Transformation of terminal alkenes into primary allylic alcohols over supported palladium hydroxide catalysts

4.1 Introduction	70
4.2 Results and discussion	74
4.3 Conclusion	96
4.4 Experimental section	96
4.5 References	100

Chapter 5. Conclusion

Acknowledgement	106
------------------------	-----

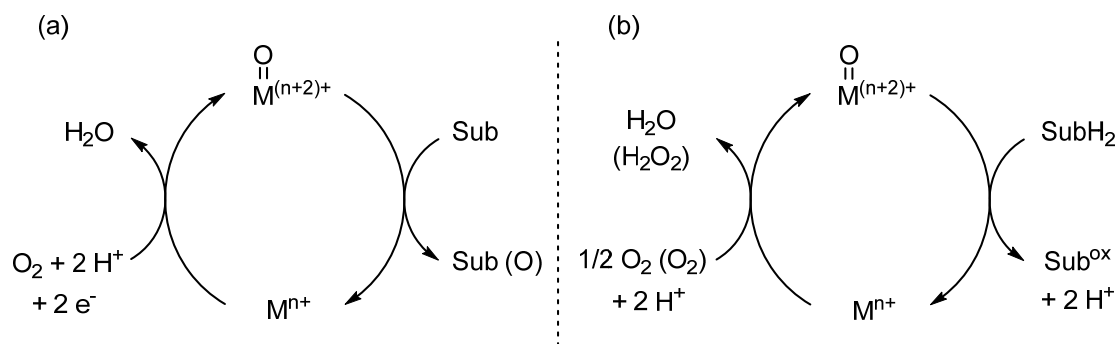
List of Publications	107
-----------------------------	-----

Chapter 1. General introduction

1.1 General introduction

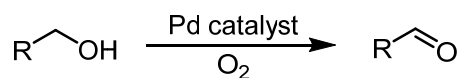
Oxidation reaction, as a fundamental and essential method, has been developed and broadly used for transformation of petrochemical feedstocks into industrial commodities such as clothes, cosmetics, paints, pharmaceuticals, and polymer materials.¹ Recently, A number of transition metal-catalyzed oxidation reactions have been investigated, such as Au-, Pd-, Ru-, Rh-, and Cu-catalyzed reactions.²⁻⁵ Among these reactions, Pd-catalyzed reactions represent the efficient method for selective C–H bond oxidations. However, the use of Pd-catalyzed oxidation reactions does involve the requirement of expensive stoichiometric oxidant such as halogens, benzoquinone (BQ), 2,3-dichloro-5,6-dicyano-*p*-benzoquinone (DDQ), tert-butyl hydroperoxide (TBHP), 2-iodoxybenzoic acid (IBX) or transition metal oxidants,⁵⁻⁹ and these oxidants may produce environmentally hazardous by-products during the reaction.

Molecular oxygen (O_2) is regarded as an ideal oxidant because of its environmental and economic concerns. However, O_2 has limited applications in transition metal catalytic systems due to its low oxidizing ability, which is ascribed to the stable triplet ground state, and disadvantages to control the products selectivity. The function of O_2 in oxidation reactions is generally classified into two types: (1) O_2 provides oxygen atom to form the oxygen atom-containing products (Scheme 1.1a), and (2) O_2 only serves as an electron or proton acceptor (Scheme 1.1b).^{2a} In contrast of these types, using O_2 as a proton or electron acceptor is quite desirable in organic synthesis, because many transition metal-catalyzed oxidations do not contain oxygen-atom transfer. Indeed, O_2 usually acts two parts in a transition metal-catalyzed oxidation, that is, oxidation of the substrate and re-oxidizing the reduced metal catalysts (Scheme 1.1b).

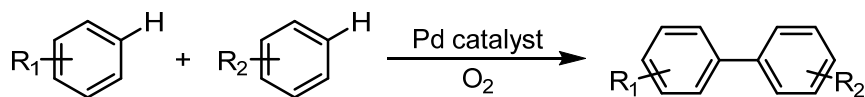


Scheme 1.1 (a) Oxygen-atom transfer from O_2 into substrates, and (b) O_2 is used as a proton or electron acceptor in the oxidation of substrates.

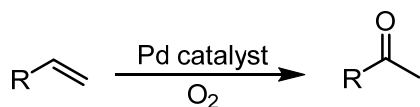
a. Oxidation of alcohols



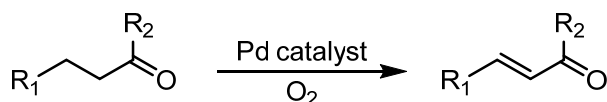
b. Oxidative biary coupling



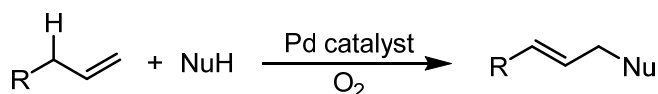
c. Wacker oxidation



d. Dehydrogenation of aldehydes and ketones



e. Allylic C-H oxidation

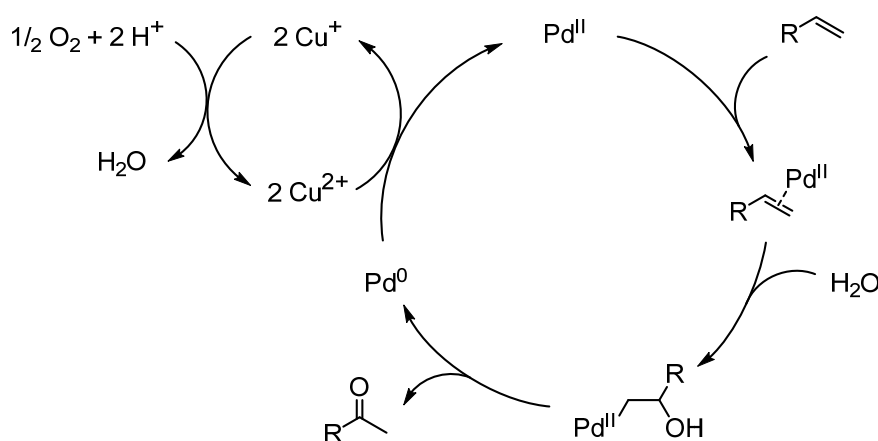


Nu: nucleophile

Scheme 1.2 Representative Pd-catalyzed oxidation reactions using O₂ as the oxidant.

Homogeneous Pd catalysts promoted oxidation reactions using O₂ as the oxidant have been extensively studied, such as oxidation of alcohols, oxidative biary coupling reactions, Wacker oxidation, dehydrogenation of aldehydes and ketones, and allylic C-H oxidations (Scheme 1.2).¹⁰⁻¹³ Conclude from previous reports, a number of challenges remain in these processes. First, the reaction is difficult to be completely achieved by using O₂ as a sole oxidant, and thus, co-catalysts or other oxidant is required to promote the reaction. For example, Wacker oxidation is widely used to synthesize carbonyl compounds from alkenes with good functional groups tolerance. The accepted reaction pathway indicates that the reaction is initially started from coordination of Pd^{II} catalyst with alkene, and water works as a nucleophile to react with η²-Pd-alkene intermediate followed by β-hydride elimination to form the product. O₂ and Cu salt are used to regenerate Pd^{II} from Pd⁰ (Scheme 1.3). In this process, the direct re-oxidation of Pd⁰ back to Pd^{II} by O₂ in water is difficult since the energy barrier is higher than that for catalyst decomposition, that is, precipitation of Pd black.¹⁴

Therefore, transfer of electrons from reduced Pd catalyst to Cu^{2+} is initially required, and Cu^+ can be oxidized by O_2 to Cu^{2+} in aqueous solution.^{14b} Second, to prevent Pd catalysts transform into catalytic inactive species (Pd black) and to improve the selectivity of product, organic ligands are usually introduced into homogeneous Pd catalytic systems. For example, $\text{Pd}(\text{OAc})_2$ catalyzed aerobic allylic acetoxylation was significantly affected by the structure of nitrogen-based ligands (Table 1.1). However, synthesis of organic ligands consumes much cost, and some of the ligands such as phosphine-based ligands are unstable under the oxidation conditions. Third, in both oxidative and non-oxidative homogeneous catalytic systems, catalysts have the disadvantages in separation and recycling, which may cause environmental pollutions. Thus, there is a compelling need to develop an environmentally friendly and efficient catalytic system for oxidative reactions using O_2 as the sole oxidant. In this thesis, I propose to use heterogeneous catalysis method, where the phase of catalyst is different from the reactant, to facilitate aerobic oxidation reactions in absence of co-catalysts and ligands.

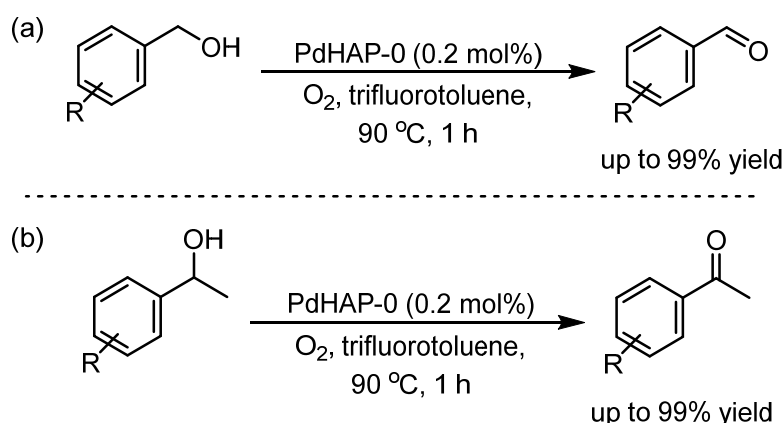


Scheme 1.3 General reaction pathway for Wacker oxidation of alkene to carbonyl compounds.

Table 1.1 Ligand effects in Pd-catalyzed aerobic allylic acetoxylation.

	$\text{C}_6\text{H}_5\text{CH}_2\text{CH}=\text{CH}_2 + \text{AcOH} \xrightarrow[\text{AcOH, 80 }^\circ\text{C, 18 h}]{\text{Pd}(\text{OAc})_2 (5 \text{ mol}\%), \text{Ligand} (5 \text{ mol}\%), \text{O}_2 (1 \text{ atm})} \text{C}_6\text{H}_5\text{CH}_2\text{CH}=\text{CH}-\text{CH}_2\text{OAc}$				
None					
4%	4%	4%	9%	81%	50%

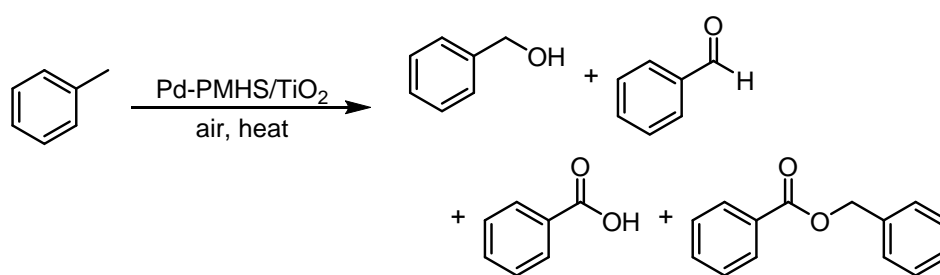
Heterogeneous catalysis can be classified into several types based on the phase of catalysts and reactants, and majority catalysts are solids and reactants are gases or liquid phase. In contrast with homogeneous catalysts, solid catalysts possess several superiorities such as thermal stability, high catalytic activity in particular for the gas phase reactions, recyclable and easy separation from the reaction mixture.^{15,16} Supported transition metal catalysts, specifically for supported Pd catalysts, have been extensively studied as efficient heterogeneous catalysts for organic synthesis. Also, a great progress has been made in oxidation reactions over supported Pd catalysts. A typical example is aerobic oxidation of alcohols to produce aldehydes and ketones. Kaneda and co-workers reported a hydroxyapatite (HAP) supported Pd catalyst for the selective oxidation of alcohols to aldehydes and ketones (Scheme 1.4).¹⁷ The catalysts were prepared by impregnation method and the mean diameter of HAP supported Pd particles was calculated at 3.8 nm with a narrow size distribution (standard deviation was 0.57 nm). The generated Pd nanoclusters on the surface of hydroxyapatite were proved to be catalytically active for alcohol oxidation by O₂.



Scheme 1.4 Hydroxyapatite supported Pd catalyzed aerobic oxidation of alcohols to (a) aldehydes and (b) ketones reported by Kaneda and co-workers.

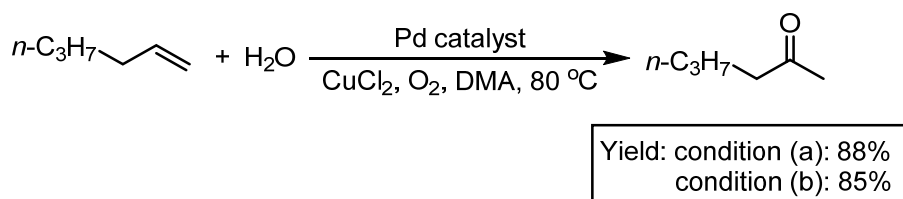
Aerobic oxidation of hydrocarbons were also achieved by supported Pd catalysts such as Pd/mesoporous silica, Pd/metal oxide, and Pd/polymer.^{18–20} Fu and co-workers reported a solvent-free selective aerobic oxidation of toluene catalyzed by TiO₂ supported Pd catalysts. Pd nanoparticles were encapsulated by polymethylhydrosilane (PMHS) during the catalyst preparation and Pd particle size was calculated at 1.3 ± 0.41 nm (by STEM).²¹ This catalyst showed better activity for oxidation of toluene than zeolite (ZSM-5) supported Pd catalyst, which was prepared by impregnation method. However, the conversion of toluene was unsatisfactory in their report, and four kinds of product

including benzyl alcohol, benzaldehyde, benzoic acid, and benzyl benzoate were detected (Scheme 1.5). Wang and co-workers reported an aerobic oxidation of hydrocarbons and alcohols over nanoporous N-doped carbon supported Pd particles with a mean size of 5.9 nm.²² In their report, doping with electron-rich nitrogen atoms in carbon material, which was prepared from a hydrothermal carbonization (HTC) method and was used to support Pd particles, could enhance the π -binding ability and basicity of catalyst, these properties resulted good catalytic activity to afford high turnover frequency (TOF) for hydrocarbon oxidation (up to 863 h⁻¹) and alcohol oxidation (up to 210,000 h⁻¹).



Scheme 1.5 Aerobic oxidation of toluene over TiO₂ supported Pd-PMHS catalyst reported by Fu and co-workers.

Supported Pd-catalyzed Wacker oxidation is received significant attention since Kaneda and co-workers reported the cationic Pd nanoclusters immobilized on the surface of TiO₂ as an efficient catalyst for transformation of 1-decene into 2-decanone in the presence of O₂ and CuCl₂ as the oxidant (Scheme 1.6a).²³ The cationic Pd₂₆₂₀ nanoclusters, which having a mean diameter and standard deviation of 3.8 ± 0.21 nm, was prepared by treatment of Pd₄phen₂(CO)₂(OAc)₄ (phen = 1,10-phenanthroline) with Cu(NO₃)₂ · 3H₂O under atmospheric O₂. Kaneda and co-workers also proved that Pd/montmorillonite could be used as a highly efficient catalyst for Wacker oxidation (Scheme 1.6b), and the catalyst was reused while maintaining high activity and selectivity.²⁴ Ikushima et al. reported a selective oxidation of styrene to acetophenone over metal oxide supported Pd-Au catalyst with hydrogen peroxide in supercritical carbon dioxide, and the informed that the reactivity and selectivity of acetophenone were directly affected by the properties of metal oxide support (Figure 1.1).²⁵ Recently, Kim and co-workers reported a Pd-Fe₃O₄ heterodimer nanocrystal to promote Wacker oxidation of styrene and derivatives to corresponding methyl ketones in excellent yields with good reusability (Scheme 1.7).²⁶



Scheme 1.6 Wacker oxidation catalyzed by (a) TiO₂ supported cationic Pd₂₆₂₀ nanoclusters, and (b) Mont supported Pd.

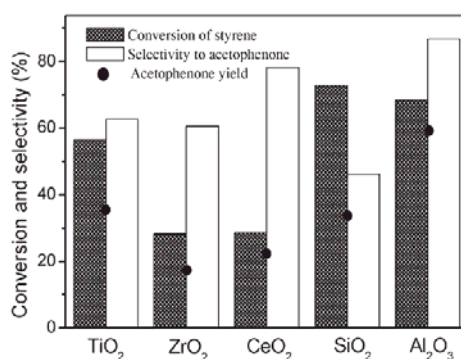
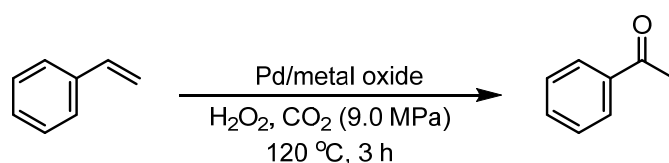
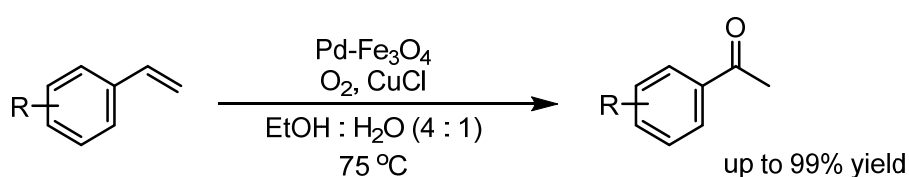
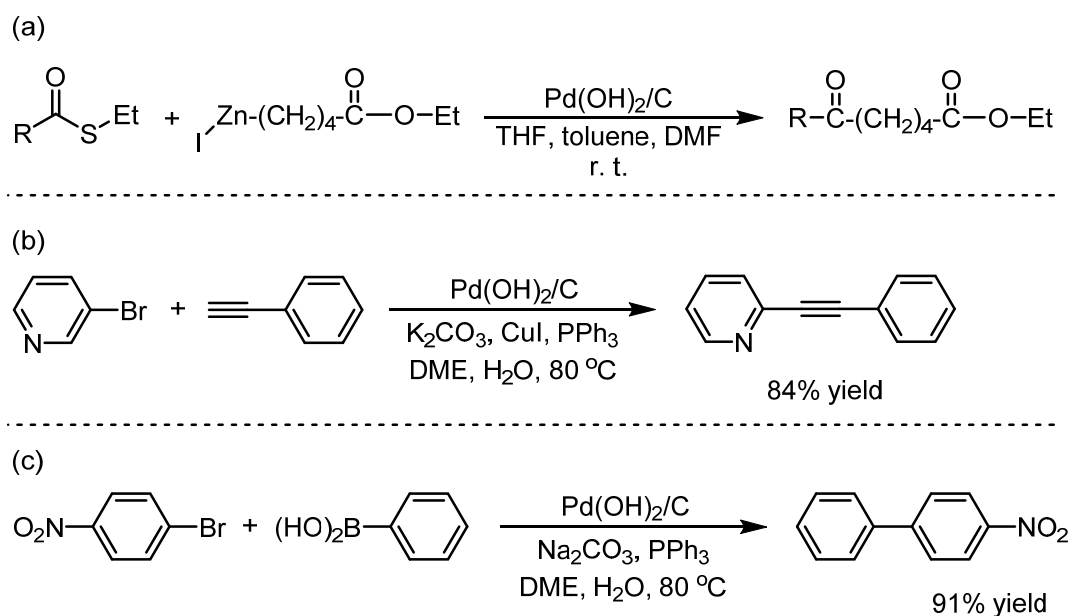


Figure 1.1 Results of selective oxidation of styrene to acetophenone over different support catalysts.



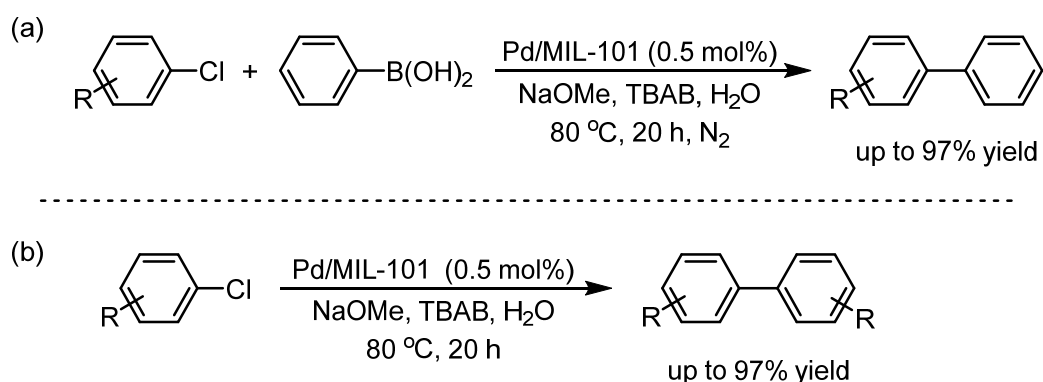
Scheme 1.7 Wacker oxidation of styrenes to acetophenones over Pd-Fe₃O₄ catalyst.

Supported Pd catalyzed C–C coupling reactions, for instance, Heck reaction, Suzuki-Miyaura reaction, Ullmann reaction, Sonogashira reaction, Stille reaction, and Fukuyama reaction, have been developed as powerful methodologies in construction of organic compounds. Pd/C and Pd/metal oxides have well been studied for these reactions.^{27–29} Additionally, Pd(OH)₂/C (Perlman's catalyst) was found to be superior to Pd/C in several coupling reactions such as Fukuyama (Scheme 1.8a), Sonogashira (Scheme 1.8b), and Suzuki-Miyaura coupling reactions (Scheme 1.8c).²⁹



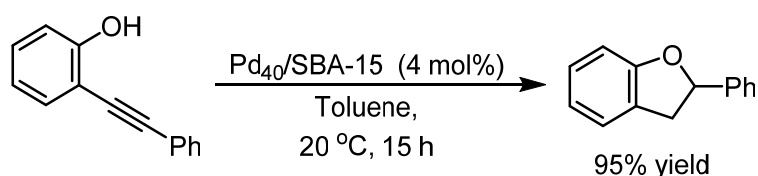
Scheme 1.8 Pd(OH)₂/C catalyzed (a) Fukuyama coupling reaction, (b) Sonogashira coupling reaction, and (c) Suzuki-Miyaura coupling reaction.

Recently, Jiang and co-workers have reported that Pd nanoparticles on zeolite type metal-organic frameworks (Pd/MIL-101) facilitated Suzuki-Miyaura and Ullmann coupling reactions of aryl chlorides in aqueous media, and excellent product yields were obtained (Scheme 1.9).³⁰ In their report, catalyst was prepared by impregnation method, and they suggested that the large surface area and properties of support may improve the catalytic activity.



Scheme 1.9 (a) Suzuki-Miyaura and (b) Ullmann coupling reactions of aryl chlorides over supported Pd catalysts reported by Jiang and co-workers.

Somorjai and co-workers reported that zeolite (SBA-15) supported Pd nanoparticle catalysts promoted hydroalkoxylation of 2-phenylethynylphenol with higher reactivity than homogeneous Pd catalyzed reactions (Scheme 1.10). They also employed this process in a continuous flow reactor, and obtained good catalytic performance.³¹



Scheme 1.10 Hydroalkoxylation of 2-phenylethynylphenol by supported 40 atom Pd nanoparticles reported by Somorjai and co-workers.

As described above, supported Pd catalysts have already exhibited outstanding catalytic performance in a number of organic reactions, and their catalytic activity primarily depends on several factors such as catalyst preparation method, chemical state of Pd, Pd particle size, properties of support, and the interaction between Pd and support. Consequently, this work attempts to optimize these factors and improve the reactivity or product selectivity for supported Pd-catalyzed organic reactions. Based on the advantages of metal oxide supported Pd catalysts, such as easy preparation and recovery, diversity properties, and good adsorption capacity for reactants,³² metal oxide supported Pd catalysts are specifically investigated. Deposition precipitation (DP) and impregnation (IMP), which have been widely utilized in chemical industry as catalyst preparation methods, are mainly employed in this work. For DP method, palladium hydroxide ions are formed by ligand exchange from precursors such as PdCl₂ and Pd(NO₃)₂ in alkaline media, and then, interact with positively charged metal oxides, thus, Pd(OH)₂ species deposited on metal oxide support such as Al₂O₃, TiO₂, ZrO₂, CeO₂ etc. The catalyst is calcined in air or reduced by H₂ at the range of 200 to 400 °C to form PdO and Pd⁰ species, respectively (Figure 1.2).³³ In IMP method, metal oxides are immersed in an aqueous solution of palladium precursors, and then, dried after the removal of H₂O. Similar to DP method, the catalyst is calcined in air and reduced by H₂ to form supported catalytic metallic particles (Figure 1.3).³⁴

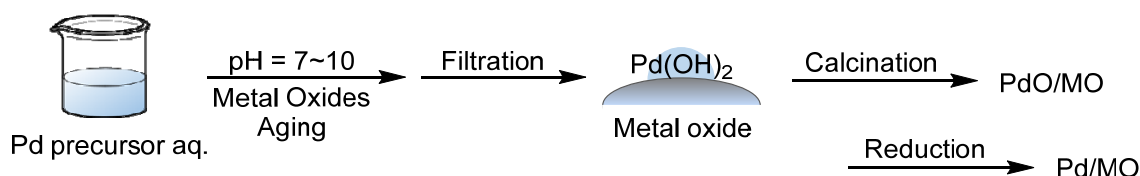


Figure 1.2 Preparation of supported Pd catalysts by deposition precipitation method.

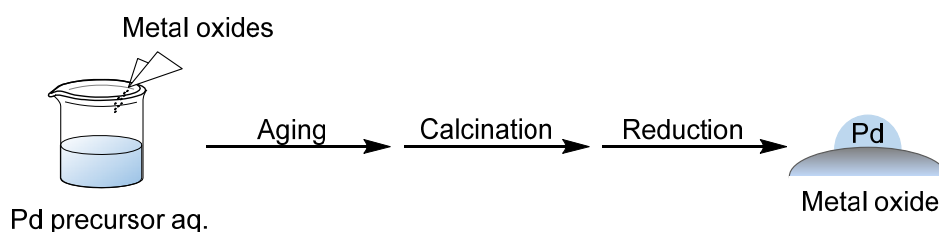
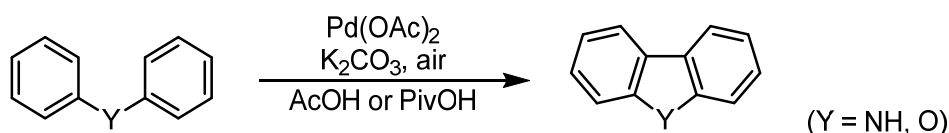


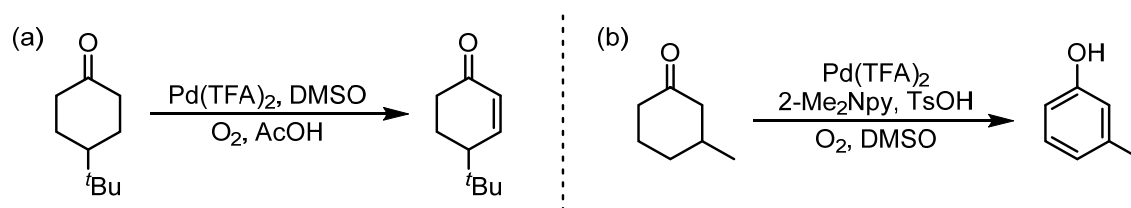
Figure 1.3 Preparation of supported Pd catalysts by impregnation method.

To evaluate the catalytic activity of metal oxide supported Pd catalysts, several oxidative reactions are investigated in this thesis. In chapter 2, intramolecular oxidative C–C bond coupling reaction is attempted to be proceeded over supported Pd catalyst. Direct intramolecular C–C bond formation reaction is regarded as a low cost and environmentally friendly method to construct conjugated aromatic structures, because pre-activation of substrates is not required and H₂O is produced as the sole by-product. A similar work was reported by Fagnou and co-workers.³⁵ In their reaction, biaryl compounds were synthesized from intramolecular oxidative biaryl couplings catalyzed by Pd(OAc)₂ with high reactivity and product selectivity (Scheme 1.11). However, the catalyst is difficult to be reused from this homogeneous catalytic system, and inorganic base was required to promote the reactions. In this work, diphenyl ethers are selected as the substrates to prepare dibenzofurans over supported Pd catalyst using O₂ as the oxidant, and in absence of base or other co-catalyst.



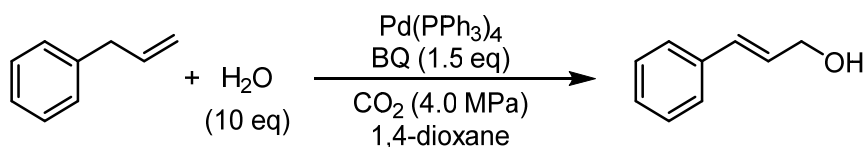
Scheme 1.11 Pd(OAc)₂ catalyzed intramolecular oxidative biaryl coupling reactions reported by Fagnou and co-workers.

Chapter 3 describes an aerobic oxidations of cyclohexanones to the corresponding products over supported Pd catalysts. Oxidations of cyclohexanones was extensively studied with homogeneous Pd catalytic systems by Stahl and co-workers.³⁶ Cyclohexenones and phenols were obtained as products from the selective oxidation conditions (Scheme 1.12). In their report, soluble Pd nanoparticles were formed in homogeneous Pd catalytic system, and they were active for the oxidation of cyclohexenone.^{36b} However, the active catalysts are limited to pseudo-homogeneous Pd nanoparticles. Heterogeneous catalysts has not yet been reported.



Scheme 1.12 Aerobic oxidations of cyclohexanones to (a) cyclohexenones, and (b) phenols reported by Stahl and co-workers.

In chapter 4, oxidative transformation of terminal alkenes into primary alcohols, which is an important process in chemical industry, is developed over supported Pd catalysts. The corresponding research in the presence of homogeneous catalysts have been developed by Nozaki,³⁷ Stahl,³⁸ Grubbs,³⁹ and Tokunaga.⁴⁰ However, some problems were involved in these catalytic systems. For example, Tokunaga and co-workers have reported a transformation of terminal alkenes into primary allylic alcohols catalyzed by Pd(PPh₃)₄ (Scheme 1.13). Although H₂O could be employed as a nucleophile to form the hydroxyl group, stoichiometric amount of benzoquinone was used as the oxidant, and to form the half-ester intermediate, high pressure of CO₂ was required. In this work, I propose to synthesize primary allylic alcohols from terminal alkenes over supported Pd catalysts using O₂ as the sole oxidant, and H₂O is also used as a nucleophile in absence of other additives. Allylbenzene is selected as a substrate to optimize reaction conditions. Catalyst performance, reaction rate, and reaction pathway are studied. In addition, the optimized reaction conditions are used to synthesize *trans*-2-butene-1,4-diol from 1,3-butadiene.



Scheme 1.12 Transformation of terminal alkenes into primary allylic alcohols reported by Tokunaga and co-workers.

From the practical and environmental point of view, the demonstrated supported Pd catalytic systems in this thesis prevail in existing homogeneous systems with many advantages. This work is expected to be a good initiation to enlarge the applications of supported transition metal catalysts in aerobic oxidation reactions and industrial processes.

1.2 References

- [1] (a) R. A. Sheldon, J. K. Kochi, *Metal-Catalyzed Oxidations of Organic Compound*, Academic Press: New York, **1981**. (b) H. A. Wittcoff, B. G. Reuben, J. S. Plotkin, *Industrial Organic Chemistry*, –2nd Ed., John Wiley & Sons: New Jersey, **2004**.
- [2] (a) S. S. Stahl, *Angew. Chem. Int. Ed.*, **2004**, 43, 3400–3420. (b) S. S. Stahl, *Science*, **2005**, 309, 1824–1826. (c) T. Punniyamurthy, S. Velusamy, J. Iqbal, *Chem. Rev.*, **2005**, 2329–2363. (d) Z. Shi, C. Zhang, C. Tang, N. Jiao, *Chem. Soc. Rev.*, **2012**, 41, 3381–3430. (e) K. M. Gligorich, M. S. Sigman, *Chem. Commun.*, **2009**, 3854–3867. (f) A. N. Campbell, S. S. Stahl, *Acc. Chem. Rev.*, **2002**, 102, 4303–4427.
- [3] (a) C. D. Pina, E. Falletta, L. Prati, M. Rossi, *Chem. Soc. Rev.*, **2008**, 37, 2077–2095. (b) A. Corma, H. García, *Chem. Soc. Rev.*, **2008**, 37, 2096–2126. (c) A. Arcadi, *Chem. Rev.*, **2008**, 108, 3266–3325.
- [4] (a) M. Yagi, M. Kaneko, *Chem. Rev.*, **2001**, 101, 21–35. (b) T. Mallat, A. Baiker, *Chem. Rev.*, **2004**, 104, 3037–3058.
- [5] G. S. Kumar, C. U. Maheswari, R. A. Kumar, M. L. Kantam, K. R. Reddy, *Angew. Chem. Int. Ed.*, **2011**, 50, 11748–11751.
- [6] (a) M. S. Chen, N. Prabakaran, N. A. Labenz, M. C. White, *J. Am. Chem. Soc.*, **2005**, 127, 6970–6971. (b) J. H. Delcamp, M. C. White, *J. Am. Chem. Soc.*, **2006**, 128, 15076–15077. (c) D. J. Covell, M. C. White, *Angew. Chem. Int. Ed.*, **2008**, 47, 6448–6451. (d) B. Morandi, Z. K. Wickens, R. H. Grubbs, *Angew. Chem. Int. Ed.*, **2013**, 52, 2944–2948. (e) M. A. Bigi, M. C.

- White, *J. Am. Chem. Soc.*, **2013**, 135, 7831–7834. (f) T. J. Osberger, M. C. White, *J. Am. Chem. Soc.*, **2013**, 136, 11176–1118. (g) J. M. Howell, W. Liu, A. J. Young, M. C. White, *J. Am. Chem. Soc.*, **2014**, 136, 5750–5754. (h) T. Diao, S. S. Stahl, *Polyhedron*, **2014**, 84, 96–102.
- [7] H. Chen, H. Jiang, C. Cai, J. Dong, W. Fu, *Org. Lett.*, **2011**, 13, 992–994.
- [8] (a) B. W. Michel, J. R. McCombs, A. Winkler, M. S. Sigman, *Angew., Chem. Int. Ed.*, **2010**, 49, 7321–7315. (b) R. J. DeLuca, J. L. Edwards, L. D. Steffens, B. W. Michel, X. Qiao, C. Zhu, S. P. Cook, M. S. Sigman, *J. Org. Chem.*, **2013**, 78, 1682–1686.
- [9] J. R. McCombs, B. W. Michel, M. S. Sigman, *J. Org. Chem.*, **2011**, 76, 3609–3613.
- [10] (a) B. A. Steinhoff, S. R. Fix, S. S. Stahl, *J. Am. Chem. Soc.*, **2002**, 124, 766–767. (b) S. Gowrisankar, H. Neumann, M. Beller, *Angew. Chem. Int. Ed.*, **2011**, 50, 5139–5143.
- [11] (a) T. A. Dwight, N. R. Rue, D. Charyk, R. Josselyn, B. DeBoed, *Org. Lett.*, **2007**, 9, 3137–3139. (b) D. R. Stuart, K. Fagnou, *Science*, **2007**, 316, 1172–1175.
- [12] (a) J. Zhu, J. Liu, R. Ma, H. Xie, J. Li, H. Jiang, W. Wang, *Adv. Synth. Catal.*, **2009**, 351, 1229–1232. (b) J. Liu, J. Zhu, H. Jiang, W. Wang, J. Li, *Chem. Commun.*, **2010**, 46, 415–417.
- [13] (a) T. Mitsudome, T. Umetani, N. Nosaka, K. Mori, T. Mizugaki, K. Ebitani, K. Kaneda, *Angew. Chem. Int. Ed.*, **2006**, 45, 481–485. (b) X. Wang, N. S. Venkataramanan, H. Kawanami, Y. Ikushima, *Green. Chem.*, **2007**, 9, 1352–1355. (c) Z. K. Wickens, B. Morandi, R. H. Grubbs, *Angew. Chem. Int. Ed.*, **2013**, 52, 11257–11260.
- [14] (a) J. Piera, J. E. Bäckvall, *Angew. Chem. Int. Ed.*, **2008**, 47, 3506–3523. (b) F. A. Cotton, G. Wilkinson, *Advanced Inorganic Chemistry*, 4th ed., Wiley, New York, **1980**.
- [15] (a) R. A. Sheldon, R. S. Downing, *Appl. Catal. A: General*, **1999**, 189, 163–183. (b) A. A. Kiss, F. Omota, A. C. Dimian, G. Rothenberg, *Top. Catal.*, **2006**, 40, 141–150. (c) J. M. Thomas, R. Raja, *Top. Catal.*, **2006**, 40, 3–17. (d) M. Heitbaum, F. Glorius, I. Escher, *Angew. Chem. Int. Ed.*, **2006**, 45, 4732–4762.
- [16] (a) R. A. Watile, K. M. Deshmukh, K. P. Dhake, B. M. Bhanage, *Catal. Sci. Technol.*, **2012**, 2, 1051–1055. (b) E. Gross, J. H. Liu, F. D. Toste, G. A. Somorjai, *Nature Chem.*, **2012**, 4, 947–952. (c) G. T. Whiting, S. A. Kondrat, C. Hammond, N. Dimitratos, Q. He, G. J. Morgan, N. F. Dummer, J. K. Bartley, C. J. Kiely, S. H. Taylor, G. J. Hutchings, *ACS Catal.*, **2015**, 5, 637–644. (d) A. Bhosale, H. Yoshida, S. Fujita, M. Arai, *Green Chem.*, **2015**, in press.
- [17] K. Mori, T. Hara, T. Mizugaki, K. Ebitani, K. Kaneda, *J. Am. Chem. Soc.*, **2004**, 126, 10657–10666.

- [18] (a) C. M. A. Parlett, D. W. Bruce, N. S. Hondow, A. F. Lee, K. Wilson, *ACS Catal.*, **2011**, 1, 636–640. (b) B. Karimi, S. Abedi, J. H. Clark, V. Budarin, *Angew. Chem. Int. Ed.*, **2006**, 45, 4776–4779
- [19] Y. Chen, H. Zheng, Z. Guo, C. Zhou, C. Wang, A. Borgna, Y. Yang, *J. Catal.*, **2011**, 283, 34–44.
- [20] (a) Z. Hou, N. Theyssen, A. Brinkmann, W. Leitner, *Angew. Chem. Int. Ed.*, **2005**, 44, 1346–1349. (b) Y. Uozumi, R. Nakao, *Angew. Chem. Int. Ed.*, **2003**, 42, 194–197.
- [21] B. Fu, X. Zhu, G. Xiao, *Appl. Catal. A: General*, **2012**, 415–416, 47–52.
- [22] P. Zhang, Y. Gong, H. Li, Z. Chen, Y. Wang, *Nature Commun.*, **2013**, 4, 1593–1603
- [23] K. Choi, T. Mizugaki, K. Ebitani, K. Kaneda, *Chem. Lett.*, **2003**, 32, 180–181.
- [24] T. Mitsudome, T. Umetani, K. Mori, T. Mizugaki, K. Ebitani, K. Kaneda, *Tetrahedron Lett.*, **2006**, 47, 1425–1428.
- [25] X. Wang, N. S. Venkataramanan, H. Kawanami, Y. Ikushima, *Green Chem.*, **2007**, 9, 1352–1355.
- [26] S. Byun, J. Chung, Y. Jang, J. Kwon, T. Hyeon, B. M. Kim, *RSC Adv.*, **2013**, 3, 16296–16299.
- [27] (a) L. Ying, J. Lisbscher, *Chem. Rev.*, **2007**, 107, 133–173. (b) Á. Molnár, *Chem. Rev.*, **2011**, 111, 2251–2320.
- [28] M. Wanger, K. Kohler, L. Djakovitch, S. Weinkauff, V. Hagen, M. Muhler, *Top. Catal.*, **2000**, 13, 319–326.
- [29] (a) Y. Mori, M. Seki, *Heterocycles*, **2002**, 58, 125–127. (b) M. Kimura, M. Seki, *Tetrahedron Lett.*, **2004**, 45, 1635–1637. (c) Y. Mori, M. Seki, *J. Org. Chem.*, **2003**, 68, 1571–1574.
- [30] B. Yuan, Y. Pan, Y. Li, B. Yin, H. Jiang, *Angew. Chem. Int. Ed.*, **2010**, 49, 4054–4058.
- [31] W. Huang, J. H. Liu, P. Alayoglu, Y. Li, C. A. Witham, C. Tsung, F. D. Toste, G. A. Somorjai, *J. Am. Chem. Soc.*, **2010**, 132, 16771–16773.
- [32] (a) S. J. Tauster, *Acc. Chem. Rev.*, **1987**, 20, 389–394. (b) K. Okumura, T. Kobayashi, H. Tanaka, M. Niwa, *Appl. Catal. B: Environ.*, **2003**, 44, 325–331. (c) W. T. Wallace, B. K. Min, D. W. Goodman, *Top. Catal.*, **2005**, 43, 17–30.
- [33] S. S. Soomro, F. L. Ansari, K. Chatziapostolou, K. Köhler, *J. Catal.*, **2010**, 273, 138–146.
- [34] N. Iwasa, T. Mayanagi, W. Nomura, M. Arai, N. Takezawa, *Appl. Catal. A: General*, **2003**, 248, 153–160.
- [35] B. Liégault, D. Lee, M. P. Huestis, D. R. Stuart, K. Fagnou, *J. Org. Chem.*, **2008**, 73, 5022–5028.

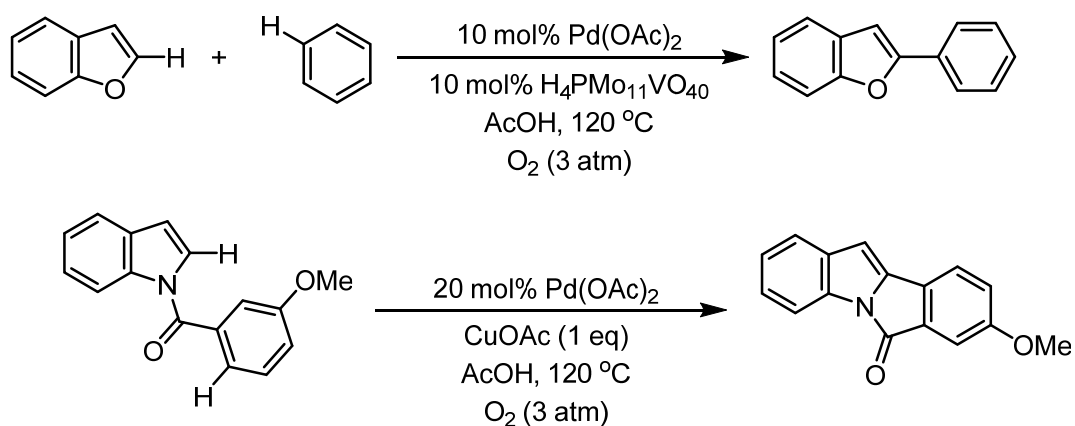
- [36] (a) T. Diao, S. S. Stahl, *J. Am. Chem. Soc.*, **2011**, 133, 14566–14569. (b) Y. Izawa, D. Pun, S. S. Stahl, *Science*, **2011**, 333, 209–213;
- [37] K. Takahashi, M. Yamashita, T. Ichihara, K. Nakano, K. Nozaki, *Angew. Chem. Int. Ed.*, **2010**, 49, 4488–4490.
- [38] A. N. Campbell, P. B. White, L. A. Guzei, S. S. Stahl, *J. Am. Chem. Soc.*, **2010**, 132, 15116–15119.
- [39] G. Dong, P. Teo, Z. K. Wickens, R. H. Grubbs, *Science*, **2011**, 16, 1609–1612.
- [40] R. Tomita, K. Mantani, A. Hamasaki, T. Ishida, M. Tokunaga, *Chem. Eur. J.*, **2014**, 20, 9914–9917.

Chapter 2.

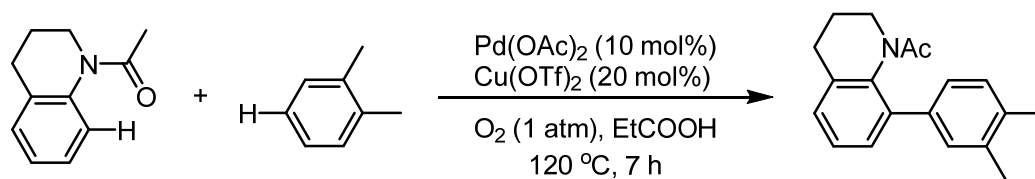
Intramolecular double C-H bond functionalization for synthesis of dibenzofurans over supported palladium hydroxide catalysts

2.1 Introduction

Recent years, palladium catalyzed C–C bond formation reactions to prepare conjugated aromatic compounds have been much attractive issues in both organic synthesis and material science based on these compounds possess good electron transfer ability and have potentiality for the manufacture of organic electron materials such as organic semiconductors and electroluminescence devices.¹ Many reactions have been employed to synthesize these compounds such as Suzuki-Miyaura, Negishi, and Ullmann coupling reactions.² However, in these methods, aryl substrates should be pre-activated into organic halides or organometallic compounds before use. Thus, multiple synthetic steps and much energy are required. Moreover, large amounts of inorganic wastes are produced. Therefore, to develop synthetic methods that avoid pre-activation of unactivated aromatic compounds for C–C bond formation reaction is of great interest.³ The first example for palladium catalyzed direct oxidative C–C bond coupling reaction to prepare biaryl products was reported by van Helden and Verberg.⁴ In their reaction, stoichiometric PdCl₂ and sodium acetate was used. DeBoef and co-workers have developed an aerobic oxidative coupling reaction with catalytic amount of Pd(OAc)₂ for synthesizing heterocoupled biaryls through the inter- and intramolecular C–C bond formation, respectively (Scheme 2.1).⁵ However, stoichiometric co-catalyst such as CuOAc was required. Shi and co-workers reported a highly selective cross-coupling of arenes in the presence of O₂, and Cu(OTf)₂ was used as co-catalyst (Scheme 2.2).⁶

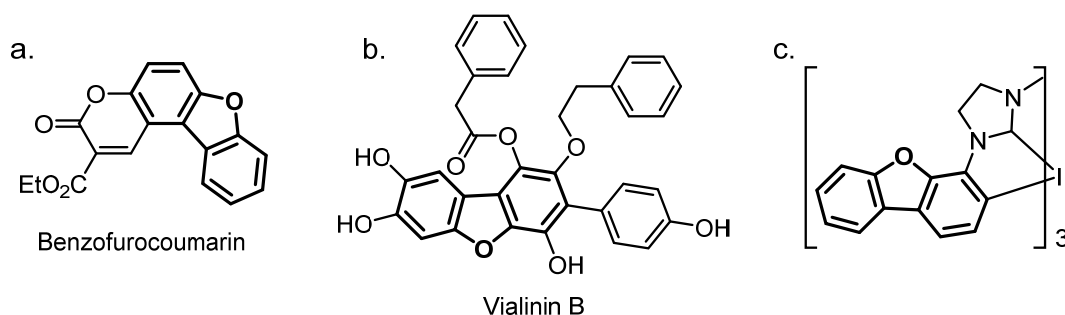


Scheme 2.1 Aerobic oxidative inter- and intramolecular C–C bond formation reaction reported by DeBoef and co-workers.



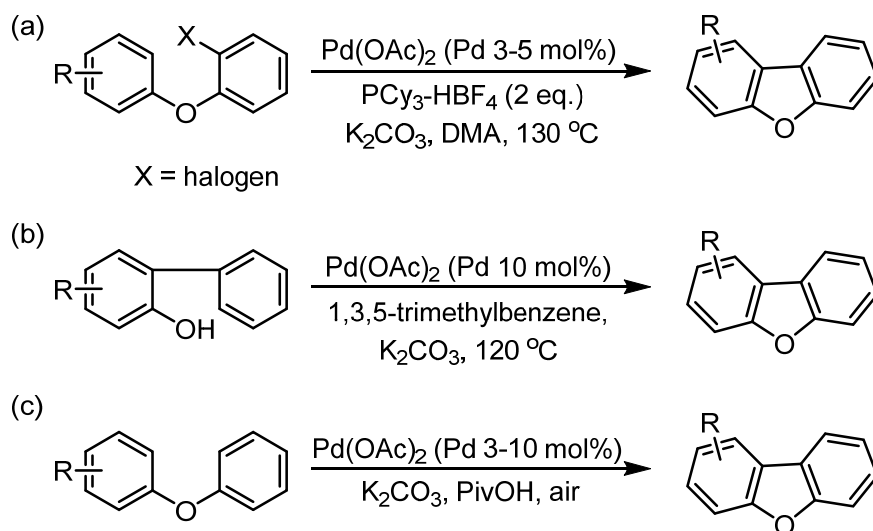
Scheme 2.2 Selective cross coupling reaction in the presence of O₂ reported by Shi and co-workers.

Dibenzofuran and its derivatives can be found in many pharmaceutical products and biological compounds such as Benzofurocoumarin and Vialinin B (Scheme 2.3a and b)⁷ and are broadly used as components of optoelectronic materials such as a deep-blue phosphorescent materials for electroluminescence devices (Scheme 2.3c).⁸



Scheme 2.3 Dibenzofuran derivatives component in (a) pharmaceutical products, (b) biological compounds, and (c) phosphorescent material on electroluminescence devices.

The common preparation method of dibenzofuran is distillation from coal tar that boils between 275 and 290 °C with low yield. Hence, developing a reliable method to synthesize dibenzofurans is desirable. There are several methods have been established to prepare dibenzofurans involving C–C or C–O bond formation reactions, for example, (a) intramolecular coupling of C–X (X = halogen) and C–H bonds,⁹ (b) intramolecular C–O bond formation,¹⁰ and (c) intramolecular coupling of two C–H bonds of diphenyl ethers (Scheme 2.4).¹¹ Among these methods, transformation of diphenyl ethers directly to dibenzofurans (Scheme 2.4c) is recognized as a low cost and environmentally friendly method, because the pre-activation of substrate is avoided, and water is produced as a sole by-product.



Scheme 2.4 Synthetic methods of dibenzofuran by (a) intramolecular coupling of C–X (X = halogen) and C–H bonds, (b) intramolecular C–O bond formation, and (c) intramolecular coupling of two C–H bonds of diphenyl ethers.

Intramolecular coupling of two C–H bonds to produce conjugated aromatic compounds using homogeneous catalytic systems have been reported by several groups such as Ohno, Pan, and Fagnou.^{11–13} However, synthesis of conjugated aromatic compounds, in particular for dibenzofuran and derivatives using heterogeneous palladium catalysts, have not yet been reported. In this chapter, a novel catalytic system using ZrO_2 supported Pd(OH)_2 catalyst is demonstrated, which can efficiently promote the transformation of diphenyl ethers to dibenzofurans without co-catalyst and using molecular oxygen as sole oxidant.

2.2 Results and discussion

2.2.1 Preparation of catalysts and characterization

Metal oxide, such as TiO_2 , Al_2O_3 , CeO_2 , and ZrO_2 , supported Pd(OH)_2 catalysts were prepared by deposition-precipitation method using palladium chloride (PdCl_2) as the precursor according to the literature with modifications.¹⁴ The metal oxide supported PdO and Pd were prepared from Pd(OH)_2 by calcination and reduction, respectively. To investigate the size of Pd nanoparticles, high angle annular dark field scanning transmission electron microscopy (HAADF-STEM) observation were performed. Figure 2.1a shows HAADF-STEM image of 20 wt% $\text{Pd(OH)}_2/\text{ZrO}_2$, and Pd nanoparticles

were well dispersed on the surface of ZrO₂. The mean diameter of Pd(OH)₂ nanoparticles was calculated to be 2.7 ± 1.3 nm (Figure 2.1b).

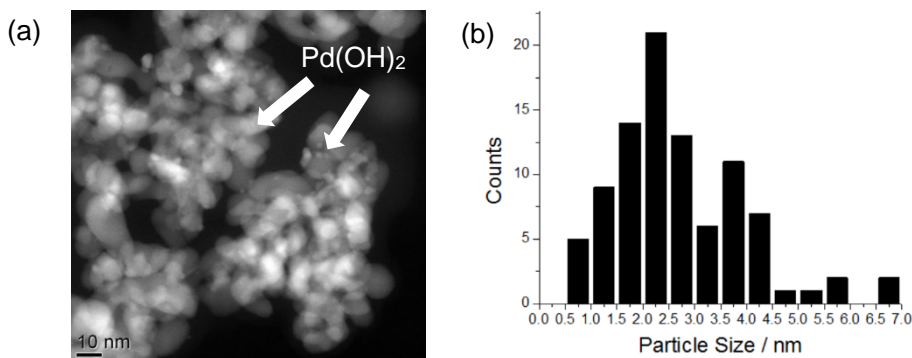


Figure 2.1 (a) HADDF-STEM image of 20 wt% Pd(OH)₂/ZrO₂, and (b) the size distribution of Pd(OH)₂ nanoparticles.

To confirm the chemical state of Pd in supported Pd(OH)₂ catalysts, Pd *K*-edge X-ray absorption near edge structure (XANES) spectra was measured, and the spectra is shown in Figure 2.2. In comparison with the references of Pd foil, PdO, and Pd(OH)₂, the chemical state of Pd in Pd(OH)₂/ZrO₂ with different loading (d–f) and 20 wt% Pd(OH)₂/TiO₂ (g) were determined as Pd^{II}, and the interaction of Pd–Pd was not observed even in high Pd loading catalyst. However, Pd(OH)₂ was not distinctly differentiated from PdO by XANES spectra, since the spectral features of Pd(OH)₂ was similar to that of PdO. In the radial structure functions (RSF) (Figure 2.3), the peaks corresponding to the interaction of Pd–O for all these catalysts were observed at 1.5 Å (phase-uncorrected). The magnitude of reference PdO for Pd–Pd interaction was higher than that of Pd(OH)₂ at 2.9 Å. These peaks corresponded to the interaction of Pd–O for the first coordination shell and both of Pd–Pd and Pd–O for the second one, respectively.¹⁵ For all the ZrO₂ and TiO₂ supported Pd(OH)₂ catalysts, the magnitude of the peaks attributed to Pd–Pd interaction were lower than reference PdO but were still higher than that of reference Pd(OH)₂. Additionally, in the *k*³-weighted extended X-ray absorption fine structure oscillations (EXAFS), the amplitude of Pd(OH)₂ was lower than that of PdO in the range of 7–11 Å⁻¹ (Figure 2.4). The amplitude of 20 wt% Pd(OH)₂/ZrO₂ was close to that of reference Pd(OH)₂.

These results indicated that the possibilities of Pd(OH)₂ exists in these catalysts, which may also consist of a small amount of PdO. Unfortunately, the formation of Pd(OH)₂ cannot be fully asserted by XAFS.

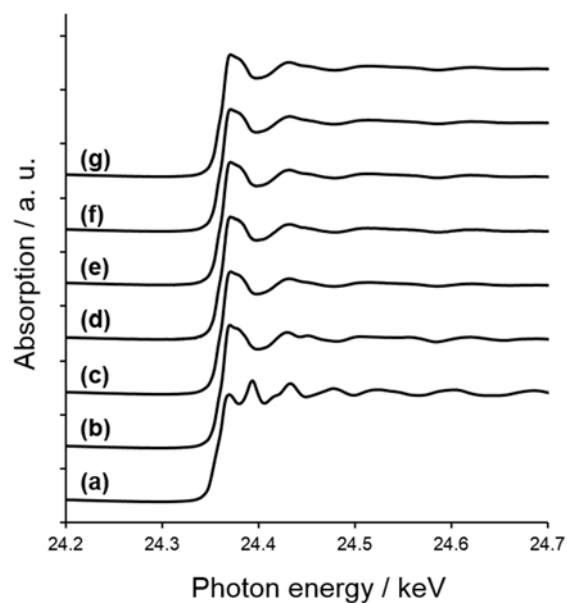


Figure 2.2 Pd *K*-edge XANES spectra of (a) Pd foil, (b) PdO, (c) Pd(OH)₂ (amorphous) (d) 10 wt% Pd(OH)₂/ZrO₂, (e) 20 wt% Pd(OH)₂/ZrO₂, (f) 30 wt% Pd(OH)₂/ZrO₂, (g) 20 wt% Pd(OH)₂/TiO₂.

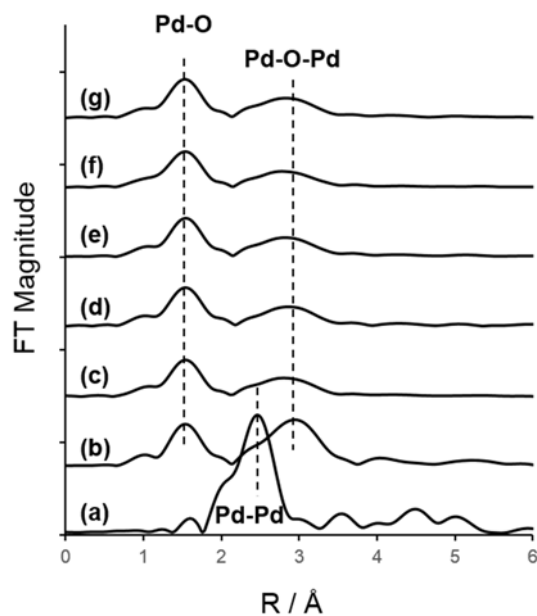


Figure 2.3 Radial structure functions of (a) Pd foil, (b) PdO, (c) Pd(OH)₂, (d) 10 wt% Pd(OH)₂/ZrO₂, (e) 20 wt% Pd(OH)₂/ZrO₂, (f) 30 wt% Pd(OH)₂/ZrO₂, (g) 20 wt% Pd(OH)₂/TiO₂.

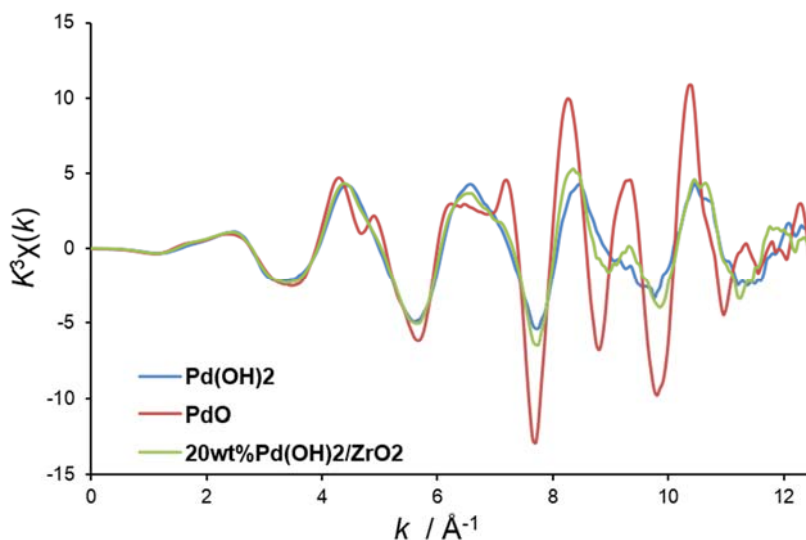
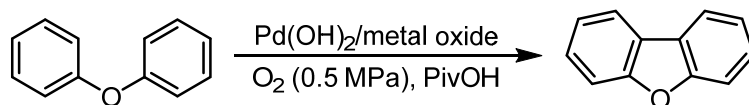


Figure 2.4 k^3 -weighted Pd K-edge EXAFS oscillations of 20 wt% Pd(OH)₂/ZrO₂ including reference PdO and Pd(OH)₂.

2.2.2 Optimization of reaction conditions

The oxidative intramolecular coupling reaction conditions were investigated for synthesis of dibenzofuran over supported Pd catalysts (Table 2.1). Fagnou and co-workers reported that pivalic acid could promote the reactions with greater reproducibility, higher yield, and broader scope than acetic acid.¹¹ Therefore, pivalic acid was also selected as the solvent this time. Several oxide supported Pd(OH)₂ catalysts were initially screened including Al₂O₃, TiO₂, CeO₂, and ZrO₂ supported catalysts using high Pd loading and long reaction time (Table 2.1, entries 1–5). These catalysts proceeded the reaction efficiently to give dibenzofuran in about 50% yield, and ZrO₂ supported Pd(OH)₂ showed better activity than other catalysts (Table 2.1, entry 5). Decreasing the reaction time to 48 h lowered the yield (Table 2.1, entry 4), whereas higher temperature improved the yield up to 60% over Pd(OH)₂/ZrO₂ (Table 2.1, entries 6 and 7). The reaction was also catalyzed by PdO/ZrO₂ and Pd/ZrO₂ with lower activity than Pd(OH)₂/ZrO₂ (Table 2.1, entries 8 and 9).

Table 2.1 Optimization of reaction conditions for the oxidative coupling diphenylether.^a

Entry	Catalyst	Pd (mol%)	Conc. (M)	Temp. (°C)	Time (h)	Conv. (%) ^b	Yield (%) ^b
1	Pd(OH) ₂ /Al ₂ O ₃	14	0.5	120	60	55	49
2	Pd(OH) ₂ /TiO ₂	14	0.5	120	60	53	49
3	Pd(OH) ₂ /CeO ₂	14	0.5	120	64	65	47
4	Pd(OH) ₂ /CeO ₂	14	0.5	120	48	44	41
5	Pd(OH) ₂ /ZrO ₂	14	0.5	120	64	61	54
6	Pd(OH) ₂ /ZrO ₂	14	0.5	130	48	65	62
7	Pd(OH) ₂ /ZrO ₂	14	0.5	140	48	96	60
8	PdO/ZrO ₂	14	0.5	130	48	59	42
9	Pd/ZrO ₂	14	0.5	130	48	38	35
10	Pd(OH) ₂ /ZrO ₂	6	0.5	130	48	69	53
11	Pd(OH) ₂ /ZrO ₂	6	0.8	130	48	83	64
12	Pd(OH) ₂ /ZrO ₂	6	0.9	130	48	86	72
13	Pd(OH) ₂ /ZrO ₂	6	1.3	130	48	88	80
14	Pd(OH) ₂ /ZrO ₂	6	1.7	130	48	93	80
15	Pd(OH) ₂ /ZrO ₂	3	1.3	130	48	80	69
16 ^c	Pd(OH) ₂ /ZrO ₂	3	-	130	48	100	26

^a Reaction conditions: diphenylether (1 mmol), Pd catalyst, PivOH, O₂ (0.5 MPa).

^b Calculated on the basis of GC analysis using tridecane as an internal standard.

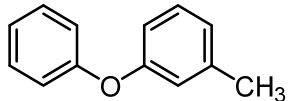
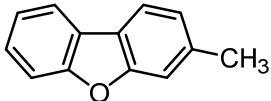
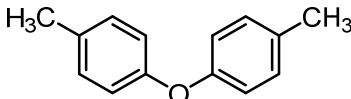
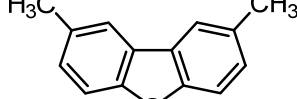
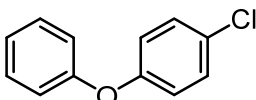
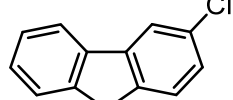
^c AcOH (3 ml).

Furthermore, both the conversion and product yield were decreased with lower Pd loading (Table 2.1, entry 10). However, the reactivity was slightly improved with higher reaction concentration (Table 2.1, entries 10–14). In entry 13, when the concentration of reaction was adjusted to 1.3 M, the reaction proceeded to give benzofuran up to 80% using 6 mol% of Pd catalyst. The yields were decreased when much lower Pd loading was tested in PivOH and AcOH, respectively (Table 2.1, entries 15 and 16). Consequently, entry 13 was selected as the optimized reaction conditions.

2.2.3 Scope of substrates

The scope of substrates was investigated, and the results are shown in Table 2.2. Reactions of diphenylethers with electron-donating groups afforded the corresponding dibenzofurans in good yields (Table 2.2, entries 1 and 2). 4-chlorodiphenylether was also transformed into 2-chlorodibenzofuran in moderate yield (Table 2.2, entry 3). In contrast, the reaction of 4-bromodiphenylether gave quite low yield (Table 2.2, entry 4), and 7% yield of debrominated diphenylether was formed. This result indicated that oxidative addition of 4-bromodiphenylether to Pd⁰, which was formed in-situ, occurred to produce diphenylether. The oxidative coupling of diphenylether in the presence of equimolar amount of bromobenzene, as a result, 14% of bromobenzene was converted, and benzene was detected. At the same time, the oxidative coupling of diphenylether was significantly inhibited. It is likely that Pd was deactivated once Pd–Br bond was formed, although Pd–Cl bond did not affect the catalytic activity (Table 2.2, entry 3). Reactions of diphenylethers with electron-withdrawing groups also proceeded to give the corresponding dibenzofurans in good yields (Table 2.2, entries 5 and 6). Notably, carbazole, which is an important compound in chemical industry, was obtained from diphenylamine in 70% yield over Pd(OH)₂/ZrO₂ with lower temperature and shorter time than those for dibenzofuran (Table 2.2, entry 7). The oxidative intramolecular coupling of diphenylthiophene and diphenylmethane also gave dibenzothiophene and fluorene, respectively, whereas the yields were low (Table 2.2, entries 8 and 9).

Table 2.2 Scope of diaryl ethers and other diaryl compounds for Pd(OH)₂/ZrO₂ catalyzed oxidative coupling.^a

Entry	Substrate	Product	Conv. (%) ^b	Yield (%) ^c
1			88	75 (59)
2 ^d			97	71 (60)
3 ^e			86	73

4			33	9
5 ^e			91	74 (52)
6			96	84 (71)
7 ^f			100	70
8			21	7
9			30	13

^a Reaction conditions: substrate (1 mmol), Pd(OH)₂/ZrO₂ (6 mol%), PivOH (0.7 g), O₂ (0.5 MPa), 130 °C, 48 h.

^b Calculated on the basis of GC analysis using tridecane as an internal standard.

^c GC yield. Yield in parentheses is isolated yield.

^d Reacted at 135 °C.

^e Reacted at 140 °C.

^f Reacted at 120 °C for 24 h.

2.2.4 Possible reaction pathway

Several experiments were carried out to discuss the reaction pathway, and the results are shown in Figure 2.5.¹⁶ The reaction pathway may consist of four steps in this process: (i) the electrophilic substitution by Pd^{II} species to form palladated species, (ii) the second substitution to form a palladacycle, (iii) reductive elimination to form dibenzofurans and Pd⁰, and (iv) the re-oxidation of Pd⁰ to Pd^{II} species by O₂.

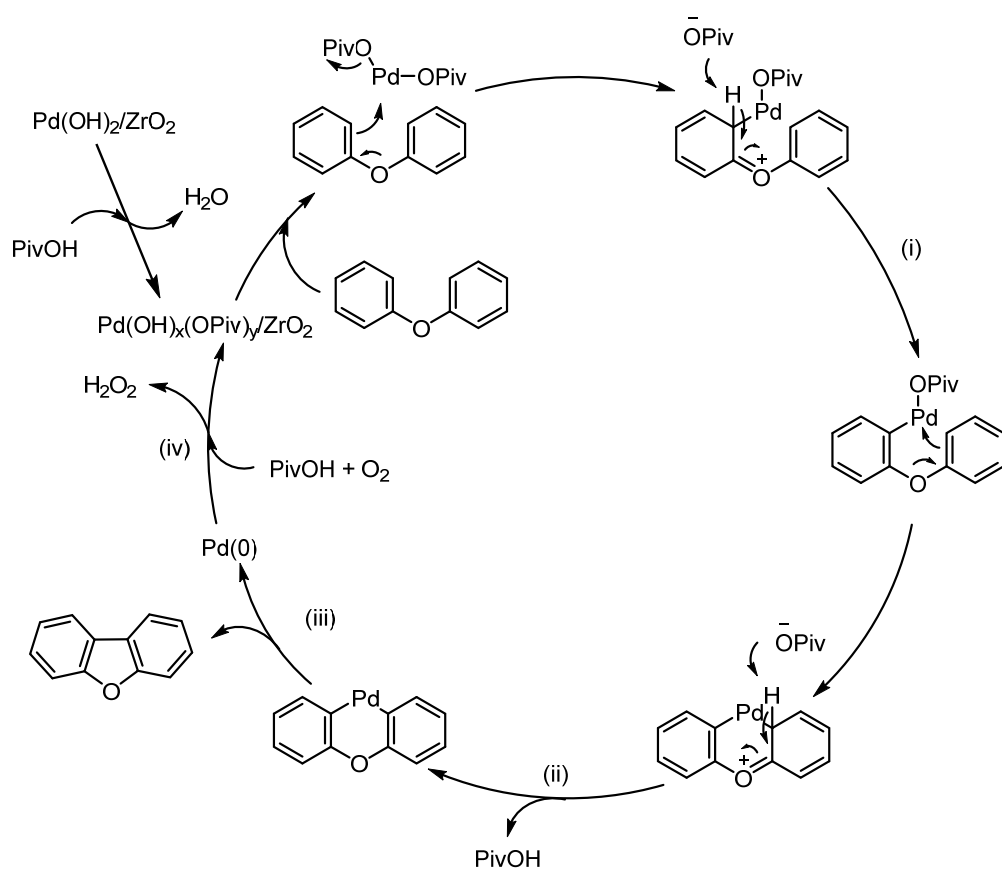


Figure 2.5 Possible reaction pathway for oxidative intramolecular coupling of diphenylether.

2.3 Conclusion

Several metal oxide supported $\text{Pd}(\text{OH})_2$ catalysts were prepared by DP method. The size of Pd particles was confirmed by HAADF-STEM, and the chemical state of Pd was determined by XAFS. Dibenzofuran was synthesized from diphenylether over the ZrO_2 supported $\text{Pd}(\text{OH})_2$ catalysts by the intramolecular oxidative coupling reaction using O_2 as the sole oxidant. The substrate scope and the reaction pathway were studied.

2.4 Experimental section

2.4.1 Materials

Palladium chloride (PdCl_2) was purchased from Tanaka Kikinzoku KK. and used as received. Al_2O_3 , TiO_2 (P-25), ZrO_2 (RC-100), and CeO_2 , were supplied by Mizusawa Chemicals, Nippon

Aerosil Co., Ltd., Daiichi Kigenso Kagaku Kogyo, and Shinetsu Chemical Co., Ltd., respectively. All commercial starting materials and reagents were used as received.

2.4.2 Instruments

Conversions and product yields were analyzed by gas chromatography (GC) using Agilent GC 6850 Series II equipped with FID and a J&W HP-1 column (0.25 μm thickness, 0.25 mm I.D., 30 m) using tridecane as an internal standard. Gas chromatography mass spectrometer (GC-MS) analysis was performed with Thermo Fisher Scientific Polaris Q equipped with a J&W HP-1 column (0.25 μm thickness, 0.25 mm I.D., 30 m). ^1H and ^{13}C NMR spectra were recorded on a JEOL JNM-ECS400 spectrometer at 400 and 100 MHz, respectively. ^1H assignment abbreviations are the following; singlet (s), doublet (d), triplet (t), double of doublet (dd), and multiplet (m). Analytical thin-layer chromatography (TLC) was performed with Merck, TLC silica gel 60 F_{254} plates. Column chromatography was performed on silica gel (Kanto Chemicals, Silica gel 60N, spherical, neutral, particle size 40–100 μm). Recycling preparative HPLC was performed on Japan Analytical Industry Co., Ltd., LC-908. Elemental analyses were carried out at the center of elementary analysis, Kyushu University

High angle annular dark-field scanning transmission electron microscopy (HAADF-STEM) observations were performed using JEOL JEM-ARM200F operating at 200 kV at the Ultramicroscopy Research Center, Kyushu University.

X-ray absorption fine structure (XAFS) measurements were performed at BL14B2 beam line of SPring-8 (Hyogo, Japan).¹⁸ The XAFS samples were ground with boron nitride in an agate mortar and were compacted into pellets. Pd K-edge (24.3 keV) XAFS spectra were measured using a Si (311) double crystal monochromator in transmission mode. Ionization chambers were used to measure the intensity of the incident and transmitted X-ray and the quick scan technique (QXAFS) was used. The spectral analysis was performed using the XAFS analysis software, Athena.¹⁸ The extraction of the extended X-ray absorption fine structure (EXAFS) oscillation from the spectra, normalization by edge-jump, and Fourier transformation were performed using the Athena software.

2.4.3 Preparation of catalysts

Metal oxide-supported $\text{Pd}(\text{OH})_2$ catalysts ($\text{Pd}(\text{OH})_2/\text{MO}_x$) were prepared according to the literature with minor modifications.¹³ Take the preparation of 20 wt% $\text{Pd}(\text{OH})_2/\text{ZrO}_2$ as an example,

PdCl₂ (417 mg) was dissolved in an aqueous solution of conc. HCl (10 mL) and distilled water (240 mL). The solution was warmed to 60 °C and the pH of the solution was adjusted to 8.0 by adding 0.1 M NaOH aqueous solution. Then, the support (1.0 g) was added to the solution and the suspension was stirred at 70 °C for 1 h. The solid was filtered, washed with water, and then dried in air at 70 °C overnight.

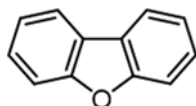
PdO/ZrO₂ catalyst was prepared from calcination of Pd(OH)₂/ZrO₂ in air at 300 °C for 4 h. Pd/ZrO₂ catalyst was prepared from reduction of Pd(OH)₂/ZrO₂ by H₂ (40 mL/min) at 200 °C for 2 h.

2.4.4 Experimental procedure for catalytic reactions

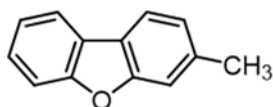
A typical experiment for synthesis of dibenzofuran from phenylether

To an autoclave was charged with diphenylether (1 mmol), catalysts (Pd 6 mol%), pivalic acid (0.7 g), and a magnetic stirring bar. The autoclave was purged and filled with O₂ until the pressure reached 0.5 MPa. The reaction mixture was stirred at 130 °C for 48 h. After the reaction, the mixture was filtered and the filtrate was analyzed by GC using tridecane as an internal standard.

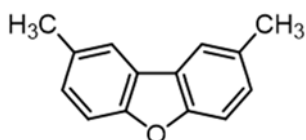
2.4.5 Characterization of the isolated compounds



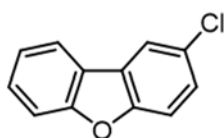
Dibenzofuran: The mixture of diphenylether (158.2 μL, 1.0 mmol), 20 wt% Pd(OH)₂/ZrO₂ (30 mg, Pd 6 mol%), in pivalic acid (0.7 g) was stirred under pressurized O₂ (0.5 MPa) at 130 °C for 48 h. After the reaction, the catalyst was filtered off and the filtrate was neutralized by NaHCO₃ aq. The organic layer was extracted with CH₂Cl₂, and then dried over Na₂SO₄. The organic solvents were removed and the crude product was purified by recycling preparative HPLC to give dibenzofuran (108.8 mg, 0.65 mmol, 65%) as a white solid. (GC yield: 80%). ¹H NMR (400 MHz, CDCl₃): δ 7.96 (d, *J* = 7.8 Hz, 2H), 7.58 (d, *J* = 8.2 Hz, 2H), 7.46 (ddd, *J* = 7.8, 7.8, 1.4 Hz, 2H), 7.35 (dd, *J* = 7.3, 7.3 Hz, 2H); ¹³C NMR (100 MHz, CDCl₃): δ 156.3, 127.2, 124.3, 122.8, 120.8, 111.8. Anal. Calcd. (%) for C₁₂H₈O: C, 85.69; H, 4.79. Found; C, 85.68; H, 4.73.



3-Methyldibenzofuran: The mixture of 3-methyldiphenylether (175.5 μ L, 1.0 mmol), 20 wt% Pd(OH)₂/ZrO₂ (30 mg, Pd 6 mol%) in pivalic acid (0.7 g) was stirred under pressurized O₂ (0.5 MPa) at 130 °C for 48 h. The catalyst was filtered off, and the filtrate was neutralized by NaHCO₃ aq. The crude product was purified by recycling preparative HPLC to give 3-methyldibenzofuran (107.8 mg, 0.59 mmol, 59%) as a white solid. (GC yield: 75%). ¹H NMR (400 MHz, CDCl₃): δ 7.92 (d, *J* = 7.4 Hz, 1H), 7.83 (d, *J* = 7.8 Hz, 1H), 7.56 (d, *J* = 7.8 Hz, 1H), 7.32-7.43 (m, 3H), 7.18 (d, *J* = 7.4 Hz, 1H), 2.54 (s, 3H); ¹³C NMR: (100 MHz, CDCl₃) δ 156.6, 156.2, 137.8, 126.6, 124.6, 124.1, 122.7, 121.8, 120.4, 120.3, 112.0, 111.7, 22.1. Anal. Calcd. (%) for C₁₃H₁₀O: C, 85.69; H, 5.53. Found; C, 85.53; H, 5.44. The structure of 3-methyldibenzofuran was determined by ¹H NMR spectra with the comparison of that of 1-methyldibenzofuran.¹⁶

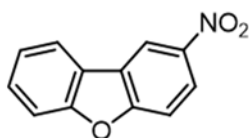


2,8-Dimethyldibenzofuran: The mixture of 4,4'-oxybis(methylbenzene) (198.3 mg, 1.0 mmol), 20 wt% Pd(OH)₂/ZrO₂ (30 mg, 6 mol%) in pivalic acid (0.7 g) was stirred under pressurized O₂ (0.5 MPa) at 130 °C for 48 h. The catalyst was filtered off, and the filtrate was neutralized by NaHCO₃ aq. The crude product was purified by recycling preparative HPLC to give 2,8-dimethyldibenzofuran (118.4 mg, 0.60 mmol, 60%) as a white solid. (GC yield: 71%). ¹H NMR (400 MHz, CDCl₃): δ 7.70 (s, 2H), 7.41 (d, *J* = 8.7 Hz, 2H), 7.23 (dd, *J* = 8.4, 1.6 Hz, 2H); ¹³C NMR: (100 MHz, CDCl₃) δ 154.9, 132.1, 128.1, 124.3, 120.6, 111.2, 21.5. Anal. Calcd. (%) for C₁₄H₁₂O: C, 85.68; H, 6.16. Found; C, 85.70; H, 6.20.

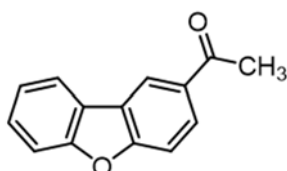


2-Chlorodibenzofuran: The mixture of 4-chlorodiphenylether (171.6 μ L, 1.0 mmol) and 20 wt% Pd(OH)₂/ZrO₂ (30 mg, Pd 6 mol%) in pivalic acid (0.7 g) was stirred under pressurized O₂ (0.5 MPa) at 130 °C for 48 h. The crude product was purified by silica-gel column chromatography (hexane:ethyl acetate = 10:1) to give 2-chlorodibenzofuran (88.7 mg, 0.44 mmol, 44%) as a white solid. (GC yield:

63%). ¹H NMR (400 MHz, CDCl₃): δ 7.91-7.89 (m, 2H), 7.56 (d, *J* = 8.2 Hz, 1H), 7.50-7.45 (m, 2H), 7.39 (dd, *J* = 8.7, 2.3 Hz, 1H), 7.35 (dd, *J* = 7.3, 7.3 Hz, 1H); ¹³C NMR (100 MHz, CDCl₃): δ 156.8, 154.6, 128.3, 128.0, 127.2, 125.8, 123.4, 123.1, 120.9, 120.6, 112.8, 112.0. Anal. Calcd. (%) for C₁₂H₇ClO: C, 71.12; H, 3.48. Found; C, 71.13; H, 3.48.



2-Nitrodibenzofuran: The mixture of 1-nitro-4-phenoxybenzene (215.2 mg, 1.0 mmol) and 20 wt% Pd(OH)₂/ZrO₂ (30 mg, Pd 6 mol%) in pivalic acid (0.7 g) was stirred under pressurized O₂ (0.5 MPa) at 140 °C for 64 h. The crude product was purified by recrystallization from the mixture of hexane and dichloromethane (1/1 v/v ratio) to obtain 2-nitrodibenzofuran as a yellow solid (111.2 mg, 0.52 mmol, 52%). (GC yield: 74%). ¹H NMR (400 MHz, CDCl₃): δ 8.83 (d, *J* = 2.3 Hz, 1H), 8.37 (dd, *J* = 6.7, 2.3 Hz, 1H), 8.00 (d, *J* = 7.4 Hz, 1H), 7.63-7.55 (m, 3H), 7.44 (dd, *J* = 7.3, 7.3 Hz, 1H); ¹³C NMR (100 MHz, CDCl₃): δ 159.2, 157.5, 143.9, 129.0, 125.1, 124.0, 123.1, 121.4, 117.2, 112.3, 112.1. Anal. Calcd. (%) for C₁₂H₇NO₃: C, 67.60; H, 3.31; N, 6.57. Found; C, 67.70; H, 3.27; N, 6.46.



1-(Dibenzofuran-2-yl)ethanone: The mixture of 1-(4-phenoxyphenyl)ethanone (212.3 mg, 1.0 mmol) and 20 wt% Pd(OH)₂/ZrO₂ (30 mg, Pd 6 mol%) in pivalic acid (0.7 g) was stirred under pressurized O₂ (0.5 MPa) at 130 °C for 48 h. The catalyst was filtered off and the crude product was purified by silica-gel column chromatography (hexane:ethyl acetate = 8:1) to give 1-(dibenzofuran-2-yl)ethanone (150.0 mg, 0.71 mmol, 71%) as a white solid. (GC yield: 84%). ¹H NMR (400 MHz, CDCl₃): δ 8.57-8.56 (m, 1H), 8.09 (ddd, *J* = 7.8, 2.7, 1.8 Hz, 1H), 7.98 (dd, *J* = 7.8, 1.8 Hz, 1H), 7.59-7.56 (m, 2 H), 7.51-7.47 (m, 1H), 7.38 (ddd, *J* = 7.4, 7.4, 0.9 Hz, 1H), 2.70 (s, 3H); ¹³C NMR (100 MHz, CDCl₃): δ 197.4, 159.0, 156.9, 132.6, 128.1, 128.1, 124.7, 123.8, 123.5, 121.7, 121.7, 112.0, 111.7, 26.9. Anal. Calcd. (%) for C₁₄H₁₀O₂: C, 79.98; H, 4.79. Found; C, 79.57; H, 4.69.

2.5 References

- [1] (a) H. Klauk, *Organic Electronics: Materials, Manufacturing and Applications*, WILEY-VCH Verlag GmbH & Co. KGaA, Weinheim, **2006**. (b) A. C. Grimsdale, K. L. Chan, R. E. Martin, P. G. Jokisz, A. B. Holmes, *Chem. Rev.*, **2009**, 109, 897–1091. (c) M. Thelakkat, H. W. Schmidt, *Adv. Mater.*, **1998**, 10, 219–223. (d) S. Yamaguchi, T. Endo, M. Uchida, T. Izumizawa, K. Furukawa, K. Tamao, *Chem. Eur. J.*, **2000**, 6, 1683–1692. (e) R. Yang, R. Tian, J. Yan, Y. Zhang, J. Yang, Q. Hou, W. Yang, C. Zhang, Y. Cao, *Macromolecules*, **2005**, 38, 244–253.
- [2] (a) L. Ying, J. Lisbscher, *Chem. Rev.*, **2007**, 107, 133–173. (b) Á. Molnár, *Chem. Rev.*, **2011**, 111, 2251–2320. (c) M. Wanger, K. Kohler, L. Djakovitch, S. Weinkauff, V. Hagen, M. Muhler, *Top. Catal.*, **2000**, 13, 319–326. (d) M. Kimura, M. Seki, *Tetrahedron Lett.*, **2004**, 45, 1635–1637; (e) Y. Mori, M. Seki, *J. Org. Chem.*, **2003**, 68, 1571–1574.
- [3] A. N. Campbell, S. S. Stahl, *Acc. Chem. Rev.*, **2002**, 102, 4303–4427.
- [4] R. van Helden, G. Verberg, *Recl. Trav. Chim. Pays-Bas*, **1965**, 84, 1263–1273.
- [5] T. A. Dwight, N. R. Rue, D. Charyk, R. Jossenlyn, B. DeBoef, *Org. Lett.*, **2007**, 9, 3137–3139.
- [6] B. J. Li, S. L. Tian, Z. Fang, Z. J. Shi, *Angew. Chem. Int. Ed.*, **2008**, 47, 1115–1118.
- [7] (a) A. M. A. G. Oliveira, M. M. M. Raposo, A. M. F. Oliveira-Campos, A. E. H. Machado, P. Puapairoj, M. Pedro, M. S. J. Nascimento, C. P. C. Afonso, M. Pinto, *Eur. J. Med. Chem.*, **2006**, 41, 367–372. (b) Y. Ye, H. Koshino, J. Onose, K. Yoshikawa, N. Abe, S. Takahashi, *Org. Lett.*, **2009**, 11, 5074–5077.
- [8] H. Sasabe, J. Takamatsu, T. Motoyama, S. Watanabe, G. Wagenblast, N. Langer, O. Molt, E. Fuchs, J. Kido, *Adv. Mater.*, **2010**, 22, 5003–5007.
- [9] L. Campeau, M. Parisien, A. Jean, K. Fagnou, *J. Am. Chem. Soc.*, **2006**, 128, 581–590.
- [10] B. Xiao, T. Gong, Z. Liu, J. Liu, D. Luo, J. Xu, L. Liu, *J. Am. Chem. Soc.*, **2011**, 133, 9250–9253.
- [11] B. Liégault, D. Lee, M. P. Huestis, D. R. Stuart, K. Fagnou, *J. Org. Chem.*, **2008**, 73, 5022–5028.
- [12] T. Watanabe, S. Oishi, N. Fujii, H. Ohno, *J. Org. Chem.*, **2009**, 74, 4720–4726.
- [13] S. Wang, H. Mao, Z. Ni, Y. Pan, *Tetrahedron Lett.*, **2012**, 53, 505–508.
- [14] S. S. Soomro, F. L. Ansari, K. Chatziapostolou, K. Köhler, *J. Catal.*, **2010**, 273, 138–146.
- [15] (a) H. Yoshida, T. Nakajima, Y. Yazawa, T. Hattori, *Appl. Catal. B: Environ.*, **2007**, 71, 70–79. (b) R. Yoshimoto, T. Ninomiya, K. Okumura, M. Niwa, *Appl. Catal. B: Environ.*, **2007**, 75, 175–181. (c) X. Guo, M. Meng, F. Dai, Q. Li, Z. Zhang, Z. Jiang, S. Zhang, Y. Huang, *Appl. Catal.*

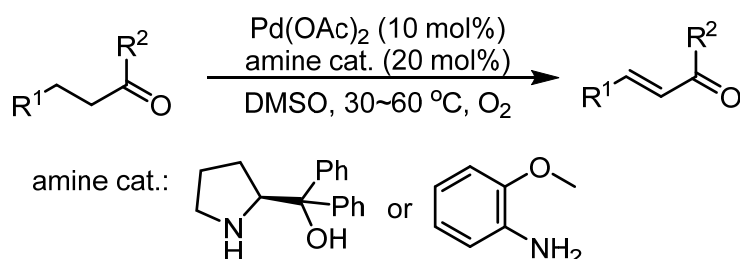
- B: Environ.*, **2013**, 142–143, 278–289. (d) M. Ren, Y. Kang, W. He, Z. Zou, X. Xue, D. L. Akins, H. Yang, S. Feng, *Appl. Catal. B: Environ.*, **2011**, 104, 49–53.
- [16] T. Ishida, R. Tsunoda, Z. Zhang, A. Hamasaki, T. Honma, H. Ohashi, T. Yokoyama, M. Tokunaga, *Appl. Catal. B: Environ.*, **2014**, 150–151, 523–531.
- [17] Y. We, N. Yoshikai, *Org. Lett.* **2011**, 13, 5504–5507.
- [18] (a) T. Honma, H. Oji, S. Hirayama, Y. Taniguchi, H. Ofuchi, M. Takagaki, *AIP Conf. Proc.*, **2010**, 1234, 13–16. (b) H. Oji, Y. Taniguchi, S. Hirayama, H. Ofuchi, M. Takagaki, T. Honma, *J. Synchrotron Rad.*, **2012**, 19, 54–59.
- [19] B. Ravel, M. Newville, *J. Synchrotron Rad.*, **2005**, 12, 537–541.

Chapter 3.

Aerobic oxidation of cyclohexanones to cyclic enones, phenols and aryl ethers over supported palladium catalysts

3.1 Introduction

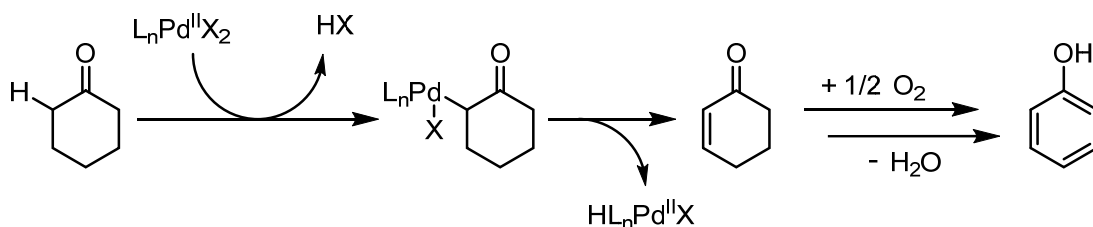
Enones, which are one kinds of unsaturated chemical compounds consisting of a conjugated structure with a C–C double bond and a carbonyl group, were widely used in organic synthesis such as Michael addition¹ and Rauhat-Currier reaction². Dehydrogenation of aldehydes and ketones to synthesize enones is recognized as a convenient and useful method.³ Since Ito and Saegusa first reported the transformation of silyl enol ethers to the corresponding enones in 1978,⁴ the Saegusa-type reactions have been studied intensely, and a catalytic system using Pd(OAc)₂ with molecular oxygen as the oxidant has been developed.⁵ However, the aldehydes or ketones must be pretreated into silyl enol ethers before attempting the reaction. Therefore, a direct aerobic oxidation of aldehydes and ketones to enones would be of great interest. Li and Wang reported a direct oxidation of aldehyde to the corresponding enones with moderate yields in the presence of Pd(OAc)₂/amine (Scheme 3.1).⁶ In their reaction, the enamine was formed from the aldehyde substrate, and then coordinated with Pd(OAc)₂ lead to a Pd–alkene complex, which was converted to a palladium adduct subsequently. The enone product was generated from β-hydride elimination and hydrolysis of iminium intermediate.



Scheme 3.1 Pd(OAc)₂/amine catalyzed direct Saegusa reaction reported by Wang and co-workers.

On the other hand, based on the broad applications in polymer production and organic synthesis,^{7,8} cyclic enones and phenols have also been studied extensively using homogeneous Pd catalysts through the aerobic oxidation of cyclohexanones.^{9,10} For instance, Tokunaga and co-workers developed a Pd(TFA)₂/bipy catalytic system for synthesizing cyclohexenones from cyclohexanones with a yield of up to 84%.^{9a} In that report, phenol was partly formed as a by-product. Stahl and co-workers reported the oxidative dehydrogenation of cyclohexanones over Pd(DMSO)₂(TFA)₂ and Pd(TFA)₂/2-dimethylaminopyridine (2-Me₂Npy) catalytic systems to produce cyclohexenones^{9c} and phenols^{10b}, respectively. In general, the cyclic enones and phenols were formed by a Pd^{II}-catalyzed α-hydrogen activation of cyclohexanones followed by β-hydride elimination or further dehydrogenation,

and oxygen was used to re-oxidize the Pd⁰ species (Scheme 3.2). Stahl concluded that DMSO inhibited to form Pd black, and soluble Pd^{II} species was highly active for the oxidation of cyclohexanone to cyclohexenone.^{9d,11} In contrast, soluble Pd nanoparticles (NPs) were formed in Pd(TFA)₂/2-Me₂Npy system, and they were more active for the oxidation of cyclohexenone to phenol than Pd^{II} species.^{10c} Although Pd NP-mediated oxidation of cyclohexanones to phenols has been proposed, active catalysts are limited to pseudo-homogeneous Pd NPs. Heterogeneous catalysts, such as Pd/C, has not yet been scarcely reported for this reaction in spite of their advantages, such as easy catalyst separation and recyclability.

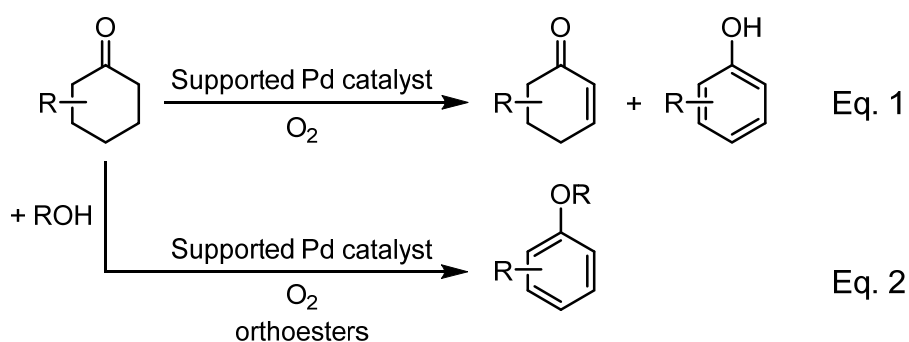


Scheme 3.2 Proposed mechanism for Pd-catalyzed dehydrogenation of cyclohexanone reported by Stahl and co-workers.

Aryl ethers are also one kind of important compounds for organic synthesis¹² and are usually obtained via the Williamson ether synthesis¹³ or Ullmann coupling reactions¹⁴. However, both these methods generally use halogen-containing substrates and need a stoichiometric amount of base to promote the reaction. Li and co-workers reported a method to prepare aryl ethers from cyclohexanones catalyzed by homogeneous Cu catalysts in the presence of N-hydroxyphthalimide (NHPI) as a co-catalyst.¹⁵ Since cyclohexenones can be obtained by Pd-catalyzed aerobic oxidation of cyclohexanones, direct transformation of aryl ethers from cyclohexanones is more simple and straightforward. Lemaire et al. recently reported the synthesis of aryl ethers from cyclohexanones over Pd/C.¹⁶ The proposed mechanism involved activation of the carbonyl group in cyclohexanone by Pd, followed by reaction with alcohols to form the hemiacetal intermediate. Elimination of the hemiacetal to enol ethers and subsequent dehydrogenation yielded the aryl ethers. In this case, alcohols were limited to those having high boiling points (>100°C), and simple alcohols, such as methanol and ethanol were not described.

Recently, we have reported a method for synthesizing carbazole and its derivatives from diphenylamines over Pd(OH)₂/ZrO₂ under oxidative reaction conditions.¹⁷ This heterogeneous catalyst

exhibited good catalytic activity for C–H bond functionalization. In this chapter, with supported Pd catalysts, aerobic oxidation of cyclohexanones to synthesize cyclic enones and phenols is studied (Scheme 3.3, Eq. 1). Moreover, preparation of aryl ethers from cyclohexanones in simple alcohols is developed over supported Pd catalysts with orthoesters, such as trimethyl orthoformate (TMOF) and triisopropyl orthoformate (TIPOF) (Eq. 2).



Scheme 3.3 Selective oxidation of cyclohexanones over supported Pd catalysts.

3.2 Results and discussion

3.2.1 Catalysts preparation and characterization

TiO₂, Al₂O₃, CeO₂, and ZrO₂, supported Pd(OH)₂ catalysts were prepared by the DP method¹⁸ as introduced in Chapter 2. Metal oxide supported PdO and Pd catalysts were prepared from supported Pd(OH)₂ catalysts by calcination in air and reduction with pure H₂, respectively. HAADF-STEM image of 10 wt% Pd(OH)₂/ZrO₂ revealed that Pd(OH)₂ NPs were well dispersed on the surface of ZrO₂, and the mean diameter was calculated to be 1.8 ± 0.9 nm (Figure 3.1). On the other hand, HAADF-STEM image of 10 wt% Pd/ZrO₂ showed that Pd NPs were aggregated to large particles during the H₂ reduction at 200 °C (Figure 3.2).

Characterization of supported Pd catalysts was performed by XAFS.¹⁹ To identify the chemical state of Pd in supported Pd(OH)₂ and Pd catalysts, Pd *K*-edge XANES spectra was measured (Figure 3.3). As we have previously reported, the chemical state of Pd in Pd(OH)₂/ZrO₂ and Pd/ZrO₂ were confirmed to be Pd^{II} and Pd⁰, respectively. In the RSF (Figure 3.4), two peaks were also observed at 1.5 and 2.9 Å (phase-uncorrected) in PdO, and these peaks corresponded to Pd–O interaction of the first coordination shell and Pd–Pd interaction of the second one, respectively. Due to the fact that both of Pd–Pd and Pd–O interactions were small as well as reference of Pd(OH)₂, Pd(OH)₂ might be present

in Pd(OH)₂/ZrO₂ as major species, although the formation of PdO could not be fully excluded by XAFS.¹⁷

The acidity and basicity of 10 wt% Pd/ZrO₂ were tested by temperature-programmed desorption of ammonia (NH₃-TPD) and temperature-programmed desorption of carbon dioxide (CO₂-TPD), respectively. However, due to the high desorption temperature of ammonia for ZrO₂, the difference of acidity between ZrO₂ and Pd/ZrO₂ could not be identified directly. In CO₂-TPD (Figure 3.5), CO₂ desorption peak was observed at 90 °C for both ZrO₂ and Pd/ZrO₂. Two broad peaks of Pd/ZrO₂, which were not observed in the profile of ZrO₂, were observed at about 290 and 420 °C (Figure 3.5b), indicating that the basicity of ZrO₂ was enhanced after deposition of Pd particles.

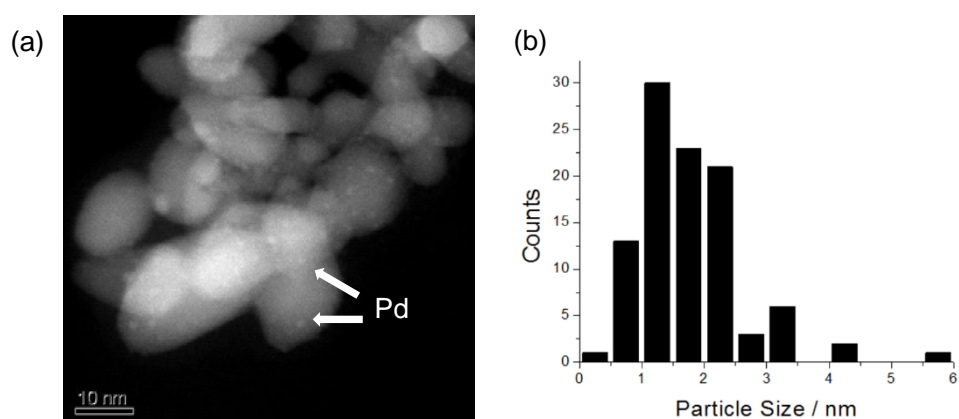


Figure 3.1 (a) HAADF-STEM image of 10 wt% Pd(OH)₂/ZrO₂ and (b) the size distribution of Pd(OH)₂.

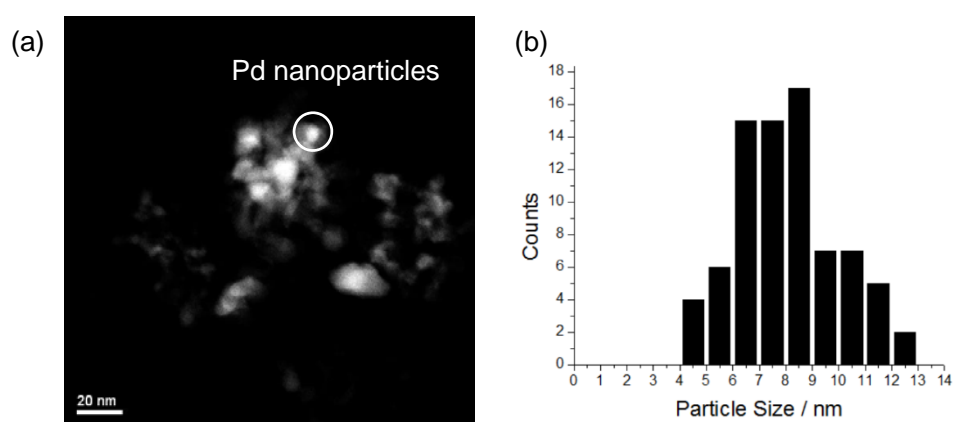


Figure 3.2 (a) HAADF-STEM image of 10 wt% Pd/ZrO₂, (b) the size distribution of Pd nanoparticles.

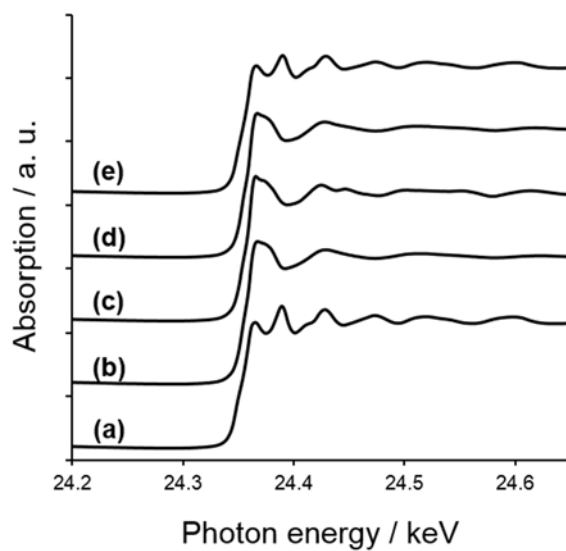


Figure 3.3 Pd K-edge XANES spectra of (a) Pd foil, (b) Pd(OH)₂, (c) PdO, (d) 10 wt% Pd(OH)₂/ZrO₂ and (e) 10 wt% Pd/ZrO₂.

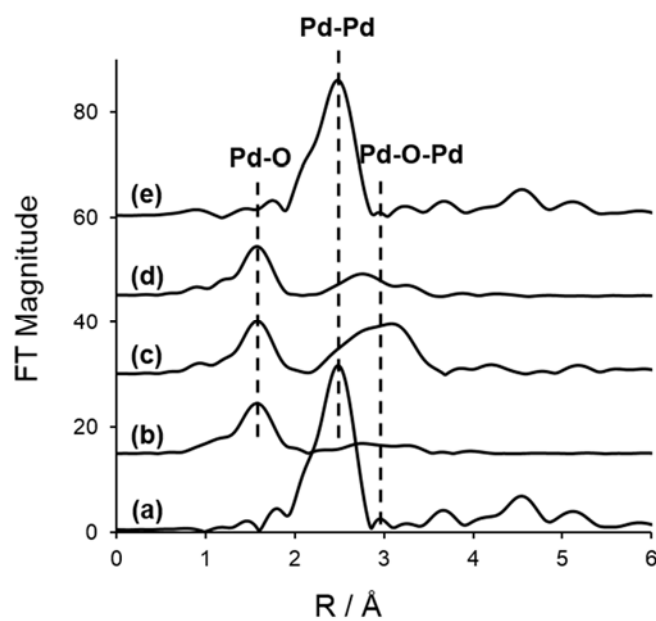


Figure 3.4 Radial structure functions of (a) Pd foil, (b) Pd(OH)₂, (c) PdO, (d) 10 wt% Pd(OH)₂/ZrO₂ and (e) 10 wt% Pd/ZrO₂.

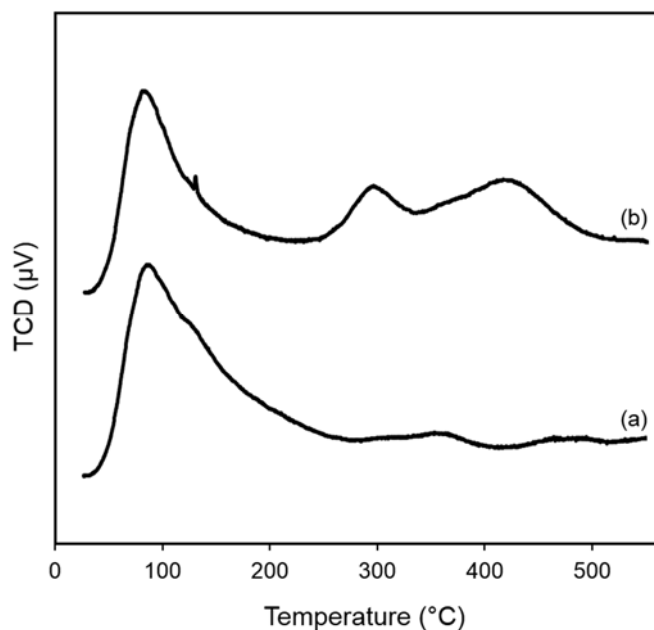


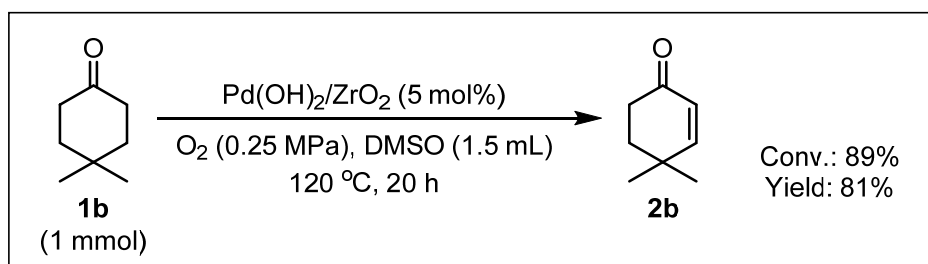
Figure 3.5 CO₂-TPD profiles of (a) ZrO₂ and (b) 10 wt% Pd/ZrO₂.

3.2.3 Synthesis of cyclohexenones and phenols

Catalytic performance of supported Pd(OH)₂ was evaluated by the transformation of cyclohexanone into cyclohexenone and phenol (Table 3.1). Initially, several metal oxide supported Pd(OH)₂ catalysts were screened in DMSO (Table 3.1, entries 1–4). Among these catalysts, the basic metal oxide (CeO₂) and the relatively acidic metal oxide (TiO₂) supported Pd(OH)₂ showed lower catalytic activity than amphoteric metal oxides (Al₂O₃ and ZrO₂) as the support. However, the selectivity to enone and phenol over Pd(OH)₂/Al₂O₃ was lower than Pd(OH)₂/ZrO₂. Thus, ZrO₂ was selected as a suitable support. Other solvents such as 1,4-dioxane, EtOAc, toluene, and PhCl were also investigated for the reaction with supported Pd(OH)₂ catalysts, whereas the selectivity to cyclohexenone or phenol were found to be unsatisfactory (Table 3.1, entries 5–10). When the catalytic amount of Pd decreased from 5 mol% to 2 mol%, the selectivity to cyclohexenone was increased to 26% yield (Table 3.1, entry 11). When Pd(OH)₂/ZrO₂ was reduced to Pd/ZrO₂ using H₂, the selectivity for phenol was improved (Table 3.1, entry 12). Decreasing the reaction temperature improved the cyclohexenone yield to 34% (Table 3.1, entry 13). Although I tried to improve the selectivity of cyclohexenone, further oxidation of cyclohexanone to phenol could not be avoided. Only exception is 4,4-dimethylcyclohexenone (**2b**) which was obtained in 81% yield, due to the absence of hydrogen atom at 4-position (Scheme 3.4). In this case, 4,4-dimethylcyclohexa-2,5-dien-1-one was not formed,

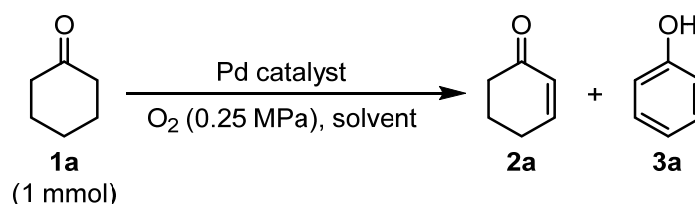
suggesting that the second oxidation to dienone did not proceed when the substrate cannot be aromatized.

Then I focused on the synthesis of phenol. Selectivity of phenol was significantly affected by the pressure of O₂. Neither cyclohexenone nor phenol was obtained under atmospheric pressure of O₂ (Table 3.1, entry 14), and an increase in O₂ pressure to 0.5 MPa gave phenol in excellent yield to 99% (Table 3.1, entry 15).



Scheme 3.4 Synthesis of 4,4-dimethylcyclohexenone from 4,4-dimethylcyclohexanone over Pd(OH)₂/ZrO₂.

Table 3.1 Synthesis of phenol from cyclohexanone.^a



Entry	Catalyst	Solvent	Temp. (°C)	Time (h)	Conv. (%) ^b	Yield of 2a (%) ^b	Yield of 3a (%) ^b
1	Pd(OH) ₂ /Al ₂ O ₃	DMSO	120	8	99	8	18
2	Pd(OH) ₂ /CeO ₂	DMSO	120	15	44	7	22
3 ^c	Pd(OH) ₂ /TiO ₂	DMSO	120	20	70	7	25
4	Pd(OH) ₂ /ZrO ₂	DMSO	120	15	90	15	38
5	Pd(OH) ₂ /Al ₂ O ₃	1,4-dioxane	120	20	66	17	25
6	Pd(OH) ₂ /CeO ₂	1,4-dioxane	120	24	83	22	16
7	Pd(OH) ₂ /ZrO ₂	1,4-dioxane	120	20	49	16	14
8	Pd(OH) ₂ /ZrO ₂	EtOAc	120	24	89	4	27
9	Pd(OH) ₂ /ZrO ₂	Toluene	120	24	40	2	16
10	Pd(OH) ₂ /ZrO ₂	PhCl	120	24	25	4	1

11 ^d	Pd(OH) ₂ /ZrO ₂	DMSO	120	15	73	26	40
12	Pd/ZrO ₂	DMSO	120	15	86	12	54
13	Pd/ZrO ₂	DMSO	100	24	81	34	36
14 ^e	Pd/ZrO ₂	DMSO	100	24	7	1	0
15 ^f	Pd/ZrO ₂	DMSO	100	24	100	<1	99

^a Reaction conditions: cyclohexanone (1 mmol), catalyst (Pd 5 mol%), solvent (2.0 mL), O₂ (0.25 MPa).

^b Calculated on the basis of GC analysis using tridecane as an internal standard.

^c Catalyst (Pd 8 mol%).

^d Catalyst (Pd 2 mol%).

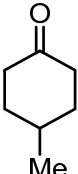
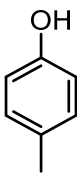
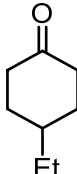
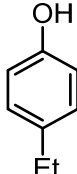
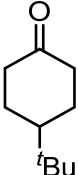
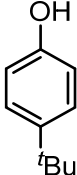
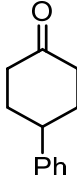
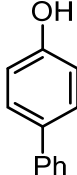
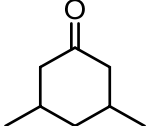
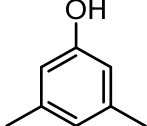
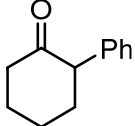
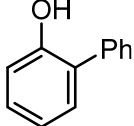
^e O₂ (1.0 atm). ^f O₂ (0.5 MPa).

Next, the scope of substrates for phenol synthesis was examined (Table 3.2). For methyl substituted cyclohexanones, the corresponding phenols were obtained in good to excellent yield (Table 3.2, entries 1–3); the reactivity order was 4- > 3- > 2-substituted cyclohexanones, and this might be ascribed to the steric effect on 3- and 2-substituted cyclohexanones for further oxidation to cyclohexa-2,5-dien-1-ones, which was considered to be formed faster than cyclohexa-2,4-dien-1-one as an intermediate before phenol formation. Other 4-substituted cyclohexanones were also tested (Table 3.2, entries 4–6). 4-Ethylcyclohexanone (**1f**) and 4-*t*-butylcyclohexanone (**1g**) exhibited excellent reactivity to form the corresponding phenols. 4-Phenylcyclohexanone (**1h**) was transformed to 4-phenylphenol (**3h**) in 82% yield by using high loading Pd catalyst. Low reactivity was observed in 3,5-dimethylcyclohexanone (**1i**) (Table 3.2, entry 7). 2-Phenyl substituted cyclohexanone (**1j**) were examined (Table 3.2, entry 8), but this compound showed poor reactivity.

Table 3.2 Substrate scope for synthesis of substituted phenols from cyclohexanones.^a

Reaction scheme: A substituted cyclohexanone (1 mmol) reacts with Pd/ZrO₂ (5 mol%), O₂ (0.5 MPa), and DMSO at 100 °C for 24 h to produce a substituted phenol.

Entry	Substrate	Product	Yield (%) ^b	Entry	Substrate	Product	Yield (%) ^b
1			63	2			78

3			99	4			99
	1e	3e			1f	3f	
5			99	6 ^c			82
	1g	3g			1h	3h	
7			13	8			46
	1i	3i			1j	3j	

^a Reaction conditions: substrate (1 mmol), 10 wt% Pd/ZrO₂ (Pd 5 mol%), DMSO (2.0 mL), O₂ (0.5 MPa).

^b Calculated on the basis of GC analysis using tridecane as an internal standard.

^c Catalyst (Pd 8 mol%).

In order to elucidate the chemical state of Pd for the synthesis of phenol, the Pd/ZrO₂ catalyst was tested by Pd *K*-edge XANES before and after the reaction, and the chemical states of Pd both on the fresh and the recycled catalysts were confirmed to be Pd⁰ (Figure 3.6a). In RSF of Pd/ZrO₂ after use, magnitude of the peak at 2.5 Å, which corresponds to the Pd–Pd bond as seen in Pd foil, decreased as compared to fresh catalyst (Figure 3.6b). In the *k*³-weighted EXAFS oscillations, the amplitude of the catalyst after reaction was also lower than the fresh catalyst (Figure 3.6c). This result indicated that possibility of the Pd NPs size was decreased during the reaction. Additionally, in the X-ray diffraction (XRD) patterns of fresh Pd/ZrO₂, the diffraction peaks at 40, 46 and 68° were assigned to (111), (200), and (220) crystalline planes of the face-centered cubic (*fcc*) lattice of Pd (PDF-2 Database, No. 01-087-0645) (Figure 3.7a). In contrast, these diffraction peaks were not present in the XRD patterns of the used Pd/ZrO₂ (Figure 3.7b). These results suggest that Pd was dissolved into the solution during the reaction and was re-deposited on ZrO₂ as small Pd NPs. The microwave plasma-atomic emission spectrometry (MP-AES) analysis result demonstrated that only 0.6 wt% Pd was lost from the fresh catalyst (Table 3.3). Although the reaction would proceed via quasi-homogeneous catalysis, most of Pd could be recovered after the reaction as supported catalysts. In addition, the

recyclability of Pd/ZrO₂ for synthesis of phenol was studied. Although the yield of phenol was slightly decreased at the fourth run, the catalyst showed good recyclability (Figure 3.8).

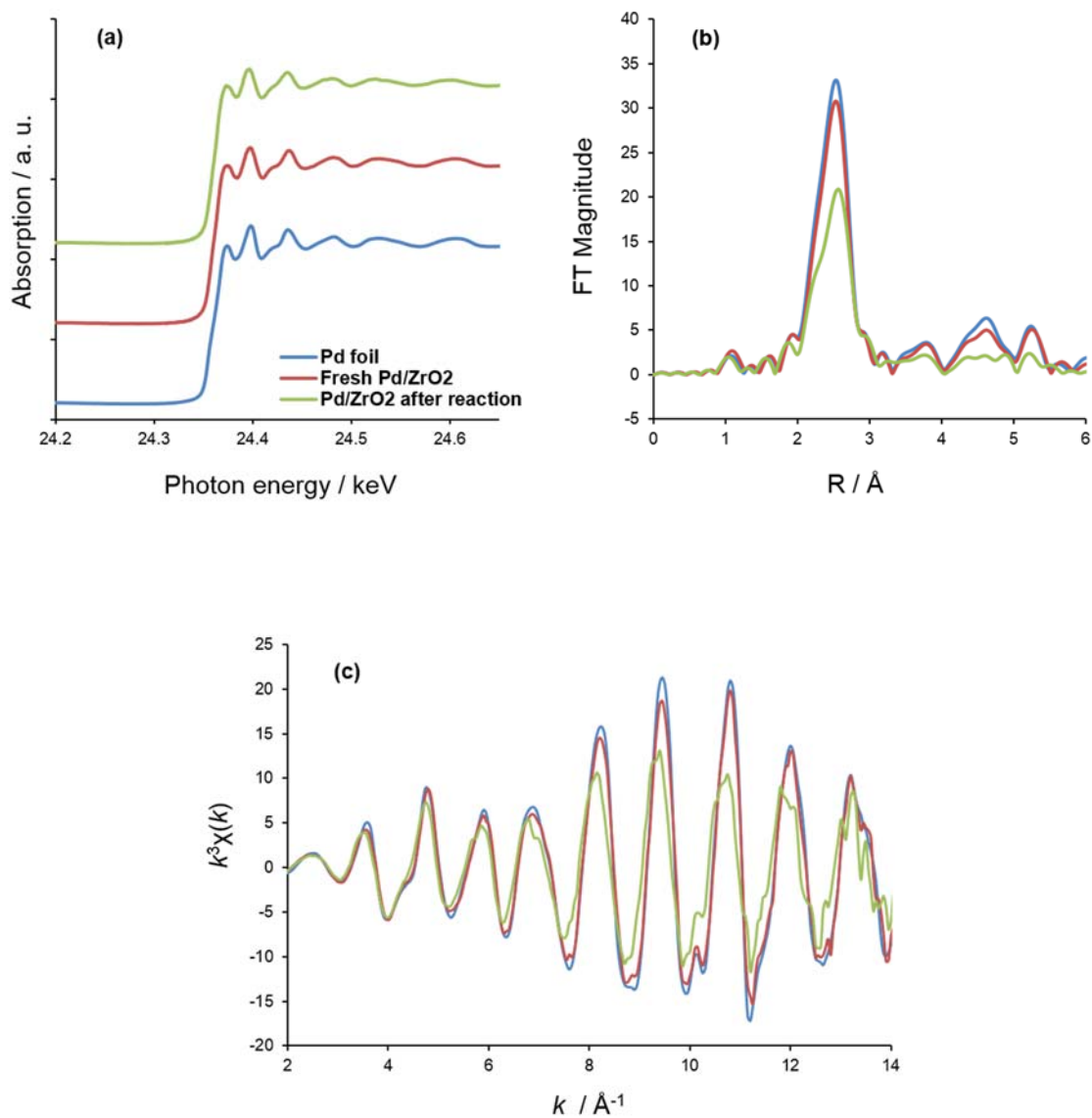


Figure 3.6 XAFS results of 10 wt% Pd/ZrO₂ after the synthesis of phenol (green) including fresh 10 wt% Pd/ZrO₂ (red) and Pd foil (blue) for comparison; (a) XANES spectra, (b) radial structure functions, and (c) k^3 -weighted EXAFS.

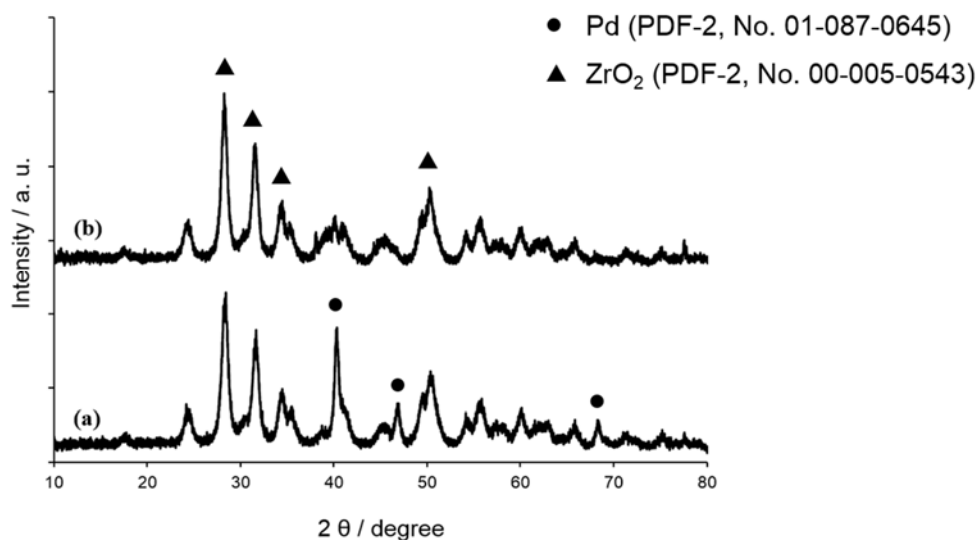


Figure 3.7 XRD patterns of (a) fresh 10 wt% Pd/ZrO₂, (b) 10 wt% Pd/ZrO₂ after reaction.

Table 3.3 Pd content of the fresh Pd/ZrO₂ catalyst and the catalyst after synthesis of phenol^a.

10 wt% Pd/ZrO ₂	Pd (wt%)
Fresh catalyst	9.7
After synthesis of phenol	9.1

^a Reaction condition: cyclohexanone (1 mmol), 10 wt% Pd/ZrO₂ (50 mg, Pd 5 mol%), DMSO (2.0 mL), O₂ (0.5 MPa), 100 °C, 24 h.

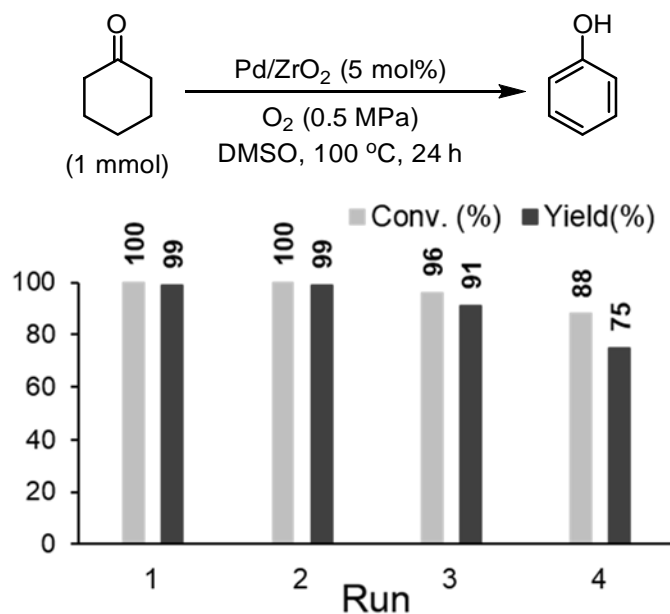


Figure 3.8 Recyclability of Pd/ZrO₂ in phenol synthesis.

The proposed reaction pathway for the synthesis of phenol over Pd/ZrO₂ is displayed in Figure 3.9. Firstly, Pd particles on Pd/ZrO₂ are dissolved into the solution, and are stabilized by DMSO. These dissolved Pd particles react with cyclohexanone to form a Pd-enolate (**A1** or **A2**). Then, intermediate **B** is generated after transfer of hydrogen atom to Pd. Cyclohexenone, which is formed followed by Pd dihydride species leave from substrate, can be further oxidized by Pd particles and O₂ to produce phenol as the final product. Simultaneously, Pd dihydride species is re-oxidized by O₂ and H₂O to form the Pd⁰ species again. After the reaction, these Pd⁰ species are re-deposited on the surface of ZrO₂.

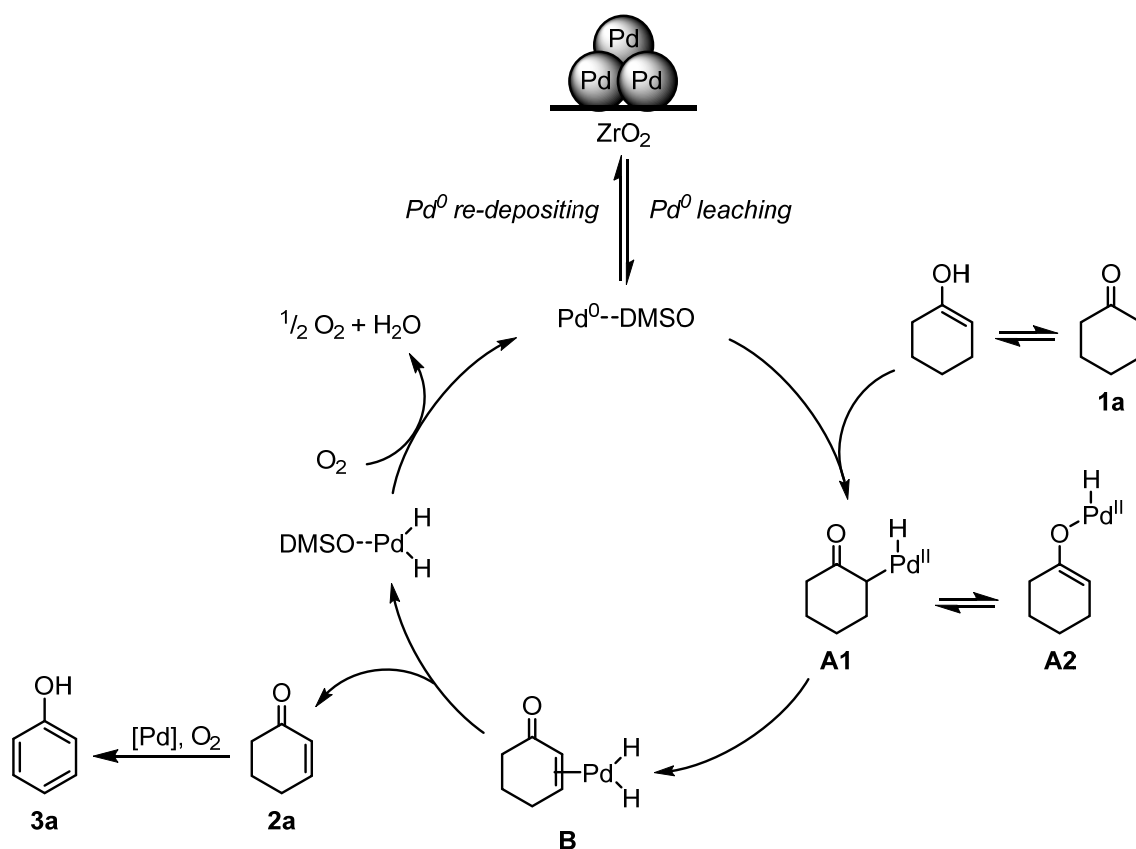


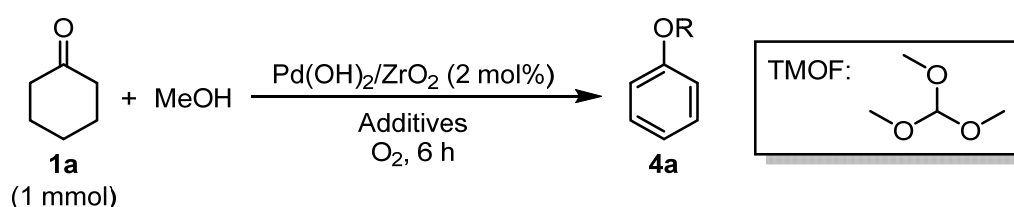
Figure 3.9 Plausible reaction pathway for the synthesis of phenol over Pd/ZrO₂.

3.2.3 Synthesis of aryl ethers

The reaction of cyclohexanone and methanol into anisole was explored under oxidative conditions. In the absence of additives, the reaction proceeded over 2 mol% Pd(OH)₂/ZrO₂ at 140 °C to afford anisole in 37% yield (Table 3.4, entry 1). Several additives such as Na₂SO₄ and molecular

sieve 4Å were added as dehydrating reagent, but the conversion decreased markedly (Table 3.4, entries 2 and 3). However, the reaction proceeded very well, yielding anisole in 66% yield, when using trimethyl orthoformate (TMOF) as the additive (Table 3.4, entry 4). The reaction also proceeded in the absence of methanol to form anisole (Table 3.4, entry 5). TMOF, which is commonly used for introduction of a protecting group in aldehydes, worked as both dehydrating and nucleophilic reagents during the reaction. After the optimization of reaction conditions, 96% yield of anisole was achieved under the following reaction conditions: 0.5 MPa of O₂, at 140 °C for 6 h (Table 3.4, entry 6). ZrO₂ supported PdO and Pd catalysts also promoted this reaction to give anisole in good yields (Table 3.4, entries 7 and 8).

Table 3.4 Synthesis of anisole from cyclohexanone.^a



Entry	Catalyst	MeOH (eq)	Additive (eq)	O ₂ (MPa)	Conv. (%) ^b	Yield (%) ^b
1	Pd(OH) ₂ /ZrO ₂	40	--	0.25	100	37
2	Pd(OH) ₂ /ZrO ₂	40	Na ₂ SO ₄ (0.5)	0.25	19	0
3	Pd(OH) ₂ /ZrO ₂	40	MS 4Å ^c	0.25	23	2
4	Pd(OH) ₂ /ZrO ₂	40	TMOF (9)	0.25	100	66
5	Pd(OH) ₂ /ZrO ₂	--	TMOF (14)	0.25	91	70
6 ^d	Pd(OH) ₂ /ZrO ₂	--	TMOF (14)	0.5	100	96
7 ^d	PdO/ZrO ₂ ^e	--	TMOF (14)	0.5	100	92
8 ^d	Pd/ZrO ₂ ^f	--	TMOF (14)	0.5	100	78

^a Reaction conditions: cyclohexanone (1 mmol), Pd(OH)₂/ZrO₂ (Pd 2 mol%), MeOH, additives, O₂ (0.5 MPa).

^b Calculated on the basis of GC analysis using tridecane as an internal standard.

^c Molecule sieve 4Å (100 mg) was added.

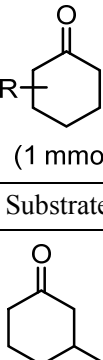
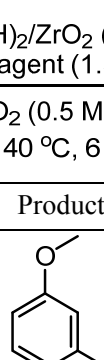
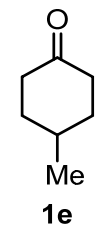
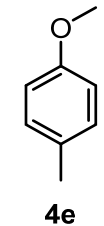
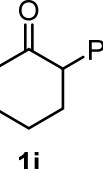
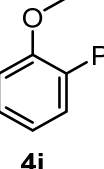
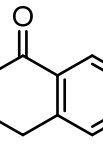
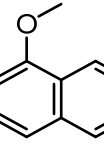
^d O₂ (0.5 MPa)

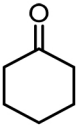
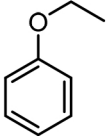
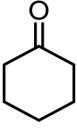
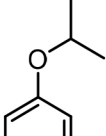
^e Catalyst was calcined at 300 °C for 4 h from Pd(OH)₂/ZrO₂.

^f Catalyst was reduced by H₂ (20 mL/min) at 200 °C for 2 h from Pd(OH)₂/ZrO₂.

With the optimized reaction conditions in hand, several substituted cyclohexanones were investigated. Methyl (**1d** and **1e**) and phenyl (**1j**) substituted cyclohexanones were transformed into their corresponding aryl ethers in moderate yields (Table 3.5, entries 1–3). 1-Tetralone (**1k**), which contains a benzocyclohexanone structure, exhibited better reactivity than other substrates and gave 1-methoxynaphthalene (**4k**) in 78% yield (Table 3.5, entry 4). Moreover, other orthoester reagents, including triethyl orthoformate (TEOF) and triisopropyl orthoformate (TIPOF), could be used instead of TMOF. Ethoxybenzene and isopropoxybenzene were obtained as the products in 49 and 11% yield, respectively (Table 3.5, entries 5 and 6). Relatively low product yields compared to high conversion were due to the formation of phenols as by-products.

Table 3.5 Scope of substrates for synthesis of aryl ethers.^a

Entry	Substrate	R'	Product	Conv. (%) ^b	Yield (%) ^b
1	 1d	Me	 4d	91	66
2	 1e	Me	 4e	85	45
3	 1i	Me	 4j	100	22
4	 1k	Me	 4k	95	78

5		Et		92	49
6		<i>i</i> Pr		79	11

^a Reaction conditions: substrate (1 mmol), Pd(OH)₂/ZrO₂ (2 mol%), orthoester reagent (1.5 mL), O₂ (0.5 MPa), 140 °C for 6 h.

^b Calculated on the basis of GC analysis using tridecane as an internal standard.

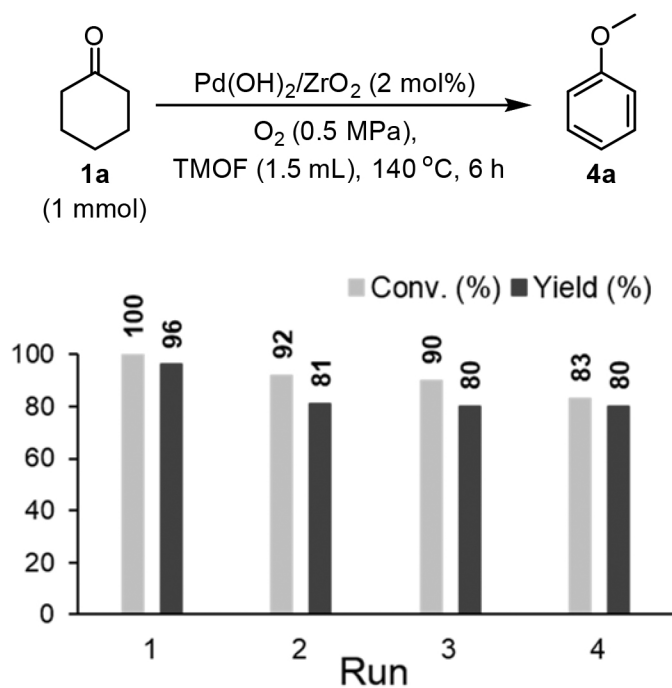


Figure 3.10 Recyclability of Pd(OH)₂/ZrO₂ for synthesis of anisole.

Next, the recyclability of the catalyst in anisole synthesis was tested (Figure 3.10). Although the catalytic activity was gradually decreased with consecutive runs, 80% yield was maintained for the fourth run. The reasons for the decrease in the catalytic activity were probably due to the leaching of Pd and/or aggregation of Pd species. Consequently, the reaction solution was measured by MP-AES, and the concentration of residual Pd in the solution after filtration was determined to be 1.33 ppm (in

1.5 mL TMOF). Moreover, after the removal of the catalyst by filtration at 42% conversion, the reaction of the filtrate stopped (Figure 3.11). These results proved that the loss of Pd could not be the cause of the decrease in catalytic activity.

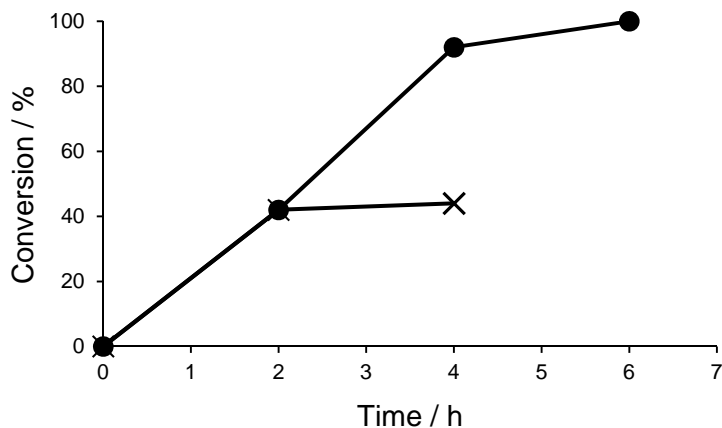
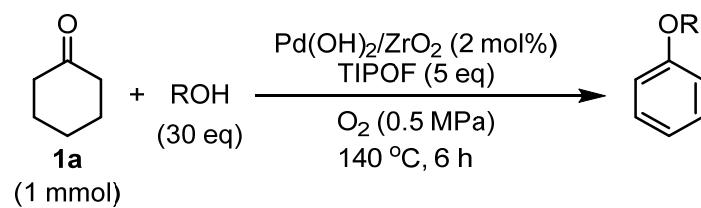
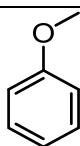
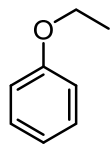
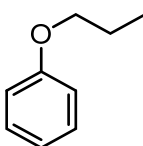
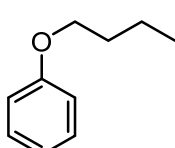
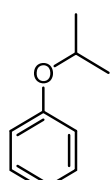
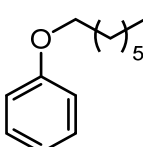
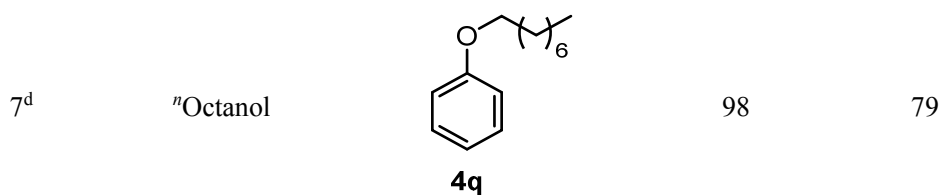


Figure 3.11 Synthesis of anisole from cyclohexanone in the presence of Pd(OH)₂/ZrO₂ (●) and after the removal of Pd(OH)₂/ZrO₂ at 2 h by filtration (×). Reaction conditions: cyclohexanone (1 mmol), 10 wt% Pd(OH)₂/ZrO₂ (20 mg Pd 2 mol%), TMOF (1.5 mL), O₂ (0.5 MPa), 140 °C.

Since TIPOF possesses lower reactivity to produce the isopropoxybenzene than TMOF and TEOF, I considered that TIPOF could be used as a dehydrating reagent in the presence of the alcohols to synthesize aryl ethers without the formation of isopropoxybenzene (Table 3.6). The ratio of alcohols and TIPOF was optimized to 6:1. In entry 1, anisole was obtained in 74% yield, which was lower than the yield obtained using only TMOF. For other primary alcohols, such as ethanol, propanol, and butanol were evaluated (Table 3.6, entries 2–4). The corresponding products, ethoxybenzene, propoxybenzene, and butoxybenzene, were obtained in good yields, and only small amounts of isopropoxybenzene and phenol (4–11% yield) were detected as by-products. This reaction also proceeded with 2-propanol to produce isopropoxybenzene (Table 3.6, entry 5), although the reaction only gave **4o** in 23% yield due to the steric hindrance in the formation of the acetal intermediate. Furthermore, higher alcohols, such as *n*-heptanol and *n*-octanol, were also employed, and the corresponding aryl ethers were afforded in good yields (Table 3.6, entries 6 and 7).

Table 3.6 Synthesis of aryl ethers from cyclohexanone with alcohols.^a

Entry	ROH	Product	Conv. (%) ^b	Yield (%) ^b
1	MeOH	 4a	100	74
2 ^c	EtOH	 4l	100	83
3	ⁿ PrOH	 4m	100	76
4	ⁿ BuOH	 4n	91	73
5	ⁱ PrOH	 4o	51	23
6 ^d	ⁿ Heptanol	 4p	95	78



^a Reaction conditions: cyclohexanone (1 mmol), Pd(OH)₂/ZrO₂ (2 mol%), ROH (30 eq), TIPOF (5 eq.), O₂ (0.5 MPa), 140 °C for 6 h.

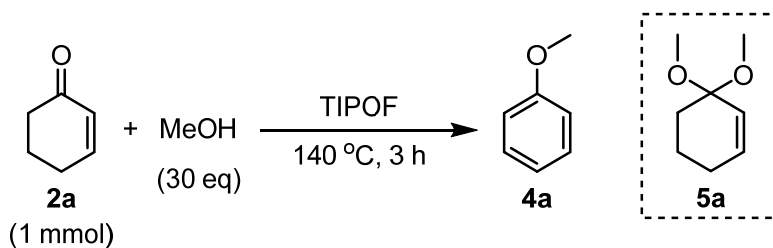
^b Calculated on the basis of GC analysis using tridecane as an internal standard.

^c Reacted at 8 h.

^d Alcohol (15 eq).

3.2.4 Possible reaction pathway

Table 3.7 Synthesis of anisole started from cyclohexenone.^a



Entry	ZrO ₂	TIPOF (eq)	Gas (MPa)	Yield (%) ^a
1	20 mg	5	O ₂ (0.5)	77
2	--	5	O ₂ (0.5)	35
3	--	--	O ₂ (0.5)	0
4	--	5	N ₂ (0.1)	0

^a Calculated on the basis of GC analysis using tridecane as an internal standard.

In order to investigate the reaction pathway for the synthesis of aryl ethers, several experiments were performed by using cyclohexenone (**2a**) as the starting material in the absence of Pd (Table 3.7). When both TIPOF and ZrO₂ were used in this process, the reaction proceeded efficiently, affording the anisole (**4a**) with a good yield in 2 h (Table 3.7, entry 1). Due to orthoesters can facilitate the formation of acetals from aldehydes and ketones, a comparative test was carried out (Table 3.7, entry 2) using the reaction conditions as entry 1 in absence of ZrO₂. The anisole yield was slightly decreased, indicating that ZrO₂ is required for this reaction. Since ZrO₂ has both Lewis acid and base sites, it could be assumed that ZrO₂ acted as a Lewis acid to promote the formation of the acetal intermediate

and/or as a Lewis base for the production of anisole by eliminations. Additionally, cyclohexenone did not react with methanol in the absence of ZrO₂ and TIPOF (Table 3.7, entry 3). Also, molecular oxygen was appeared to be essential to produce aryl ethers, because only dimethylacetal (**5a**) was detected under N₂ atmosphere (Table 3.7, entry 4).

The proposed reaction pathway for the synthesis of cyclohexenone, phenol, and aryl ethers is presented in Figure 3.12. The mechanism for the synthesis of cyclohexenone (**2a**) from cyclohexanone (**1a**) has been studied in previous reports.^{9c,10b} Similarly, cyclohexanone is activated by Pd(OH)₂ on metal oxide surface to produce Pd-enolate intermediate (**A**), and cyclic enone is formed, followed by β-hydride elimination. Pd⁰ is regenerated to Pd^{II} by oxidation with molecular oxygen. In the second step, the cyclic enone reacts with alcohol to form acetal (**5**), and aryl ether is obtained by further elimination and oxidation. These steps are promoted by ZrO₂ as Lewis acid-base catalyst and by orthoesters as efficient dehydrating reagent. Alternatively, cyclic enone could be transformed into dienones **6a** and **6b**, and dienones were tautomerized to phenol.

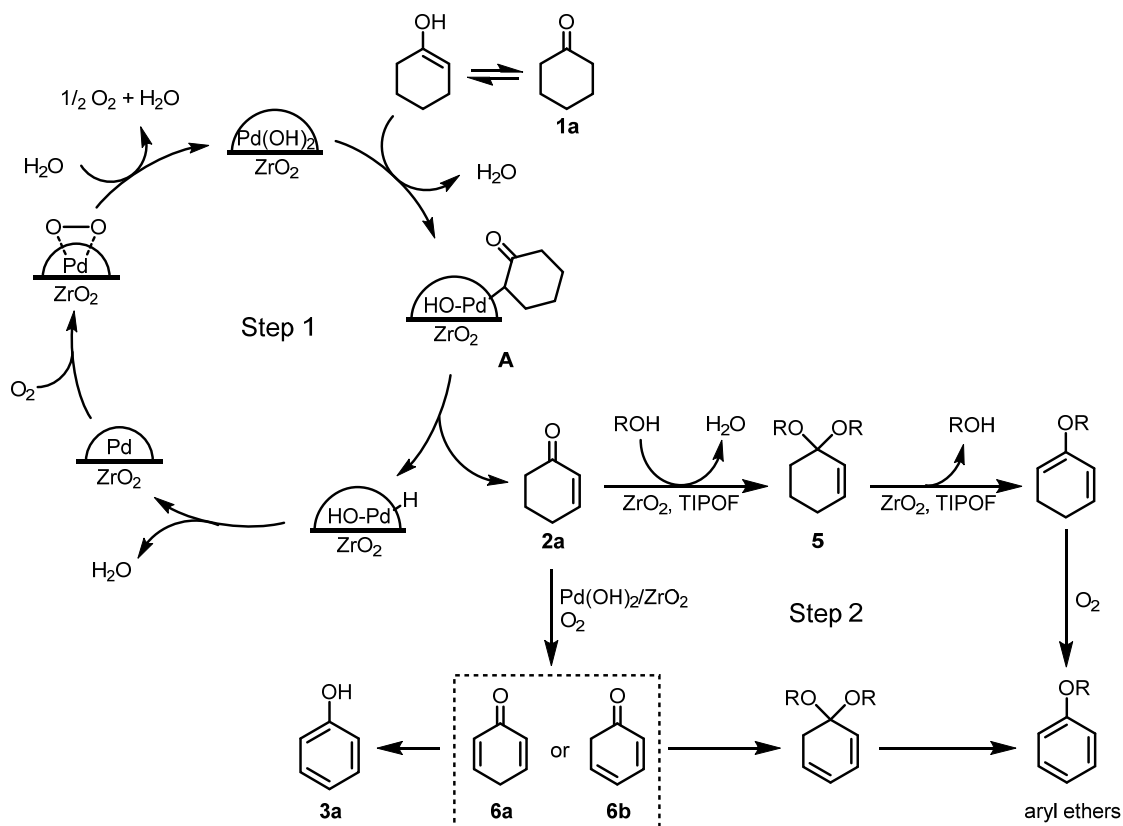


Figure 3.12 Possible Reaction pathway for synthesis of cyclohexenone, phenol, aryl ethers from cyclohexanone.

3.3 Conclusion

In conclusion, a method for the direct aerobic oxidation of cyclohexanones to cyclic enones, phenols, and aryl ethers was developed over supported Pd⁰ or Pd^{II} catalysts using molecular oxygen as the sole oxidant. Although the reaction exhibited low selectivity for the transformation of cyclohexanone to cyclohexenone, 4,4-dimethylcyclohexenone could be obtained in 81% yield from the corresponding cyclohexanone. For the synthesis of phenols, ZrO₂ supported Pd⁰ catalyst showed better catalytic activity than other supported Pd^{II} catalysts, and the corresponding phenols were obtained in moderate to excellent yields. Notably, two novel catalytic protocols were proposed for the preparation of aryl ethers from cyclohexanones with ZrO₂ supported Pd(OH)₂ as catalyst. Cyclohexanones could be converted to aryl ethers in the presence of the corresponding orthoesters, which act as the nucleophilic and dehydrating reagents. In the direct reaction with alcohols, the orthoesters (TIPOF) only acted as an efficient dehydrating reagent. In contrast with previous works, both these processes provide synthetically useful and convenient methods to prepare aryl ethers which have low boiling points, such as anisole, ethoxybenzene, and propoxybenzene.

3.4 Experimental section

3.4.1 Materials

Palladium chloride (PdCl₂) was purchased from Tanaka Kikinzoku KK. and used as received. Al₂O₃, TiO₂ (P-25), ZrO₂ (RC-100), and CeO₂, were supplied by Mizusawa Chemicals, Nippon Aerosil Co., Ltd., Daiichi Kigenso Kagaku Kogyo, and Shinetsu Chemical Co., Ltd., respectively. All commercial starting materials and reagents were used as received.

3.4.2 Instruments

Conversions and product yields were analyzed by gas chromatography (GC) using Agilent GC 6850 Series II equipped with FID and a J&W HP-1 column (0.25 μm thickness, 0.25 mm I.D., 30 m) using tridecane as an internal standard. Gas chromatography mass spectrometer (GC-MS) analysis was performed with Thermo Fisher Scientific Polaris Q equipped with a J&W HP-1 column (0.25 μm thickness, 0.25 mm I.D., 30 m). ¹H and ¹³C NMR spectra were recorded on a JEOL JNM-ECS400 spectrometer at 400 and 100 MHz, respectively. ¹H assignment abbreviations are the following; singlet (s), doublet (d), triplet (t), quartet (q), quintet (quin), sextet (sext), septet (sep), double of doublet (dd),

double of triplet (dt), multiplet (m) and broad peak (br). Analytical thin-layer chromatography (TLC) was performed with Merck, TLC silica gel 60 F₂₅₄ plates. Column chromatography was performed on silica gel (Kanto Chemicals, Silica gel 60N, spherical, neutral, particle size 40–100 μm).

Palladium contents in the catalysts and leaching of palladium into the reaction solutions were analyzed by microwave plasma-atomic emission spectrometry (MP-AES) by Agilent, 4100 MP-AES. The reaction solution was filtered to remove solid catalysts and the filtrate was analyzed by MP-AES.

X-ray powder diffraction (XRD) patterns were obtained on a Rigaku MiniFlex600 at a scanning rate of 20°/min and a sampling angle interval of 0.02° in 2θ that ranged from 10 to 80°: the instrument was equipped with a high-intensity Cu Kα radiation source (λ = 0.154178 nm). The operating voltage and the current were 40 kV and 15 mA, respectively. The phases of components were identified by matching diffraction patterns to powder diffraction files (PDF-2 Database).

HAADF-STEM and XAFS measurements were performed by using the same methods as described in Chapter 2.

Temperature-programmed desorption of carbon dioxide (CO₂-TPD) profiles were performed by BEL Japan Inc., BEL-CAT CAT-66. Samples were pretreated at 100 °C under He (40 mL/min) for 1 h, and then, 5 vol% CO₂ in He was introduced at a flow rate of 40 mL/min at 30 °C for 1 h. Unbound CO₂ was removed by flowing He at 30 °C for 30 min. The CO₂-TPD profiles were obtained by heating at a rate of 10 °C/min in a flow of He (40 mL/min). The desorbed CO₂ was detected by Q-MASS.

3.4.3 Preparation of catalysts

Preparation of metal oxides supported Pd(OH)₂ catalysts

Metal oxide-supported Pd(OH)₂ catalysts (Pd(OH)₂/MO_x) were prepared by DP method as introduced in Chapter 2. As for 10 wt% Pd(OH)₂/ZrO₂, PdCl₂ (177 mg) was dissolved in an aqueous solution of conc. HCl (10 mL) and distilled water (400 mL). The solution was warmed to 70 °C, and the pH of the solution was adjusted to 8.0 by adding 0.1 M NaOH aqueous solution. Then, the support (1.0 g) was added to the solution, and the suspension was stirred at 70 °C for 1 h. The solid was filtered, washed with water, and then dried in air at 70 °C overnight.

Preparation of metal oxides supported PdO and Pd catalysts

PdO/ZrO₂ was prepared from calcination of 10 wt% Pd(OH)₂/ZrO₂ in air at 300 °C for 4 h. Pd/ZrO₂ was prepared by the reduction of 10 wt% Pd(OH)₂/ZrO₂ in a stream of pure H₂ (40 mL/min) at 200 °C for 2 h.

3.4.4 Experimental procedure for catalytic reactions

A typical experiment for synthesis of cyclohexenones and phenols from cyclohexanones

To an autoclave was charged with cyclohexanone (1 mmol), catalyst (Pd 5 mol%), DMSO (2 mL), and a magnetic stirring bar. The autoclave was purged and filled with O₂ until the pressure reached 0.5 MPa. The reaction mixture was stirred at 100 °C for 24 h. After the reaction, the mixture was filtered, and the filtrate was analyzed by GC using tridecane as an internal standard.

A typical experiment for synthesis of aryl ethers from cyclohexanones

To an autoclave was charged with cyclohexanone (1 mmol), catalyst (Pd 2 mol%), orthoester (1.5 mL), and a magnetic stirring bar. The autoclave was purged and filled with O₂ until the pressure reached 0.5 MPa. The reaction mixture was stirred at 140 °C for 6 h. After the reaction, the mixture was filtered, and the filtrate was analyzed by GC using tridecane as an internal standard.

A typical experiment for synthesis of aryl ethers from cyclohexanones and alcohols

To an autoclave was charged with cyclohexanone (1 mmol), catalyst (Pd 2 mol%), alcohol (30 eq) TIOF (5 eq), and a magnetic stirring bar. The autoclave was purged and filled with O₂ until the pressure reached 0.5 MPa. The reaction mixture was stirred at 140 °C for 6 h. After the reaction, the mixture was filtered, and the filtrate was analyzed by GC using tridecane as an internal standard.

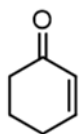
Recycling test for synthesis of anisole from cyclohexanone

After the reaction, the autoclave was cooled down to room temperature, and the catalyst was recovered by filtration, washed with CH₂Cl₂ and MeOH, and then, dried in air at 100 °C for 12 h. The catalyst was used for the next run.

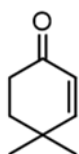
Experiment for removal of catalyst

To an autoclave was charged with cyclohexanone (1 mmol), Pd(OH)₂/ZrO₂ (Pd 2 mol%), TMOF (1.5 mL), and a magnetic stirring bar. The autoclave was purged and filled with O₂ until the pressure reached 0.5 MPa. The reaction mixture was stirred at 140 °C for 2 h, and then, the autoclave was cooled down to room temperature. The catalyst was filtered. The filtrate solution was filled into autoclave, which was purged and filled with 0.5 MPa O₂ again. The reaction solution was stirred at 140 °C for another 2 h. After reaction, the reaction solution was analyzed by GC using tridecane as an internal standard for each steps.

3.4.5 Characterization of the isolated compounds

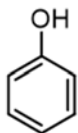


Cyclohexenone (2a): The mixture of cyclohexanone (104 μL, 1.0 mmol) and 10 wt% Pd(OH)₂/ZrO₂ (20 mg, Pd 2 mol%) in DMSO (2.0 mL) was stirred under pressurized O₂ (0.25 MPa) at 120 °C for 15 h. After the reaction, the catalyst was filtered off, and the filtrate was washed with H₂O. The organic layer was extracted with ethyl acetate, and then dried over Na₂SO₄. The organic solvents were removed, and the crude product was purified by silica-gel column chromatography (hexane:ethyl acetate = 15:1) to give cyclohexenone (20.0 mg, 0.21 mmol, 21%) as a yellow liquid (GC yield 26%). ¹H NMR (400 MHz, CDCl₃): δ 6.94–6.90 (m, 1H), 5.91 (d, *J* = 10.0 Hz, 1H), 2.31 (t, *J* = 6.4 Hz, 1H), 2.28–2.24 (m, 1H), 1.92 (quin, *J* = 6.8 Hz, 1H); ¹³C NMR (100 MHz, CDCl₃): δ 199.9, 150.9, 129.8, 38.1, 25.7, 22.7.

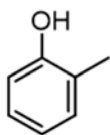


4,4-Dimethylcyclohexenone (2b): The mixture of 4,4-dimethylcyclohexanone (126 mg, 1.0 mmol) and 10 wt% Pd(OH)₂/ZrO₂ (50 mg, Pd 5 mol%) in DMSO (2.0 mL) was stirred under pressurized O₂ (0.25 MPa) at 120 °C for 20 h. After the reaction, the catalyst was filtered off, and the filtrate was washed with H₂O. The organic layer was extracted with ethyl acetate, and then dried over Na₂SO₄. The organic solvents were removed, and the crude product was purified by silica-gel column chromatography (hexane:ethyl acetate = 15:1) to give 4,4-dimethylcyclohexenone (91 mg, 0.75 mmol,

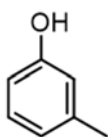
75%) as a yellow liquid (GC yield 81%). ^1H NMR (400 MHz, CDCl_3): δ 6.64 (d, $J = 10.0$ Hz, 1H), 5.81 (d, $J = 10.0$ Hz, 1H), 2.43 (t, $J = 6.8$ Hz, 2H), 1.84 (t, $J = 6.8$ Hz, 2H), 1.14 (s, 6H); ^{13}C NMR (100 MHz, CDCl_3): δ 199.9, 160.1, 126.9, 36.1, 34.5, 32.9, 27.8.



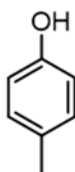
Phenol (3a): The mixture of cyclohexanone (104 μL , 1.0 mmol) and 10 wt% $\text{Pd}(\text{OH})_2/\text{ZrO}_2$ (50 mg, Pd 5 mol%) in DMSO (2.0 mL) was stirred under pressurized O_2 (0.5 MPa) at 100 $^\circ\text{C}$ for 24 h. After the reaction, the catalyst was filtered off, and the filtrate was washed with H_2O . The organic layer was extracted with ethyl acetate, and then dried over Na_2SO_4 . The organic solvents were removed, and the crude product was purified by silica-gel column chromatography (hexane:ethyl acetate = 10:1) to give phenol (73 mg, 0.77 mmol, 77%) as a colorless liquid (GC yield 99%). ^1H NMR (400 MHz, CDCl_3): δ 7.24 (dd, $J = 8.8, 7.2$ Hz, 2H), 6.93 (t, $J = 7.2$ Hz, 1H), 6.83 (d, $J = 8.4$ Hz, 2H), 5.02 (s, 1H); ^{13}C NMR (100 MHz, CDCl_3): δ 155.6, 129.8, 120.9, 115.4.



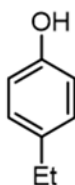
2-Methylphenol (3c): The mixture of 2-methylcyclohexan-1-one (123 μL , 1.0 mmol) and 10 wt% $\text{Pd}(\text{OH})_2/\text{ZrO}_2$ (50 mg, Pd 5 mol%) in DMSO (2.0 mL) was stirred under pressurized O_2 (0.5 MPa) at 100 $^\circ\text{C}$ for 24 h. After the reaction, the catalyst was filtered off, and the filtrate was washed with H_2O . The organic layer was extracted with ethyl acetate, and then dried over Na_2SO_4 . The organic solvents were removed, and the crude product was purified by silica-gel column chromatography (hexane:ethyl acetate = 10:1) to give 3-methylphenol (53 mg, 0.48 mmol, 48%) as a yellow liquid. (GC yield 63%). ^1H NMR (400 MHz, CDCl_3): δ 7.15 (d, $J = 7.6$ Hz, 1H), 7.11 (dt, $J = 7.4, 1.2$ Hz, 1H), 6.88 (t, $J = 7.2$ Hz, 1H), 6.79 (d, $J = 7.6$ Hz, 1H), 5.02 (s, 1H), 2.28 (s, 3H); ^{13}C NMR: (100 MHz, CDCl_3) δ 153.8, 131.2, 124.0, 123.9, 120.9, 115.0, 15.9.



3-Methylphenol (3d): The mixture of 3-methylcyclohexan-1-one (123 μ L, 1.0 mmol) and 10 wt% Pd(OH)₂/ZrO₂ (50 mg, Pd 5 mol%) in DMSO (2.0 mL) was stirred under pressurized O₂ (0.5 MPa) at 100 °C for 24 h. After the reaction, the catalyst was filtered off, and the filtrate was washed with H₂O. The organic layer was extracted with ethyl acetate, and then dried over Na₂SO₄. The organic solvents were removed, and the crude product was purified by silica-gel column chromatography (hexane:ethyl acetate = 10:1) to give 3-methylphenol (65 mg, 0.61 mmol, 61%) as a colorless liquid (GC yield 78%). ¹H NMR (400 MHz, CDCl₃): δ 7.12 (t, *J* = 7.6 Hz, 1H), 6.75 (d, *J* = 7.2 Hz, 2H), 6.66 (dt, *J* = 10.0, 11.6 Hz, 1H), 5.41 (s, 1H), 2.30 (s, 3H); ¹³C NMR (100 MHz, CDCl₃): δ 155.6, 139.9, 129.5, 121.7, 116.2, 112.4, 21.5.

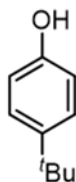


4-Methylphenol (3e): The mixture of 4-methylcyclohexan-1-one (122 μ L, 1.0 mmol) and 10 wt% Pd(OH)₂/ZrO₂ (50 mg, Pd 5 mol%) in DMSO (2.0 mL) was stirred under pressurized O₂ (0.5 MPa) at 100 °C for 24 h. After the reaction, the catalyst was filtered off, and the filtrate was washed with H₂O. The organic layer was extracted with ethyl acetate, and then dried over Na₂SO₄. The organic solvents were removed, and the crude product was purified by silica-gel column chromatography (hexane:ethyl acetate = 10:1) to give 4-methylphenol (85 mg, 0.78 mmol, 78%) as a colorless liquid (GC yield 99%). ¹H NMR (400 MHz, CDCl₃): δ 7.04 (d, *J* = 8.4 Hz, 2H), 6.75 (d, *J* = 8.0 Hz, 2H), 5.38 (s, 1H), 2.28 (s, 3H); ¹³C NMR (100 MHz, CDCl₃): δ 153.3, 130.2, 130.1, 115.2, 20.6.

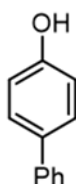


4-Ethylphenol (3f): The mixture of 4-ethylcyclohexan-1-one (141 μ L, 1.0 mmol) and 10 wt% Pd(OH)₂/ZrO₂ (50 mg, Pd 5 mol%) in DMSO (2.0 mL) was stirred under pressurized O₂ (0.5 MPa) at 100 °C for 24 h. After the reaction, the catalyst was filtered off, and the filtrate was washed with H₂O. The organic layer was extracted with ethyl acetate, and then dried over Na₂SO₄. The organic solvents were removed, and the crude product was purified by silica-gel column chromatography (hexane:ethyl acetate = 10:1) to give 4-ethylphenol (85 mg, 0.7 mmol, 70%) as a white solid (GC yield 99%). ¹H

NMR (400 MHz, CDCl₃): δ 7.08 (d, J = 8.8 Hz, 2H), 6.79 (d, J = 8.4 Hz, 2H), 5.52 (s, 1H), 2.30 (q, J = 7.6 Hz, 2H), 1.22 (t, J = 8.0 Hz, 3H); ¹³C NMR (100 MHz, CDCl₃): δ 153.4, 136.7, 129.1, 115.3, 28.1, 16.0.

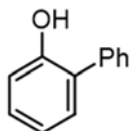


4-(*t*-Butyl)phenol (3g): The mixture of 4-*t*-butylcyclohexan-1-one (154 mg, 1.0 mmol) and 10 wt% Pd(OH)₂/ZrO₂ (50 mg, Pd 5 mol%) in DMSO (2.0 mL) was stirred under pressurized O₂ (0.5 MPa) at 100 °C for 24 h. After the reaction, the catalyst was filtered off, and the filtrate was washed with H₂O. The organic layer was extracted with ethyl acetate, and then dried over Na₂SO₄. The organic solvents were removed, and the crude product was purified by silica-gel column chromatography (hexane:ethyl acetate = 10:1) to give 4-(*t*-butyl)phenol (94 mg, 0.63 mmol, 63%) as a white solid (GC yield 99%). ¹H NMR (400 MHz, CDCl₃): δ 7.29 (d, J = 8.8 Hz, 2H), 6.83 (d, J = 8.4 Hz, 2H), 5.87 (brs, 1H), 1.34 (s, 9H); ¹³C NMR (100 MHz, CDCl₃): δ 153.0, 143.8, 126.6, 115.0, 34.2, 31.7.

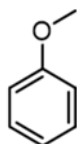


[1,1'-Biphenyl]-4-ol (3h): The mixture of 4-phenylcyclohexan-1-one (174 mg, 1.0 mmol) and 10 wt% Pd(OH)₂/ZrO₂ (50 mg, Pd 5 mol%) in DMSO (2.0 mL) was stirred under pressurized O₂ (0.5 MPa) at 100 °C for 24 h. After the reaction, the catalyst was filtered off, and the filtrate was washed with H₂O. The organic layer was extracted with ethyl acetate, and then dried over Na₂SO₄. The organic solvents were removed, and the crude product was purified by silica-gel column chromatography (hexane:ethyl acetate = 8:1) to give [1,1'-Biphenyl]-4-ol (148 mg, 0.87 mmol, 87%) as a white solid (GC yield 82%). ¹H NMR (400 MHz, CDCl₃): δ 7.54 (dd, J = 8.8, 1.6 Hz, 2H), 7.48 (d, J = 8.8 Hz, 2H), 7.42 (t, J = 7.2 Hz, 2H), 7.31 (t, J = 7.2 Hz, 1H), 6.91 (d, J = 8.0 Hz, 2H), 5.26 (brs, 1H); ¹³C NMR (100 MHz, CDCl₃): δ 155.2, 140.8, 134.1, 128.9, 128.5, 126.8, 115.8.

Characterization of 3,5-dimethylphenol (**3i**) was performed by GC-MS to confirmed the molecule weight, and GC by the comparison of authentic sample which was purchased from Tokyo Chemical Industry Co., Ltd.



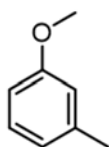
[1,1'-Biphenyl]-2-ol (3j): The mixture of cyclohexanone (174 mg, 1.0 mmol) and 10 wt% Pd(OH)₂/ZrO₂ (50 mg, Pd 5 mol%) in DMSO (2.0 mL) was stirred under pressurized O₂ (0.5 MPa) at 100 °C for 24 h. After the reaction, the catalyst was filtered off, and the filtrate was washed with H₂O. The organic layer was extracted with ethyl acetate, and then dried over Na₂SO₄. The organic solvents were removed, and the crude product was purified by silica-gel column chromatography (hexane:ethyl acetate = 8:1) to give [1,1'-Biphenyl]-2-ol (65 mg, 0.38 mmol, 38%) as a white solid (GC yield 46%). ¹H NMR (400 MHz, CDCl₃): δ 7.52 (d, *J* = 4.8 Hz, 4H), 7.45–7.42 (m, 1H), 7.33–7.29 (m, 2H), 7.07–7.01 (m, 2H), 5.40 (s, 1H); ¹³C NMR (100 MHz, CDCl₃): δ 152.5, 137.3, 130.5, 129.4, 129.3, 129.3, 128.3, 128.0, 121.0, 116.0.



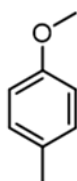
Anisole (4a): Synthesis from cyclohexanone with trimethyl orthoformate: The mixture of cyclohexanone (98 mg, 1.0 mmol) and 10 wt% Pd(OH)₂/ZrO₂ (20 mg, Pd 2 mol%) in trimethyl orthoformate (1.5 mL) was stirred under pressurized O₂ (0.5 MPa) at 140 °C for 6 h. After the reaction, the catalyst was filtered off, and the filtrate was washed with H₂O. The organic layer was extracted with diethyl ether, and then dried over Na₂SO₄. The organic solvents were removed, and the crude product was purified by silica-gel column chromatography (heptane:diethyl ether = 30:1) to give anisole (70 mg, 0.65 mmol, 65%) as a yellow liquid (GC yield 96%).

Synthesis of anisole (4a) from cyclohexanone with methanol: The mixture of cyclohexanone (98 mg, 1.0 mmol) and 10 wt% Pd(OH)₂/ZrO₂ (20 mg, Pd 2 mol%) in triisopropyl orthoformate (1.1 mL) and methanol (1.9 mL) was stirred under pressurized O₂ (0.5 MPa) at 140 °C for 6 h. After the reaction,

the catalyst was filtered off, and the filtrate was washed with H₂O. The organic layer was extracted with diethyl ether, and then dried over Na₂SO₄. The organic solvents were removed and the crude product was purified by silica-gel column chromatography (heptane:diethyl ether = 30:1) to give anisole (56 mg, 0.52 mmol, 52%) as a yellow liquid (GC yield 74%). ¹H NMR (400 MHz, CDCl₃): δ 7.39–7.35 (m, 2H), 7.05–6.98 (m, 3H), 3.86 (s, 3H); ¹³C NMR (100 MHz, CDCl₃): δ 159.8, 129.6, 120.8, 114.1, 55.2.

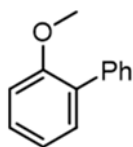


3-Methylanisole (4d): The mixture of 3-methylcyclohexanone (112 mg, 1.0 mmol) and 10 wt% Pd(OH)₂/ZrO₂ (20 mg, Pd 2 mol%) in trimethyl orthoformate (1.5 mL) was stirred under pressurized O₂ (0.5 MPa) at 140 °C for 6 h. After the reaction, the catalyst was filtered off, and the filtrate was washed with H₂O. The organic layer was extracted with diethyl ether, and then dried over Na₂SO₄. The organic solvents were removed, and the crude product was purified by silica-gel column chromatography (heptane:diethyl ether = 30:1) to give 3-methylanisole (60 mg, 0.49 mmol, 49%) as a yellow liquid (GC yield 66%). ¹H NMR (400 MHz, CDCl₃): δ 7.20 (t, *J* = 7.2 Hz, 1H), 6.80–6.72 (m, 3H), 3.81 (s, 3H), 2.36 (s, 3H); ¹³C NMR (100 MHz, CDCl₃): δ 159.7, 139.6, 129.3, 121.6, 114.8, 110.9, 55.2, 21.6.

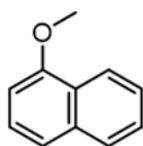


4-Methylanisole (4e): The mixture of 4-methylcyclohexanone (112 mg, 1.0 mmol) and 10 wt% Pd(OH)₂/ZrO₂ (20 mg, Pd 2 mol%) in trimethyl orthoformate (1.5 mL) was stirred under pressurized O₂ (0.5 MPa) at 140 °C for 6 h. After the reaction, the catalyst was filtered off, and the filtrate was washed with H₂O. The organic layer was extracted with diethyl ether, and then dried over Na₂SO₄. The organic solvents were removed, and the crude product was purified by silica-gel column chromatography (heptane:diethyl ether = 30:1) to give 3-methylanisole (42 mg, 0.38 mmol, 38%) as a colorless liquid (GC yield 45%). ¹H NMR (400 MHz, CDCl₃): δ 7.10 (d, *J* = 8.0 Hz, 2H), 6.81 (dd,

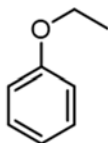
$J = 6.8, 2.4$ Hz, 2H), 3.79 (s, 3H), 2.30 (s, 3H); ^{13}C NMR (100 MHz, CDCl_3): δ 157.5, 130.0, 129.9, 113.8, 55.4, 20.6.



2-Methoxybiphenyl (4j): The mixture of 2-phenylcyclohexanone (175 mg, 1.0 mmol) and 10 wt% $\text{Pd}(\text{OH})_2/\text{ZrO}_2$ (20 mg, Pd 2 mol%) in trimethyl orthoformate (1.5 mL) was stirred under pressurized O_2 (0.5 MPa) at 140 °C for 6 h. After the reaction, the catalyst was filtered off, and the filtrate was washed with H_2O . The organic layer was extracted with diethyl ether, and then dried over Na_2SO_4 . The organic solvents were removed, and the crude product was purified by silica-gel column chromatography (hexane:diethyl ether = 30:1) to give 2-methoxybiphenyl (32 mg, 0.17 mmol, 17%) as a colorless liquid (GC yield 22%). ^1H NMR (400 MHz, CDCl_3): δ 7.72 (d, $J = 6.8$ Hz, 2H), 7.59–7.55 (m, 3H), 7.51–7.45 (m, 2H), 7.21–7.17 (m, 1H), 7.12 (d, $J = 7.8$ Hz, 1H), 3.92 (s, 3H); ^{13}C NMR (100 MHz, CDCl_3): δ 156.7, 138.8, 131.2, 131.0, 129.8, 128.9, 128.3, 127.2, 121.1, 111.5, 55.7.

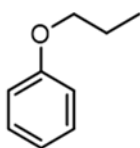


1-Methoxynaphthalene (4k): The mixture of α -tetralone (146 mg, 1.0 mmol) and 10 wt% $\text{Pd}(\text{OH})_2/\text{ZrO}_2$ (20 mg, Pd 2 mol%) in trimethyl orthoformate (1.5 mL) was stirred under pressurized O_2 (0.5 MPa) at 140 °C for 6 h. After the reaction, the catalyst was filtered off, and the filtrate was washed with H_2O . The organic layer was extracted with diethyl ether, and then dried over Na_2SO_4 . The organic solvents were removed, and the crude product was purified by silica-gel column chromatography (hexane:diethyl ether = 30:1) to give 1-methoxynaphthalene (111 mg, 0.70 mmol, 70%) as a yellow liquid (GC yield 78%). ^1H NMR (400 MHz, CDCl_3): δ 8.40–8.37 (m, 1H), 7.91–7.87 (m, 1H), 7.59–7.44 (m, 4H), 6.87 (d, $J = 7.2$ Hz, 1H), 4.04 (s, 3H); ^{13}C NMR (100 MHz, CDCl_3): δ 155.6, 134.7, 127.7, 126.6, 126.0, 125.8, 125.4, 122.2, 120.4, 104.0, 55.6.



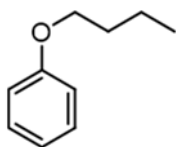
Ethoxybenzene (41): Synthesis from cyclohexanone with triethyl orthoformate: The mixture of cyclohexanone (98 mg, 1.0 mmol) and 10 wt% Pd(OH)₂/ZrO₂ (20 mg, Pd 2 mol%) in triethyl orthoformate (1.5 mL) was stirred under pressurized O₂ (0.5 MPa) at 140 °C for 6 h. After the reaction, the catalyst was filtered off, and the filtrate was washed with H₂O. The organic layer was extracted with diethyl ether, and then dried over Na₂SO₄. The organic solvents were removed, and the crude product was purified by silica-gel column chromatography (heptane:diethyl ether = 30:1) to give ethoxybenzene (37 mg, 0.30 mmol, 30%) as a yellow liquid (GC yield 49%).

Synthesis of ethoxybenzene (41) from cyclohexanone with ethanol: The mixture of cyclohexanone (98 mg, 1.0 mmol) and 10 wt% Pd(OH)₂/ZrO₂ (20 mg, Pd 2 mol%) in triisopropyl orthoformate (1.1 mL) and ethanol (1.8 mL) was stirred under pressurized O₂ (0.5 MPa) at 140 °C for 6 h. After the reaction, the catalyst was filtered off, and the filtrate was washed with H₂O. The organic layer was extracted with diethyl ether, and then dried over Na₂SO₄. The organic solvents were removed, and the crude product was purified by silica-gel column chromatography (heptane:diethyl ether = 30:1) to give ethoxybenzene (76 mg, 0.62 mmol, 62%) as a yellow liquid (GC yield 83%). ¹H NMR (400 MHz, CDCl₃): δ 7.43–7.38 (m, 2H), 7.09–7.01 (m, 3H), 4.11 (q, *J* = 6.8 Hz, 2H), 1.53 (t, *J* = 6.8 Hz, 3H); ¹³C NMR (100 MHz, CDCl₃): δ 159.2, 129.6, 120.7, 114.7, 63.4, 15.0.

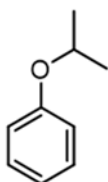


Propoxybenzene (4m): The mixture of cyclohexanone (98 mg, 1.0 mmol) and 10 wt% Pd(OH)₂/ZrO₂ (20 mg, Pd 2 mol%) in triisopropyl orthoformate (1.1 mL) and 1-propanol (2.2 mL) was stirred under pressurized O₂ (0.5 MPa) at 140 °C for 6 h. After the reaction, the catalyst was filtered off, and the filtrate was washed with H₂O. The organic layer was extracted with diethyl ether, and then dried over Na₂SO₄. The organic solvents were removed, and the crude product was purified by silica-gel column chromatography (heptane:diethyl ether = 30:1) to give propoxybenzene (86 mg, 0.63 mmol, 63%) as a yellow liquid (GC yield 76%). ¹H NMR (400 MHz, CDCl₃): δ 7.29–7.25 (m, 2H), 7.04–6.98 (m,

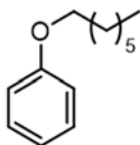
3H), 3.99 (t, $J = 6.8$ Hz, 2H), 1.89 (sext, $J = 7.6$ Hz, 2H), 1.13 (t, $J = 7.2$ Hz, 3H); ^{13}C NMR (100 MHz, CDCl_3): δ 159.3, 129.4, 120.5, 114.6, 69.5, 22.8, 10.7.



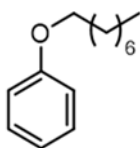
Butoxybenzene (4n): The mixture of cyclohexanone (98 mg, 1.0 mmol) and 10 wt% $\text{Pd}(\text{OH})_2/\text{ZrO}_2$ (20 mg, Pd 2 mol%) in triisopropyl orthoformate (1.1 mL) and 1-butanol (2.7 mL) was stirred under pressurized O_2 (0.5 MPa) at 140 °C for 6 h. After the reaction, the catalyst was filtered off, and the filtrate was washed with H_2O . The organic layer was extracted with diethyl ether, and then dried over Na_2SO_4 . The organic solvents were removed, and the crude product was purified by silica-gel column chromatography (heptane:diethyl ether = 30:1) to give butoxybenzene (90 mg, 0.60 mmol, 60%) as a yellow liquid (GC yield 73%). ^1H NMR (400 MHz, CDCl_3): δ 7.29–7.25 (m, 2H), 6.94–6.89 (m, 3H), 3.96 (t, $J = 6.4$ Hz, 2H), 1.77 (quin, $J = 8.4$ Hz, 2H), 1.49 (sext, $J = 8.0$ Hz, 2H), 0.97 (t, $J = 7.6$ Hz, 3H); ^{13}C NMR (100 MHz, CDCl_3): δ 159.2, 129.5, 120.5, 114.6, 67.6, 31.4, 19.4, 14.0.



Isopropoxybenzene (4o): The mixture of cyclohexanone (98 mg, 1.0 mmol) and 10 wt% $\text{Pd}(\text{OH})_2/\text{ZrO}_2$ (20 mg, Pd 2 mol%) in triisopropyl orthoformate (1.1 mL) and 2-propanol (2.3 mL) was stirred under pressurized O_2 (0.5 MPa) at 140 °C for 6 h. After the reaction, the catalyst was filtered off, and the filtrate was washed with H_2O . The organic layer was extracted with diethyl ether, and then dried over Na_2SO_4 . The organic solvents were removed, and the crude product was purified by silica-gel column chromatography (heptane:diethyl ether = 30:1) to give isopropoxybenzene (30 mg, 0.22 mmol, 22%) as a colorless liquid (GC yield 23%). ^1H NMR (400 MHz, CDCl_3): δ 7.27 (dt, $J = 7.6, 6.8$ Hz, 2H), 6.94–6.88 (m, 3H), 4.55 (sep, $J = 6.0$ Hz, 1H), 1.34 (d, $J = 6.0$ Hz, 6H); ^{13}C NMR (100 MHz, CDCl_3): δ 157.9, 129.5, 120.6, 116.0, 69.8, 22.2.



Heptyloxybenzene (4p): The mixture of cyclohexanone (98 mg, 1.0 mmol) and 10 wt% Pd(OH)₂/ZrO₂ (20 mg, Pd 2 mol%) in triisopropyl orthoformate (1.1 mL) and 1-heptanol (2.1 mL) was stirred under pressurized O₂ (0.5 MPa) at 140 °C for 6 h. After the reaction, the catalyst was filtered off, and the filtrate was washed with H₂O. The organic layer was extracted with diethyl ether, and then dried over Na₂SO₄. The organic solvents were removed, and the crude product was purified by silica-gel column chromatography (heptane:diethyl ether = 30:1) to give heptyloxybenzene (123 mg, 0.64 mmol, 64%) as a yellow liquid (GC yield 78%). ¹H NMR (400 MHz, CDCl₃): δ 7.29–7.25 (m, 2H), 6.94–6.88 (m, 3H), 3.95 (q, *J* = 6.0 Hz, 2H), 1.77 (quin, *J* = 7.6 Hz, 2H), 1.46–1.30 (m, 8H), 0.89 (t, *J* = 6.0 Hz, 3H); ¹³C NMR (100 MHz, CDCl₃): δ 159.2, 129.5, 120.5, 114.6, 68.0, 31.9, 29.4, 29.2, 26.1, 22.7, 14.2.



Octyloxybenzene (4q): The mixture of cyclohexanone (98 mg, 1.0 mmol) and 10 wt% Pd(OH)₂/ZrO₂ (20 mg, Pd 2 mol%) in triisopropyl orthoformate (1.1 mL) and 1-octanol (2.4 mL) was stirred under pressurized O₂ (0.5 MPa) at 140 °C for 6 h. After the reaction, the catalyst was filtered off, and the filtrate was washed with H₂O. The organic layer was extracted with diethyl ether, and then dried over Na₂SO₄. The organic solvents were removed, and the crude product was purified by silica-gel column chromatography (heptane:diethyl ether = 30:1) to give octyloxybenzene (138 mg, 0.67 mmol, 67%) as a yellow liquid. (GC yield 79%). ¹H NMR (400 MHz, CDCl₃): δ 7.30–7.24 (m, 2H), 6.94–6.88 (m, 3H), 3.94 (t, *J* = 6.4 Hz, 2H), 1.77 (quin, *J* = 7.6 Hz, 2H), 1.48–1.28 (m, 10H), 0.88 (t, *J* = 6.8 Hz, 3H); ¹³C NMR (100 MHz, CDCl₃): δ 159.2, 129.5, 120.5, 114.6, 68.0, 31.9, 29.5, 29.4, 29.3, 26.2, 22.8, 14.2.

3.5 References

- [1] (a) Y. Chi, S. H. Gellman, *Org. Lett.*, **2005**, 7, 4253–4256. (b) T. Ooi, D. Ohara, K. Kukumoto, K. Maruoka, *Org. Lett.*, **2005**, 7, 3195–3197. (c) F. Wu, H. Li, R. Hong, L. Deng, *Angew. Chem. Int. Ed.*, **2006**, 45, 947–950. (d) W. Li, W. Wu, J. Yang, X. Liang, J. Ye, *Synthesis*, **2011**, 1085–1091. (e) D. Sharma, Bandna, A. K. Shil, B. Singh, P. Das, *Synlett.*, **2012**, 23, 1199–1204.
- [2] (a) C. E. Aroyan, A. Dermenci, S. J. Miller, *Tetrahedron*, **2009**, 65, 4069–4084. (b) E. Marqués-López, R. P. Herrera, T. Marks, W. C. Jacobs, D. Könnig, R. M. de Figueiredo, M. Christmann, *Org. Lett.*, **2009**, 11, 4116–4119. (c) W. Liu, G. Zhao, *Org. Biomol. Chem.*, **2014**, 12, 832–835.
- [3] (a) S. B. Herzon, L. Lu, C. M. Woo, S. L. Gholap, *J. Am. Chem. Soc.*, **2011**, 133, 7260–7263. (b) H. Yokoe, C. Mitsuhashi, Y. Matsuoka, T. Yoshimura, M. Yoshida, K. Shishido, *J. Am. Chem. Soc.*, **2011**, 133, 8854–8857.
- [4] Y. Ito, T. Hirao, T. Saegusa, *J. Org. Chem.*, **1978**, 43, 1011–1013.
- [5] R. C. Larock, T. R. Hightower, G. A. Hahn, P. Kraus, D. Zhang, *Tetrahedron Lett.*, **1995**, 36, 2423–2426.
- [6] J. Zhu, J. Liu, R. Ma, H. Xie, J. Li, H. Jiang, W. Wang, *Adv. Synth. Catal.*, **2009**, 351, 1229–1232.
- [7] (a) D. J. Hart, K-I. Kanai, *J. Am. Chem. Soc.*, **1983**, 105, 1255–1263. (b) J. H. Lee, Y. Zhang, S. J. Danishefsky, *J. Am. Chem. Soc.*, **2010**, 132, 14330–14333. (c) Q. Xu, R. Zhang, T. Zhang, M. Shi, *J. Org. Chem.*, **2010**, 75, 3935–3937. (d) A. L. Gottumukkala, J. F. Teichert, D. Heijnen, N. Eisink, S. van Dijk, C. Ferrer, A. van den Hoogenband, A. J. Minnaard, *J. Org. Chem.*, **2011**, 76, 3498–3501. (e) M. Moritaka, K. Nakano, Y. Ichikawa, H. Kotsuki, *Heterocycles*, **2013**, 87, 2351–2360.
- [8] (a) B. B. Snider, *Tetrahedron Lett.*, **1980**, 21, 1133–1136. (b) E. C. Angell, F. Fringuelli, M. Guo, L. Minuti, A. Taticchi, E. Wenkert, *J. Org. Chem.*, **1988**, 53, 4325–4328. (c) M. G. Organ, P. Anderson, *J. Chem. Educ.*, **1996**, 73, 1193–1196. (d) J. H. P. Tyman, *Synthetic and Natural Phenols*, **1996**, Elsevier, New York.
- [9] (a) M. Tokunaga, S. Harada, T. Iwasawa, T. Obora, Y. Tsuji, *Tetrahedron Lett.*, **2007**, 48, 6860–6862. (b) X. Zhang, D. Y. Wang, T. J. Emge, A. S. Goldman, *Inorg. Chim. Acta.*, **2011**, 369, 253–259. (c) T. Diao, S. S. Stahl, *J. Am. Chem. Soc.*, **2011**, 133, 14566–14569. (d) T. Diao, D. Pun, S. S. Stahl, *J. Am. Chem. Soc.*, **2013**, 135, 8205–8212.
- [10] (a) Y. Shov, A. H. I. Arisha, *J. Org. Chem.*, **1998**, 63, 5640–5642. (b) Y. Izawa, D. Pun, S. S.

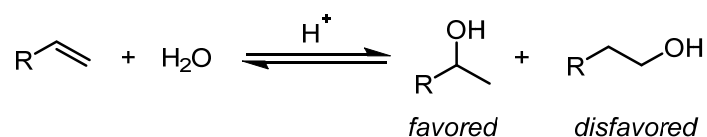
- Stahl, *Science*, **2011**, 333, 209–213. (c) D. Pun, T. Diao, S. S. Stahl, *J. Am. Chem. Soc.*, **2013**, 135, 8213–8221.
- [11] (a) B. A. Steinhoff, S. R. Fix, S. S. Stahl, *J. Am. Chem. Soc.*, **2002**, 124, 766–767. (b) R. I. McDonald, S. S. Stahl, *Angew. Chem. Int. Ed.*, **2010**, 49, 5529–5532.
- [12] G. Evano, N. Blanchard, M. Toumi, *Chem. Rev.*, **2008**, 108, 3054–3131.
- [13] K. P. C. Volhardt, N. E. Schore, *Organic Chemistry: Structure and Function (4th Edition)*, W. H. Freeman & Co. through Japan UNI Agency, Inc., Tokyo, P. 378.
- [14] R. A. Altman, A. Shafir, A. Choi, P. A. Lichtor, S. L. Buchwald, *J. Org. Chem.*, **2008**, 73, 284–286.
- [15] M. O. Simon, S. A. Girard, C. J. Li, *Angew. Chem. Int. Ed.*, **2012**, 51, 7537–7540.
- [16] (a) M. Sutter, R. Lafon, Y. Raoul, E. Métay, M. Lemaire, *Eur. J. Org. Chem.*, **2013**, 5902–5916. (b) M. Sutter, N. Sotto, Y. Raoul, E. Métay, M. Lemaire, *Green Chem.*, **2013**, 15, 347–352.
- [17] T. Ishida, R. Tsunoda, Z. Zhang, A. Hmasaki, T. Honma, H. Ohashi, T. Yokoyama, M. Tokunaga, *Appl. Catal. B: Environ.*, **2014**, 150–151, 523–531.
- [18] S. S. Soomro, F. L. Ansari, K. Chatziapostolou, K. Köhler, *J. Catal.*, **2010**, 273, 138–146.
- [19] (a) T. Honma, H. Oji, S. Hirayama, Y. Taniguchi, H. Ofuchi, M. Takagaki, *AIP Conf. Proc.*, **2010**, 1234, 13–16. (b) H. Oji, Y. Taniguchi, S. Hirayama, H. Ofuchi, M. Takagaki, T. Honma, *J. Synchrotron Rad.*, **2012**, 19, 54–59.
- [20] B. Ravel, M. Newville, *J. Synchrotron Rad.*, **2005**, 12, 537–541.

Chapter 4.

Transformation of terminal alkenes into primary allylic alcohols over supported palladium hydroxide catalysts

4.1 Introduction

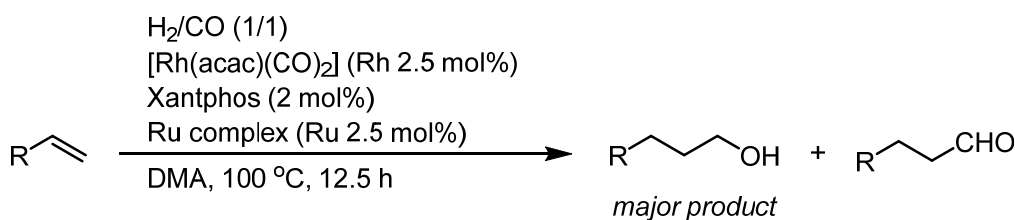
Direct addition of valuable functional groups to terminal alkenes is an appealing and significant subject in organic chemistry. In particular, transformation of terminal alkenes into primary alcohols is quite desirable in both bulk and fine chemical synthesis.¹ However, in accordance with Markovnikov's rule, secondary and tertiary alcohols are generated by ordinary acid-catalyzed hydration process (Scheme 4.1).² Thus, synthesis of primary alcohols from terminal alkenes has been regarded as one of the "ten challenges in catalysis".³



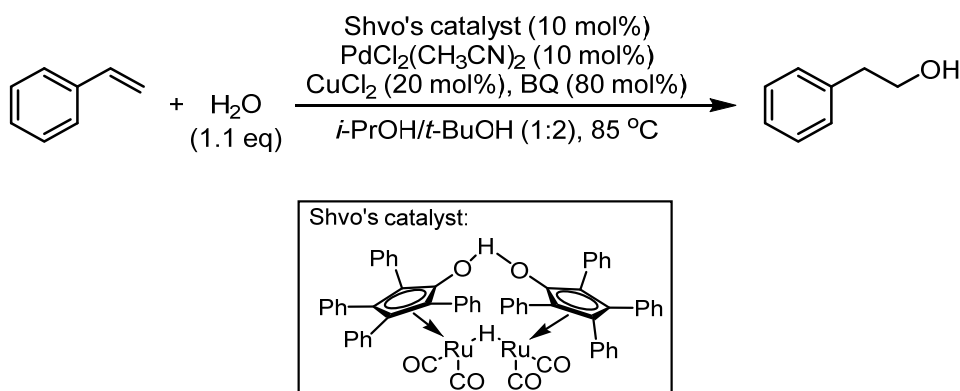
Scheme 4.1 Acid-catalyzed hydration of alkenes in accordance with Markovnikov's rule.

Hydroboration-oxidation was used as a two-steps method to produce anti-Markovnikov products from terminal alkenes. However, stoichiometric amount of expensive boron reagent is normally required.²

Recently, several homogeneous transition metal-catalyzed reactions have been developed to afford the products with anti-Markovnikov selectivity. For instance, Nozaki and co-workers reported a method to prepare primary alcohols using Rh/Ru dual catalytic system via a tandem hydroformylation-reduction process (Scheme 4.2).⁴ Rh/Xantphos was employed to promote the hydroformylation of terminal alkenes, and Ru complex was used to reduce the aldehyde to primary alcohol. Grubbs et al. achieved a one-pot process using Pd and Ru catalysts for conversion of styrene derivatives to the corresponding primary alcohols (Scheme 4.3).⁵ In their reaction, the terminal-selective Wacker oxidation was initially performed with *t*-BuOH as a nucleophile over Pd catalyst followed by acid-catalyzed hydrolysis and Ru-catalyzed reduction to form the desired product.⁵ Previously, aldehyde-selective Wacker oxidation was reported by Grubbs et al. using a catalytic system with PdCl₂(MeCN)₂, 1,4-benzoquinone (BQ), and *t*-BuOH.⁶ The regioselectivity of products was significantly affected by the bulkiness of *t*-BuOH despite the partial positive charge (δ^+) on the internal position of the terminal alkenes.⁶ However, stoichiometric amount of BQ was required as an oxidant in their reports. Although BQ has been widely used in Pd-catalyzed reactions, such as acetoxylation⁷, aminations⁸, and alkylations⁹, a methods that do not rely on BQ or its derivatives is of great interesting because of practical and environmental concerns.



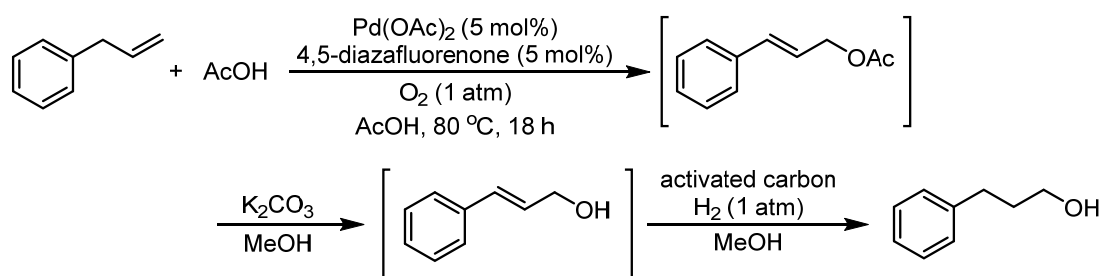
Scheme 4.2 Tandem hydroformylation-reduction process for synthesis of primary alcohols reported by Nozaki and co-workers.



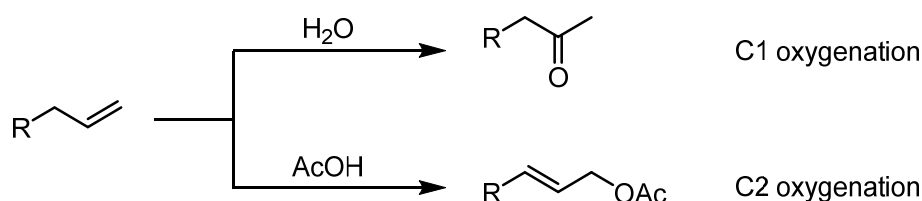
Scheme 4.3 Synthesis of 2-phenylethan-1-ol from styrene catalyzed by Pd/Ru catalytic system reported by Grubbs and co-workers.

On the other hand, allylic C-H oxidations were also developed to form anti-Markovnikov products from terminal alkenes. Stahl and co-workers developed a Pd-catalyzed allylic C-H acetoxylation of allylbenzene and its derivatives.¹⁰ In this case, π -allyl-Pd^{II} intermediate was formed from activation of allylic C-H bond of allylbenzene, and acetic acid served as a nucleophile to attack the terminal position to give the acetoxylation product, which could be transformed into primary alcohol by hydrolysis and reduction in a one-pot manner without addition of other metal catalysts (Scheme 4.4). It is noteworthy that replacement of BQ has been attempted by using molecular oxygen as the oxidant. Kaneda and co-workers reported the combination of PdCl₂ and DMA allowed highly effective oxygenation of terminal alkenes in the absence of other co-catalyst and oxidant.¹¹ The use of a different nucleophile (H₂O and AcOH) led to a complete switch in regioselectivity between the C1 and C2 position (Scheme 4.5). Showa Denko have commercialised the acetoxylation of propene to allyl acetate over Pd catalyst, and the allyl acetate could be converted to prop-2-en-1-ol by a hydrolysis process (Scheme 4.6).¹² Manyik et al. reported a method for direct transformation of 1,3-butadiene

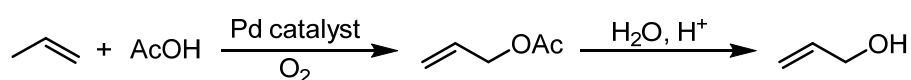
into a primary allyl alcohol (2,7-octadien-1-ol) in the presence of CO₂ (Scheme 4.7).¹³ In their reaction, substrate was activated by the Pd catalyst, and the reaction underwent the addition of carbonic acid to a bis- π -allyl Pd intermediate followed by decarboxylation. This reaction has been successfully used in industry. Tokunaga and co-workers reported a Pd-complex catalyzed direct transformation of terminal alkenes into primary allylic alcohols using H₂O as the nucleophile (scheme 4.8).¹⁴ In this reaction, HCO₃⁻ ion, which was formed from CO₂ and H₂O, attacked the terminal carbon of π -allyl-Pd^{II} intermediate to afford a half-ester, and then, followed by release of CO₂ to give the product. Other methods for preparation of primary alcohols were also developed, such as chemoenzymatic method¹⁵ and diastereoselective hydrohydroxyalkylation of 1,3-diene¹⁶. However, Pd-catalyzed allylic C-H oxidation reactions generally suffer from low activity and selectivity, limited substrate scope, non-recyclable catalyst, and in particular for requirement of stoichiometric oxidants and/or expensive organic ligands.



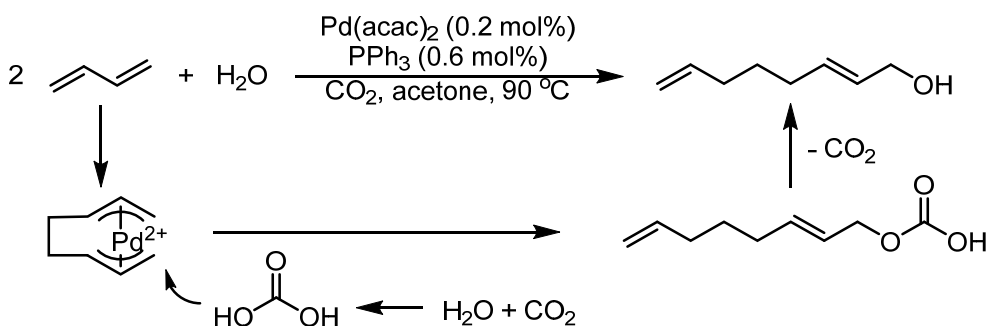
Scheme 4.4 Transformation of allylbenzene to 3-phenyl-propan-1-ol via a one-pot, three-step sequence reported by Stahl and co-workers.



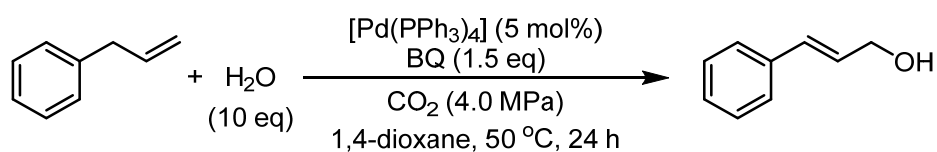
Scheme 4.5 Selectively incorporation of an oxygen atom at the C1 or C2 position reported by Kaneda and co-workers.



Scheme 4.6 Acetoxylation of propene and hydrolysis process.

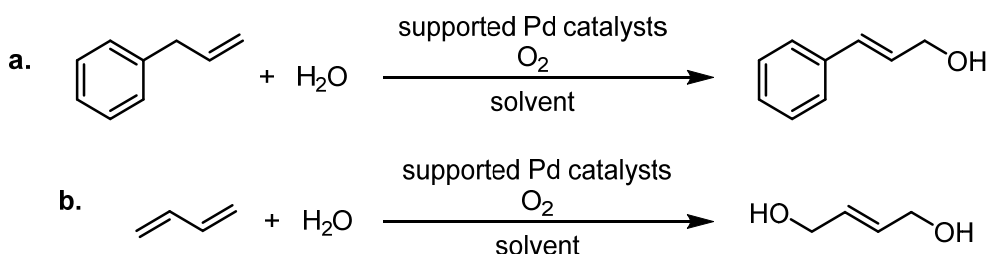


Scheme 4.7 Direct conversion of 1,3-butadiene to 2,7-octadienol reported by Manyik and co-workers.



Scheme 4.8 Homogeneous Pd catalyzed transformation of allylbenzene to cinnamyl alcohol reported by Tokunaga and co-workers.

As we have previously described, metal oxide supported Pd catalysts exhibited efficient catalytic activity in several organic reactions.^{17,18} In this work, I attempted to develop a direct transformation of terminal alkenes into primary alcohols over supported Pd catalysts using molecular oxygen as a sole oxidant. Synthesis of cinnamyl alcohol from allylbenzene was selected as a model reaction to assess the feasibility of the research purpose (Scheme 4.9a). Additionally, transformation of 1,3-butadiene to *trans*-2-butene-1,4-diol, which is recognized as an important intermediate for production of 1,4-butandiol in chemical industry, was also performed over supported Pd catalytic system (Scheme 4.9b).



Scheme 4.9 Transformation of allylbenzene into cinnamyl alcohol (a), and synthesis of 1,3-butenediol from 1,4-butadiene (b).

4.2 Results and discussion

4.2.1 Catalyst preparation and characterization

Supported Pd catalysts were prepared by deposition precipitation (DP)¹⁹ and impregnation (IMP)²⁰ according to the literatures with modifications. Al₂O₃, CeO₂, TiO₂, ZrO₂, CuO, MgO, NiO, La₂O₃, and ZnO were used as supports. Effect of surface area of ZrO₂ and CeO₂ was also examined for supported Pd(OH)₂ catalysts. In the case of Pd(OH)₂/CeO₂ with 5 wt% Pd of initial loading, actual Pd loading was determined to be 4.97 wt% by MP-AES.

XAFS measurements were used to characterize the catalysts, and some of the prepared catalysts in this chapter were listed in Table 4.1. Pd *K*-edge XANES spectra demonstrated that the chemical state of Pd was confirmed as Pd^{II} for the catalysts that prepared from Pd(NO₃)₂ (Figure 4.1, I and III), and the interaction of Pd–O was observed in RSF for all the catalysts (Figure 4.1, II and IV).¹⁷ Unfortunately, the catalysts with different supports could not be differentiated by XAFS analysis. Then, 5 wt% Pd(OH)₂/CeO₂ was tested by an *in situ* XAFS experiment. The catalyst was examined from room temperature to 200 °C and the results are shown in Figure 4.2 and Figure 4.3. In Pd *K*-edge XANES spectra, the chemical state of Pd was changed from Pd^{II} to Pd⁰ with temperature increasing. In RSF, it could be observed that the peak of Pd–O interaction was decreased through the temperature increase, and Pd–Pd was observed in the catalyst. These results demonstrated that CeO₂ supported Pd(OH)₂ was not stable in high temperature due to that the dispersed Pd particles were easy to be aggregated together to form the Pd clusters.

Table 4.1 Standard and catalyst samples for XAFS analysis.

No.	Sample	Specific surface area of Support (m ² /g)	No.	Sample	Specific surface area of Support (m ² /g)
a	Pd foil	--	g	Pd(OH) ₂ /CeO ₂	15
b	Pd(OH) ₂	--	h	Pd(OH) ₂ /CeO ₂	65
c	PdO	--	i	Pd(OH) ₂ /CeO ₂	81
d	CeO ₂	58	j	Pd(OH) ₂ /CeO ₂	123
e	Pd(OH) ₂ /ZrO ₂	91	k	Pd(OH) ₂ /CeO ₂	156
f	Pd(OH) ₂ /CeO ₂	58	l	Pd(OH) ₂ /CeO ₂	173

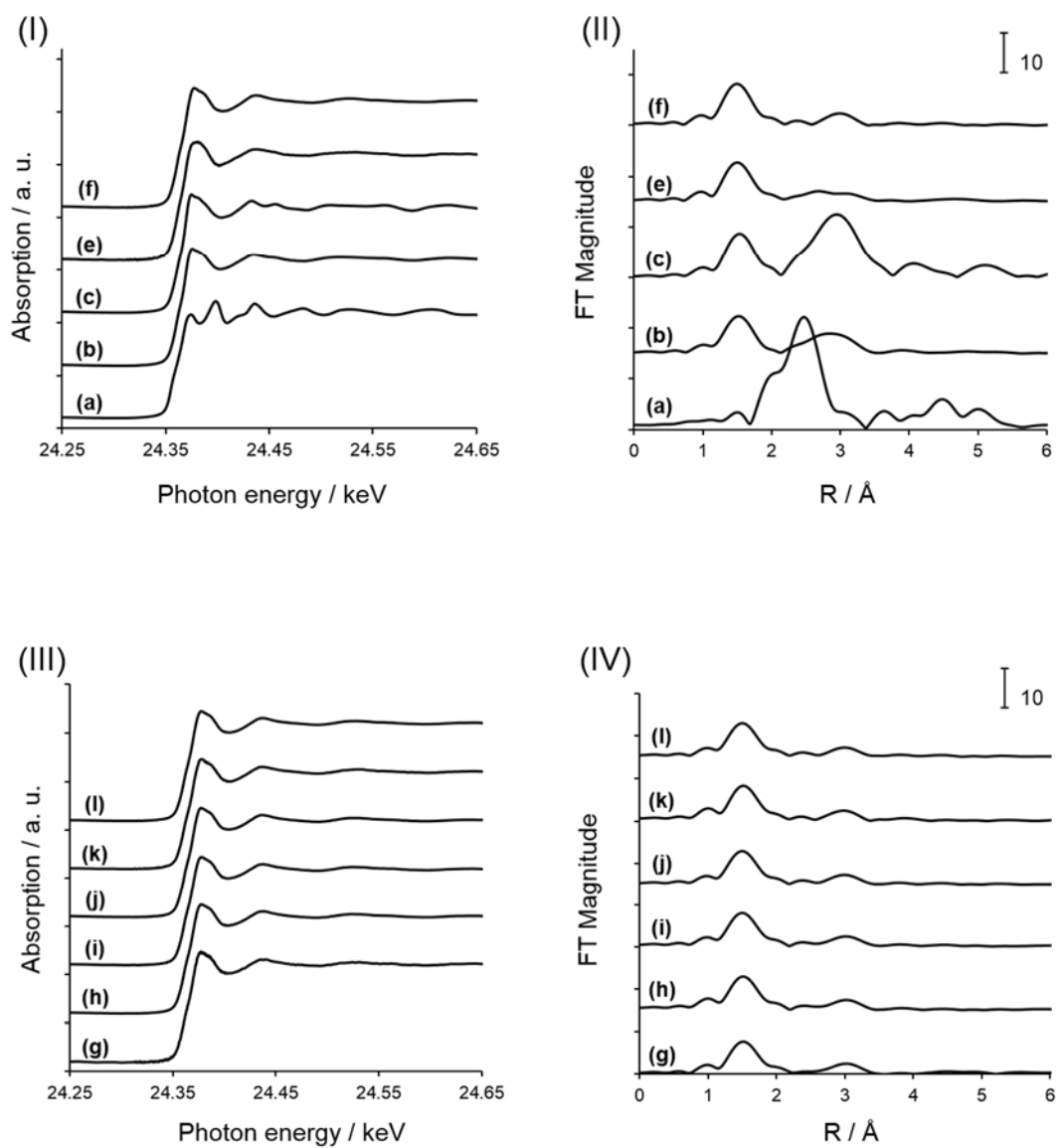


Figure 4.1 Pd K-edge XANES spectra (I, III) and radial structure functions (II, IV) of ZrO₂ and CeO₂ supported Pd(OH)₂ catalysts.

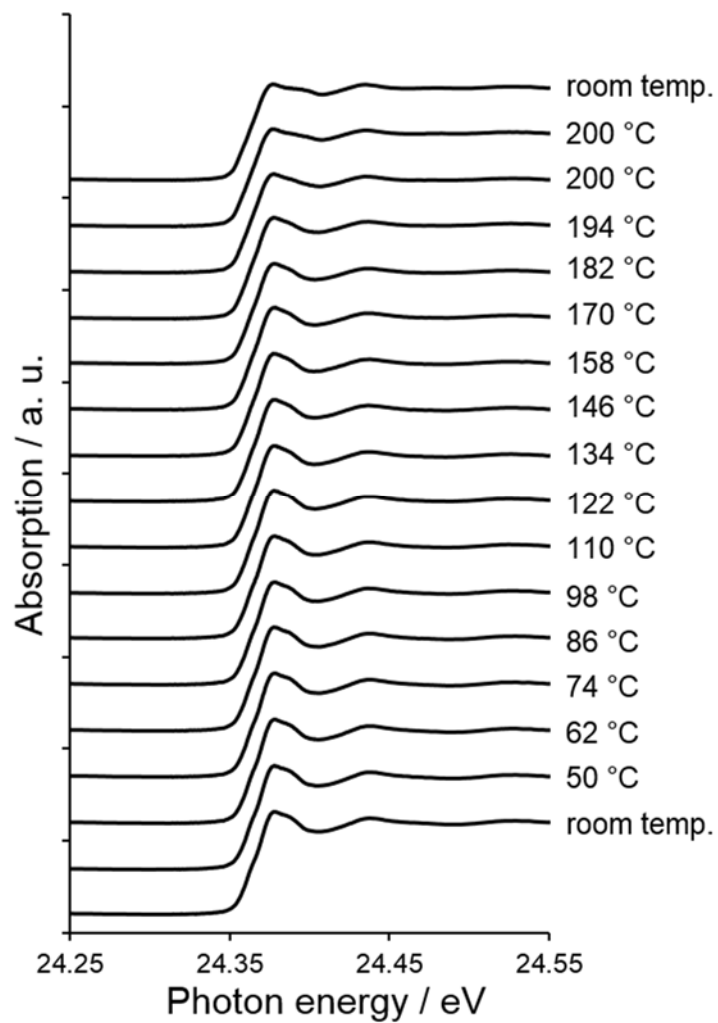


Figure 4.2 In situ Pd K-edge XANES spectra CeO₂ supported Pd(OH)₂ catalyst at elevated temperatures (3 °C/min).

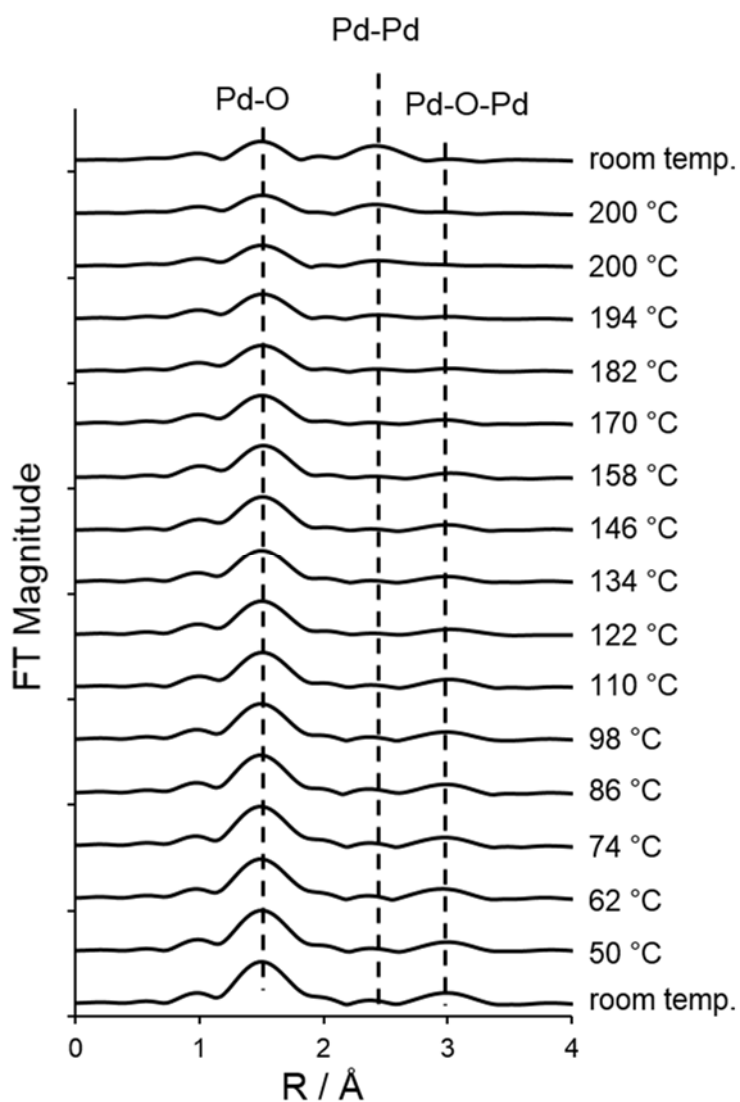


Figure 4.3 In situ radial structure functions of CeO_2 supported $\text{Pd}(\text{OH})_2$ catalyst at elevated temperatures ($3\text{ }^\circ\text{C}/\text{min}$).

CO_2 -TPD measurement was used to identify the basicity of $\text{Pd}(\text{OH})_2/\text{CeO}_2$ (CeO_2 : $58\text{ m}^2/\text{g}$). Standard $\text{Pd}(\text{OH})_2$ and CeO_2 were also tested. CO_2 desorption peak of $\text{Pd}(\text{OH})_2$ was observed at $180\text{ }^\circ\text{C}$, and two peaks at 120 and $440\text{ }^\circ\text{C}$ were observed in CeO_2 (Figure 4.4a and 4.4b). The CO_2 desorption peaks of $\text{Pd}(\text{OH})_2/\text{CeO}_2$ was shifted to $250\text{ }^\circ\text{C}$ with two shoulder peaks at 100 and $400\text{ }^\circ\text{C}$ (Figure 4.4c). This result indicated that basicity of CeO_2 became stronger by the deposition of $\text{Pd}(\text{OH})_2$.

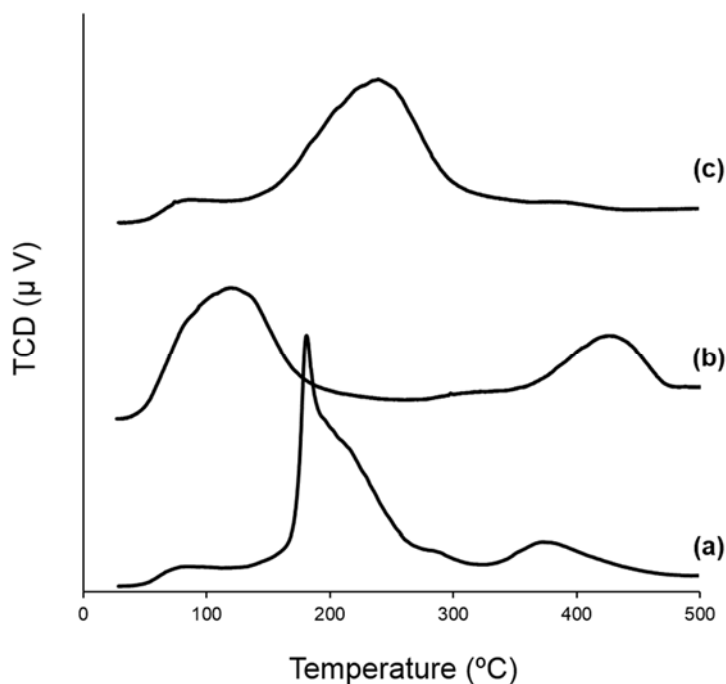
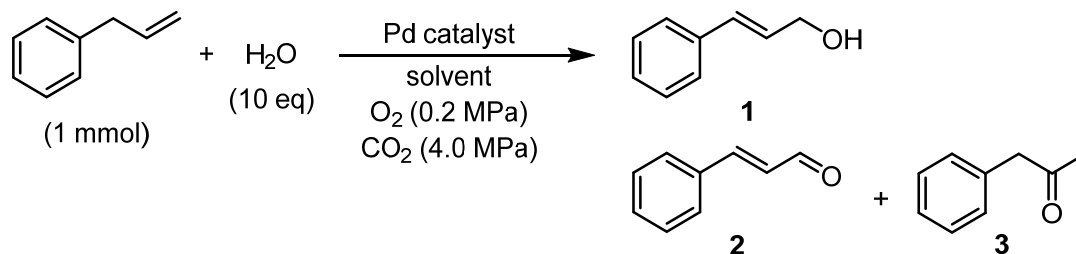


Figure 4.4 CO₂-TPD profiles of (a) Pd(OH)₂, (b) CeO₂ (58 m²/g), and (c) Pd(OH)₂/CeO₂ (58 m²/g).

4.2.2 Transformation of allylbenzene into cinnamyl alcohol

Supported Pd catalysts were initially screened for transformation of allylbenzene into primary alcohol. In analogy to the homogeneous catalytic system, high pressure of CO₂ combined with O₂ was used.^{13,14} In Table 4.2, cinnamyl alcohol (**1**), cinnamaldehyde (**2**), and phenyl acetone (**3**) were detected as products. Metal oxide supported Pd(OH)₂ showed poor catalytic activity (Table 4.2, entries 1–4). Several kinds of solvents were screened, such as 1,4-dioxane, N,N-dimethylformamide (DMF), ethyl acetate, octane, and *t*-butyl alcohol, DMSO was slightly better than other solvents in terms of yield of **1** (Table 4.2, entries 5–8), even increasing the reaction time and temperature (Table 4.2, entry 9). Interestingly, using Pd/Al₂O₃ as the catalyst, phenyl acetone, which might be formed via Wacker oxidation process, was obtained in 46% yield (Table 4.2, entry 11). Wacker oxidation using other substrates including styrene and 1-octene will be discussed later. H₂O₂ was regarded as an ideal oxidant based on several advantages such as miscible with water and relatively easy to handle.²¹ However, replacement of H₂O to H₂O₂ did not affect the conversion of allylbenzene to the corresponding products (Table 4.2, entries 6, 7, and 10). A few amount of the telomerization compounds were detected by GC as by-products, resulting in the poor mass balance in this table, although the structure of these byproducts was not clear.

Table 4.2 Reaction optimization for transformation of allylbenzene into cinnamyl alcohol in the presence of CO₂.^a



Entry	Catalyst ^b	Solvent	Temp. (°C)	T (h)	Conv. (%) ^c	Yield ^c		
						1 (%)	2 (%)	3 (%)
1	Pd(OH) ₂ /Al ₂ O ₃	DMSO	80	24	67	5	3	6
2	Pd(OH) ₂ /CeO ₂	DMSO	80	24	49	6	2	6
3	Pd(OH) ₂ /TiO ₂	DMSO	80	24	39	2	1	5
4	Pd(OH) ₂ /ZrO ₂	DMSO	80	24	52	8	0	8
5	Pd(OH) ₂ /Al ₂ O ₃	DMF	90	24	48	0	6	0
6 ^d	Pd(OH) ₂ /Al ₂ O ₃	EtOAc	90	24	10	0	1	1
7 ^d	Pd(OH) ₂ /Al ₂ O ₃	Octane	90	24	14	0	0	0
8	Pd(OH) ₂ /Al ₂ O ₃	<i>t</i> BuOH	90	24	21	0	3	0
9	Pd(OH) ₂ /Al ₂ O ₃	1,4-Dioxane	90	40	38	1	7	3
10 ^d	Pd/ZrO ₂	DMSO	90	24	23	0	1	2
11	Pd/Al ₂ O ₃	DMSO	80	48	90	0	16	46

^a Reaction conditions: allylbenzene (1 mmol), catalyst (Pd 1.5 mol%), H₂O (10 mmol), solvent (1.5 mL), CO₂ (4.0 MPa), O₂ (0.5 MPa).

^b These catalysts were prepared by DP method using PdCl₂ as a precursor.

^c Calculated on the basis of GC analysis using tridecane as an internal standard.

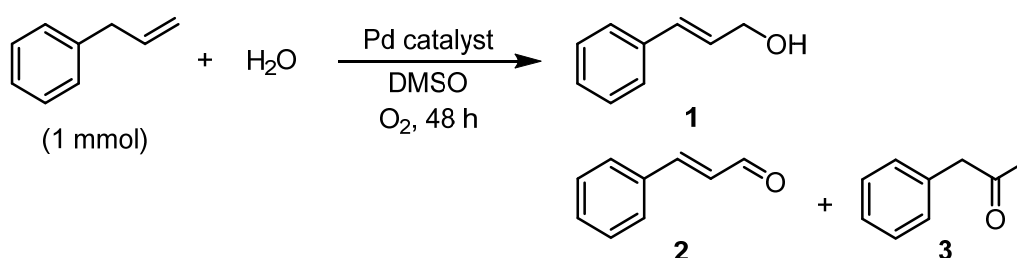
^d H₂O₂ (10 eq) was used instead of H₂O.

Next, catalyst preparation methods were optimized. Replacing PdCl₂ with Pd(NO₃)₂ as the precursor improved the catalytic activity (Table 4.3, entries 1–3). Besides, the reaction proceeded well in the absence of CO₂. In entry 4, Pd/ZrO₂ was prepared by IMP method showed good catalytic activity, but cinnamaldehyde and phenyl acetone were obtained as major products. Amount of H₂O significantly affected the reactivity, and 10 equivalent of H₂O gave the highest yield of cinnamyl alcohol (Table 4.3, entries 2 vs. 5 and 6). The concentration of substrate was optimized to 0.5 M, and

cinnamyl alcohol was obtained in 23% yield over Pd/Al₂O₃ (Table 4.3, entry 8). In addition, the pressure of oxygen was discussed. In contrast with air and O₂ balloon conditions (Table 4.3, entries 10 and 11), increasing the pressure of O₂ resulted better reactivity and selectivity to cinnamyl alcohol (Table 4.3, entry 12). A comparison of reaction temperature suggested that 80 °C would be suitable (Table 4.3, entry 12). Moreover, an increase in the amount of Pd improved the yield of cinnamyl alcohol to 37% (Table 4.3, entry 15).

Based on the result that basic metal oxide (CeO₂) supported catalyst showed higher catalytic activity than amphoteric metal oxides (ZrO₂ and Al₂O₃) as support. Several kinds of basic metal oxides were screened as support, including MgO, NiO, La₂O₃, and ZnO (Table 4.3, entry 16–19). MgO supported Pd catalyst exhibited poor catalytic activity was possibly caused by two reasons: the low specific surface area and impurities of MgO; or a stable structure, which coordinated of Pd(OH)₂ with MgO, inhibited Pd particles to the catalytic cycle. Although NiO, La₂O₃, and ZnO, supported Pd(OH)₂ catalysts showed good selectivity to anti-Markovnikov selective products (cinnamyl alcohol and cinnamaldehyde), the mass balance and the yield of cinnamyl alcohol were unsatisfactory. Other supported transition metal catalysts, such as iridium, ruthenium, and gold catalysts, showed negligible catalytic activity (Table 4.3, entries 20–22). Through optimization of reaction conditions in Table 4.2 and Table 4.3, supported Pd^{II} catalysts exhibited better catalytic activity to prepare anti-Markovnikov products (**1** and **2**) than supported Pd⁰ catalyst. This result is consistent with homogeneous catalytic systems that Pd^{II} can initially activate the α -H of allylbenzene to form a π -allyl Pd^{II} intermediate.^{10,14} In addition, I consider that the hydroxyl group on Pd(OH)₂ might react with α -H to produce H₂O, and promote the reaction. Therefore, the reaction conditions were discussed further with supported Pd(OH)₂ catalysts.

Table 4.3 Catalyst screening for transformation of allylbenzene into cinnamyl alcohol in the absence of CO₂.^a



Entry	Catalyst ^b (1.5 mol%)	H ₂ O (eq)	Conc. (M)	O ₂ (MPa)	Temp. (°C)	Conv. (%) ^c	Yield ^c		
							1 (%)	2 (%)	3 (%)
1	Pd(OH) ₂ /Al ₂ O ₃	10	0.7	0.5	80	97	17	10	30
2	Pd(OH) ₂ /ZrO ₂	10	0.7	0.5	80	82	32	11	14
3	Pd/Al ₂ O ₃	10	0.7	0.5	80	83	20	12	15
4	Pd/ZrO ₂ ^d	10	0.7	0.5	80	92	0	21	14
5	Pd(OH) ₂ /ZrO ₂	0	0.7	0.5	80	21	0	4	0
6	Pd(OH) ₂ /ZrO ₂	20	0.7	0.5	80	98	11	20	27
7	Pd/Al ₂ O ₃	10	1.0	0.5	80	94	15	21	14
8	Pd/Al ₂ O ₃	10	0.5	0.5	80	63	23	9	6
9	Pd/Al ₂ O ₃	10	0.4	0.5	80	44	19	10	6
10	Pd(OH) ₂ /ZrO ₂	10	0.5	0.1 ^e	80	21	2	4	2
11	Pd(OH) ₂ /ZrO ₂	10	0.5	0.1 ^f	80	37	12	6	5
12	Pd(OH) ₂ /ZrO ₂	10	0.5	1.0	80	86	40	9	13
13	Pd(OH) ₂ /ZrO ₂	10	0.5	0.5	70	54	26	5	7
14	Pd(OH) ₂ /ZrO ₂	10	0.5	0.5	90	89	26	13	23
15 ^g	Pd(OH) ₂ /ZrO ₂	10	0.5	0.5	80	94	37	16	19
16 ^g	Pd(OH) ₂ /MgO	15	0.5	2.0	80	19	0	2	0
17 ^g	Pd(OH) ₂ /NiO	15	0.5	2.0	80	95	24	18	2
18 ^g	Pd(OH) ₂ /La ₂ O ₃	15	0.5	2.0	80	63	13	15	2
19 ^g	Pd(OH) ₂ /ZnO	15	0.5	2.0	80	88	24	19	1
20	Ir(OH) ₃ /Al ₂ O ₃	10	0.5	1.0	80	5	0	0	0
21	Ru(OH) ₃ /Al ₂ O ₃	10	0.5	1.0	80	9	0	0	0
22	Au(OH) ₃ /Al ₂ O ₃	10	0.5	1.0	80	11	0	0	0

^a Reaction conditions: allylbenzene (1 mmol), catalyst (Pd 1.5 mol%), H₂O, DMSO, O₂, 48 h.

^b These catalysts were prepared by DP method using Pd(NO₃)₂ as a precursor.

^c Calculated on the basis of GC analysis using tridecane as an internal standard.

^d The catalyst was prepared by IMP method.

^e Air (0.1 MPa)

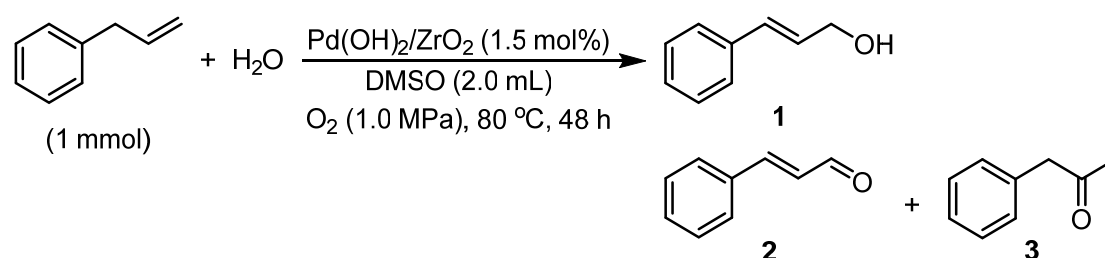
^f O₂ balloon.

^g Pd 2.5 mol%.

To evaluate support effects, several ZrO₂ with different specific surface area supported Pd(OH)₂ were prepared. As shown in Table 4.4, the catalytic activity and selectivity were altered by the specific

surface area. Pd(OH)₂ supported on ZrO₂ with 30 m²/g showed low catalytic activity and selectivity to cinnamyl alcohol (Table 4.4, entry 1), suggesting that these Pd particles on the small specific surface area ZrO₂ were easy to be aggregated into large particles, which might cause the low catalytic activity for transformation of allylbenzene. In contrast, Pd particles supported on ZrO₂ with high surface area could be well-distributed, and this result higher catalytic activity. Indeed, Pd(OH)₂ supported on ZrO₂ with 91 and 94 m²/g showed better results than entry 1 (Table 4.4, entries 2 and 3). ZrO₂ with 194 and 280 m²/g are non-crystalline solids (amorphous), and Pd(OH)₂ supported on these ZrO₂ exhibited low catalytic activity (Table 4.4, entries 4 and 5).

Table 4.4 Optimization of reaction conditions with ZrO₂ supported Pd(OH)₂.^a



Entry	Specific surface area of ZrO ₂ (m ² /g)	Conv. (%) ^b	1 (%)	Yield ^b 2 (%)	3 (%)
1	30	67	25	6	9
2	91	86	40	9	13
3	94	84	34	13	17
4	194	57	20	5	3
5	280	86	23	9	14

^a Reaction conditions: allylbenzene (1 mmol), Pd(OH)₂/ZrO₂ (Pd 1.5 mol%), H₂O (10 mmol), DMSO (2.0 mL), O₂, 80 °C, 48 h.

^b These catalysts were prepared by DP method using Pd(NO₃)₂ as a precursor.

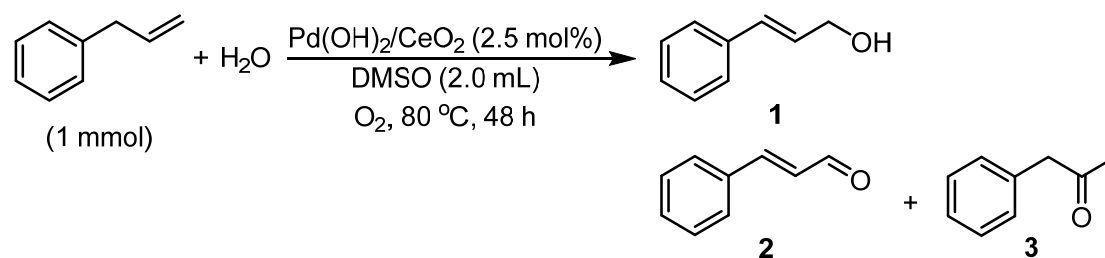
^c Calculated on the basis of GC analysis using tridecane as an internal standard.

Pd(OH)₂ supported on various types of CeO₂ were also investigated, and the results are shown in Table 4.5. The basicity of CeO₂ is relatively higher than ZrO₂,²² and thus, CeO₂ supported Pd(OH)₂ catalyst is regarded as a more stable catalyst than Pd(OH)₂/ZrO₂. Similar to Table 4.4, Pd(OH)₂ supported on CeO₂ (58 m²/g) exhibited higher catalytic activity than CeO₂ with 15 m²/g supported Pd(OH)₂ (Table 4.5, entries 1 and 2). CeO₂ with 65, 81, 123, and 173 m²/g supported Pd(OH)₂ catalysts

also displayed good catalytic activity (Table 4.5, entries 3–5 and 7), but the selectivity to cinnamyl alcohol was lower than Pd(OH)₂/CeO₂ (CeO₂: 58 m²/g). The impurities, such as small molecules, atoms, and ions, are easy to be adsorbed on the metal oxide with high specific surface area, and this might cause the decreasing of catalytic activity for supported Pd(OH)₂ catalysts. Therefore, using CeO₂ (58 m²/g) with high purity (> 99.99%) and moderate specific surface area as the support, giving a better performance than other types of CeO₂ supported catalysts. In addition, catalytic activity of Pd(OH)₂/CeO₂ was not only affected by the specific surface area of support. For example, CeO₂ (157 m²/g) supported Pd(OH)₂ was inactive for transformation of allylbenzene (Table 4.5, entry 6), and this might be caused by other physical properties of CeO₂ such as high ignition loss (7.99%), low pore volume (2.82 ml/g), and preparation methods (Table 4.6). The physical properties of CeO₂ with 65, 81, and 123 m²/g were also summarized in Table 4.6. In Table 4.7, physical properties of Pd(OH)₂ catalysts supported on different CeO₂ were tested by Brunauer-Emmett-Teller (BET) method. In contrast with Table 4.6, both the specific surface area and pore volume of CeO₂ were slightly decreased after preparation of catalysts, suggesting that Pd(OH)₂ particles were deposited on the surface of support. Unfortunately, the details about the support effects and catalytic activity or product selectivity were not included in this thesis, this work need to be further studied.

Other reaction conditions were optimized with Pd(OH)₂/CeO₂ (58 m²/g), when the pressure of O₂ was increased to 2.0 MPa, the yield of cinnamyl alcohol was improved to 51% (Table 4.5, entry 8). When the amount of H₂O was increased to 15 mmol, the yield was also improved to 65% (Table 4.5, entry 9).

Table 4.5 Optimization of reaction conditions with CeO₂ supported Pd(OH)₂.^a



Entry	Specific surface area of CeO ₂ (m ² /g)	H ₂ O (eq)	O ₂ (MPa)	Conv. (%) ^b	1 (%)	Yield ^b 2 (%)	3 (%)
1	15	10	0.5	67	20	6	4
2	58	10	0.5	81	46	13	10

3	65	10	0.5	88	30	22	10
4	81	10	0.5	96	42	21	14
5	123	10	0.5	97	37	23	17
6	157	10	0.5	20	0	0	0
7	173	10	2.0	95	39	21	14
8	58	10	2.0	92	60	14	11
9	58	10	3.0	89	51	12	11
10	58	15	2.0	98	65	18	16

^a Reaction conditions: allylbenzene (1 mmol), Pd(OH)₂/CeO₂ (Pd 2.5 mol%), H₂O, DMSO (2.0 mL), O₂, 80 °C, 48 h.

^b These catalysts were prepared by DP method using Pd(NO₃)₂ as a precursor.

^c Calculated on the basis of GC analysis using tridecane as an internal standard.

Table 4.6 Physical properties for CeO₂ with 157, 123, 81, and 65 m²/g.

No.	JRC-CEO-1	JRC-CEO-2	JRC-CEO-3	JRC-CEO-4
Purity (%)	99.99	99.97	99.97	99.80
Ignition loss (%)	7.99	2.28	0.59	-
Specific surface area (m ² /g)	157	123	81	65
Mean pore diameter (nm)	2.82	7.08	11.6	-
Total pore volume (ml/g)	0.11	0.23	0.24	-
Crystallite diameter (nm)	7.4	8.7	11.0	12.6
Preparation methods	calcination of cerium (III) carbonate at 300 °C	calcination of cerium (IV) hydroxide carbonate at 400 °C	calcination of cerium (IV) hydroxide carbonate at 600 °C	Chemical vapor deposition method at 2000 °C

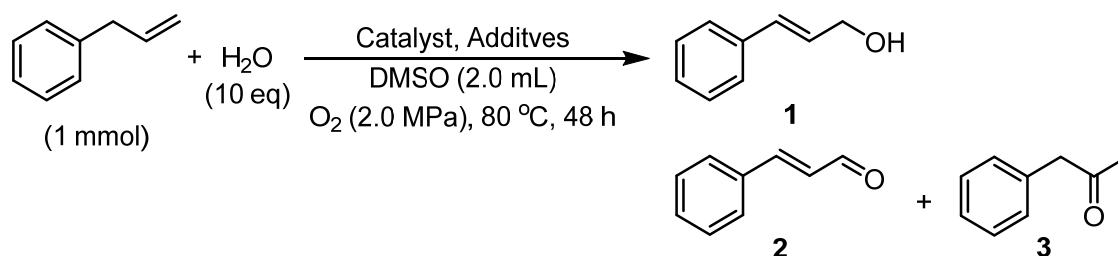
Table 4.7 Physical properties for Pd(OH)₂ supported on different CeO₂ tested using BET method.

Catalyst	5 wt% Pd(OH) ₂ /CeO ₂	5 wt% Pd(OH) ₂ /CeO ₂	5 wt% Pd(OH) ₂ /CeO ₂	5 wt% Pd(OH) ₂ /CeO ₂
CeO ₂	JRC-CEO-1	JRC-CEO-2	JRC-CEO-3	JRC-CEO-4
Specific surface area (m ² /g)	130	105	74	31

Mean pore diameter (nm)	3.2	7.8	10.7	17.0
Total pore volume (ml/g)	0.10	0.20	0.20	0.13
Preparation methods	DP	DP	DP	DP

Then, several additives were examined, and inorganic bases, for example, NaOH and K₂CO₃, were added. However, the catalytic activity significantly decreased (Table 4.8, entries 1 and 2). Organic base was also tested, whereas the reaction almost stopped over Pd(OH)₂/ZrO₂ (Table 4.8, entries 3 and 4). Acid additives, such as AcOH and PivOH, did not affect the catalytic activity and selectivity of this reaction (Table 4.8, entries 5 and 6). Next, several oxidants, including organic and inorganic oxidants, were employed. Fe₃O₄ and CuO are usually used as inorganic oxidants or co-catalysts for oxidative processes. However, the addition of them were not effective (Table 4.8, entries 7 and 8). When benzoquinone (BQ) was used, the yield of cinnamyl alcohol was improved to 67% (Table 4.8, entry 9). When 2,5-di-*tert*-butyl-benzoquinone (2,5-*t*Bu₂-BQ), which was reported as a good oxidant in homogeneous catalytic system,¹⁴ was added, the catalytic activity was markedly improved, affording cinnamyl alcohol in 74% yield (Table 4.8, entry 10). In previous studies, BQs may act three roles in the allylic C–H acetoxylation of terminal alkenes: (1) promotion of nucleophilic attack; (2) displacement of allylic products from Pd⁰; and (3) re-oxidizing Pd⁰ to Pd^{II}.²³ In this work, although 2,5-*t*Bu₂-BQ could improve the yield of cinnamyl alcohol to 74%, supported Pd catalytic system in the presence of O₂ exhibited good catalytic activity as well.

Table 4.8 Optimization of reaction conditions with additives.^a



Entry	Catalyst (mol%) ^b	Additives (mmol)	Conv. (%) ^c	Yield ^c		
				1 (%)	2 (%)	3 (%)
1	Pd(OH) ₂ /ZrO ₂ (1.5)	NaOH (0.1)	35	3	5	0
2	Pd(OH) ₂ /ZrO ₂ (1.5)	K ₂ CO ₃ (0.1)	40	6	7	0

3	Pd(OH) ₂ /ZrO ₂ (1.5)	NEt ₃ (0.2)	19	0	0	0
4	Pd(OH) ₂ /ZrO ₂ (1.5)	DIPEA (0.2)	27	0	0	0
5	Pd(OH) ₂ /ZrO ₂ (1.5)	AcOH (0.2)	75	31	9	14
6	Pd(OH) ₂ /ZrO ₂ (1.5)	PivOH (0.2)	76	32	11	21
7	Pd(OH) ₂ /CeO ₂ (2.5)	Fe ₃ O ₄ (0.2)	64	24	12	11
8	Pd(OH) ₂ /CeO ₂ (2.5)	CuO (0.2)	33	0	0	0
9	Pd(OH) ₂ /CeO ₂ (2.5)	BQ (0.2)	99	67	10	20
10	Pd(OH) ₂ /CeO ₂ (2.5)	2,5- <i>t</i> Bu ₂ -BQ (0.2)	99	74	12	13

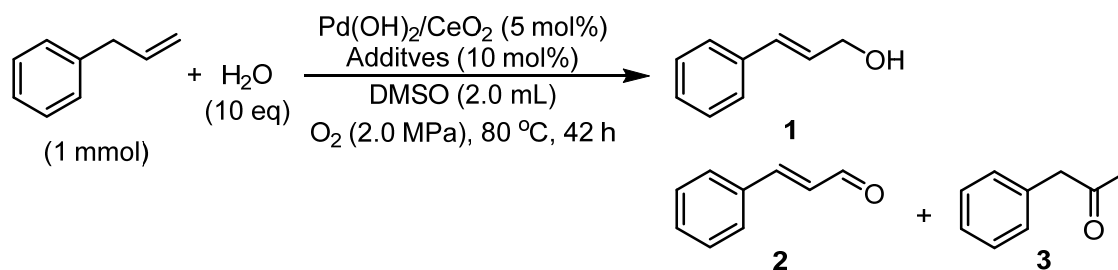
^a Reaction conditions: allylbenzene (1 mmol), Pd(OH)₂/MO (Pd 1.5 or 2.5 mol%), H₂O (10 mmol), additives, DMSO (2.0 mL), O₂ (2.0 MPa), 80 °C, 48 h.

^b These catalysts were prepared by DP method using Pd(NO₃)₂ aqueous solution as precursor. The surface area of ZrO₂ and CeO₂ was 91 m²/g and 58 m²/g, respectively.

^c Calculated on the basis of GC analysis using tridecane as an internal standard.

Other additives were screened, and the results are summarized in Table 4.9. The standard reaction conditions are shown in entry 1. In the presence of 5 mol% Pd catalyst, cinnamyl alcohol was obtained in 51% yield. BQs with different substituents were used as additives. Adding 2-methyl substituted BQ slightly improved the yield of cinnamyl alcohol, although phenyl acetone was increased (Table 4.9, entry 2). In entry 3, the addition of 10 mol% 2-*tert*-butyl-BQ gave the highest yield (69%) of cinnamyl alcohol. In analogy to the result for addition of 2,5-*t*Bu₂-BQ, electron-donating groups decreased the oxidizing ability of BQ, and steric effect decreased the coordination ability of BQ to Pd center. This might improve the coordination of Pd catalyst to substrates and lead to high yield. Several phosphine ligands were also screened (Table 4.9, entries 8–13). However, the selectivity of cinnamyl alcohol could not be improved. In particular, the yield was reduced in the presence of the phosphine with strong electron-donating substituents. Moreover, the reactions were completely inhibited with using nitrogen-containing ligands, which might coordinated with Pd center, and inhibit the catalytic cycle by generating the stable Pd intermediate (Table 4.9, entries 14–16).

Table 4.9 Optimization of reaction conditions with other additives.^a



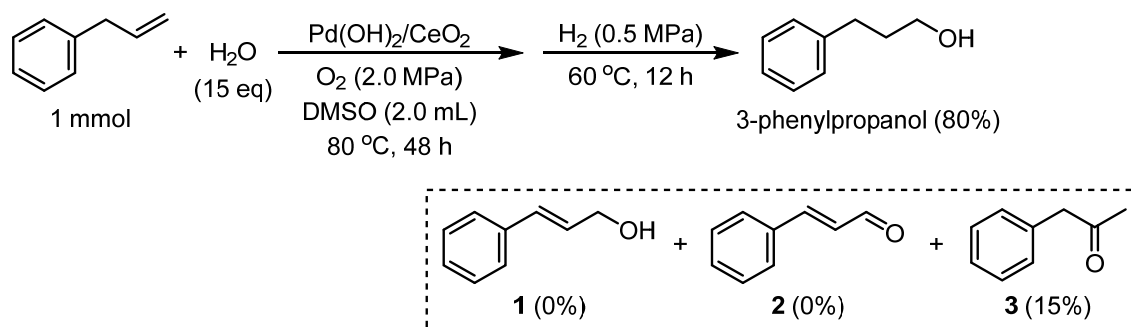
Entry	Additive	Conv. (%) ^b	Yield ^b		
			1 (%)	2 (%)	3 (%)
1	--	92	51	20	15
2		98	57	12	21
3		100	69	15	14
4		89	47	19	14
5		98	57	17	21
6		100	59	13	25
7		98	51	12	26
8	PPh ₃	98	58	18	19
9		85	47	14	9

10		97	49	18	17
11		59	18	12	2
12		94	44	16	15
13		92	41	19	24
14		1	0	0	0
15		8	0	0	0
16		5	0	0	0

^a Reaction conditions: allylbenzene (1 mmol), Pd(OH)₂/MO (Pd 1.5 or 2.5 mol%), H₂O (10 mmol), additives (0.1 mmol), DMSO (2.0 mL), O₂ (2.0 MPa), 80 °C, 42 h.

^b Calculated on the basis of GC analysis using tridecane as an internal standard.

To evaluate the feasibility for the synthesis of 3-phenylpropanol from allylbenzene, a sequential allylic oxidation and hydrogenation were performed in a one-pot process (Scheme 4.10). The yield of 3-phenylpropanol was 80%, and 15% of phenylacetone was also observed. This result suggested that the double bonds and formyl groups could be reduced over Pd(OH)₂/CeO₂ by H₂.



Scheme 4.10 One-pot process to synthesize 3-phenylpropanol from allylbenzene.

4.2.3 Reaction progress in allylic oxidation of allylbenzene

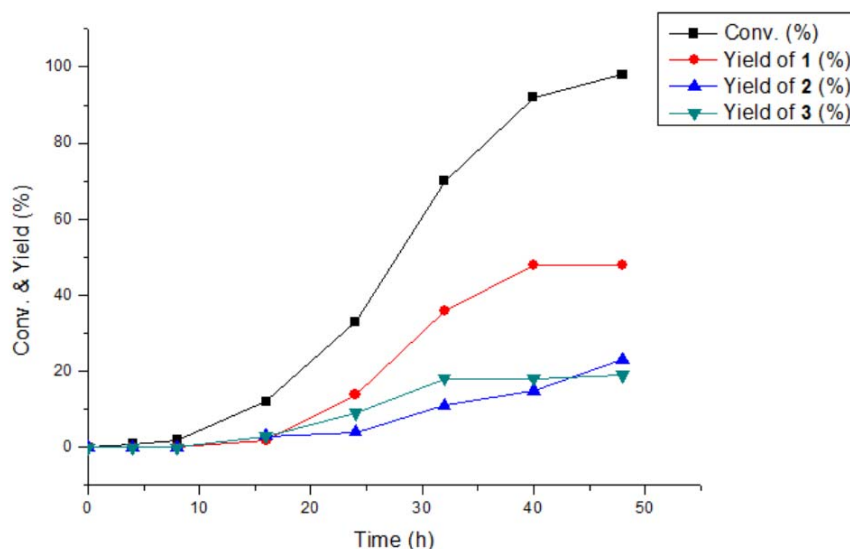
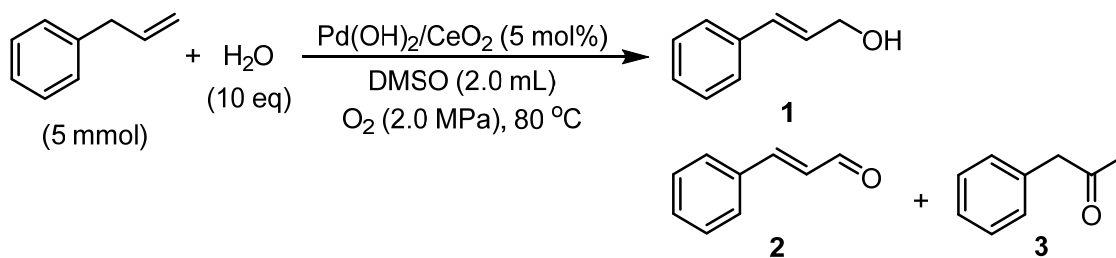
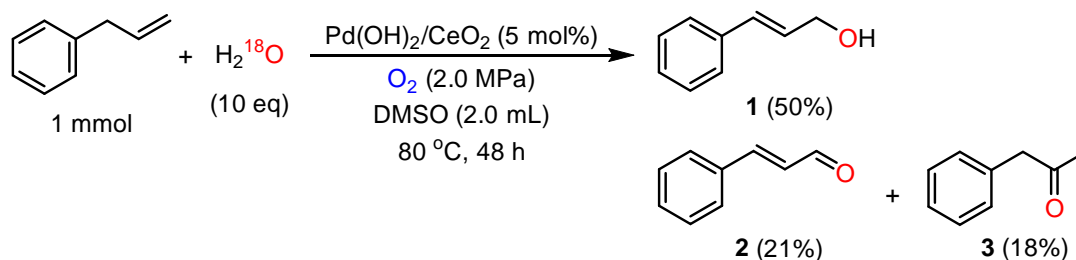


Figure 4.5 Time-conversion curve for the oxidation of allylbenzene.

To monitor the reaction progress, the reaction mixtures were detected by GC at intervals. In Figure 4.5, the reaction conversion increased rapidly after 8 h, but the yields of all the products were low. After 16 h, the conversion was increased to 12%, and three products were produced simultaneously. The selectivity was low at this stage, because telomerization compounds from allylbenzene were also observed as by-products. The yield of cinnamyl alcohol was increased more efficiently than other two compounds (**2** and **3**) after 24 h. Consequently, cinnamyl alcohol was yielded in 48% after 40 h, and cinnamaldehyde gradually increased. These results suggested that 40 h was a suitable reaction time for the synthesis of cinnamyl alcohol, and cinnamaldehyde might be produced from cinnamyl alcohol by over oxidation.

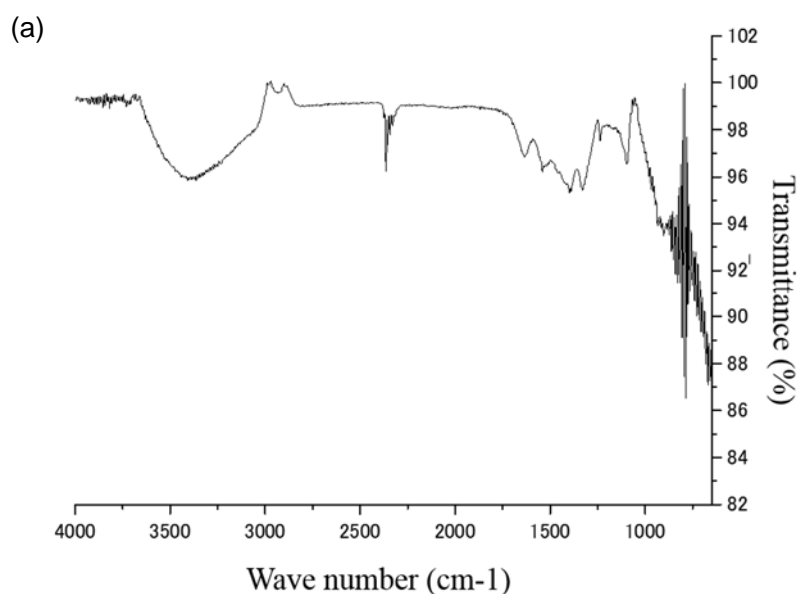
4.2.5 Reaction pathway for the allylic oxidation of terminal alkenes into primary allylic alcohols

To probe the reaction pathway, $\text{H}_2(^{18}\text{O})$ was used to determine the source of oxygen atoms in products. As shown in Scheme 4.11, ^{18}O was incorporated into all the products.



Scheme 4.11 $\text{H}_2(^{18}\text{O})$ examination for oxidation of allylbenzene.

Next, I attempted to identify the coordination ability of DMSO to Pd(OH)_2 , because DMSO has been reported as a ligand for homogeneous Pd-catalyzed reactions.²⁴ $\text{Pd(OH)}_2/\text{CeO}_2$ was treated in DMSO at 80°C for 24 h, filtrated, and dried in air overnight after washing by acetone. As shown in Figure 4.6, $\text{Pd(OH)}_2/\text{CeO}_2$ after treatment with DMSO showed a weak peak at 1030 cm^{-1} corresponding to the stretch vibration of S=O bond,²⁵ and this peak was not observed when only CeO_2 was treated in DMSO with same conditions. These results indicated that DMSO might coordinate to Pd(OH)_2 during the reaction.



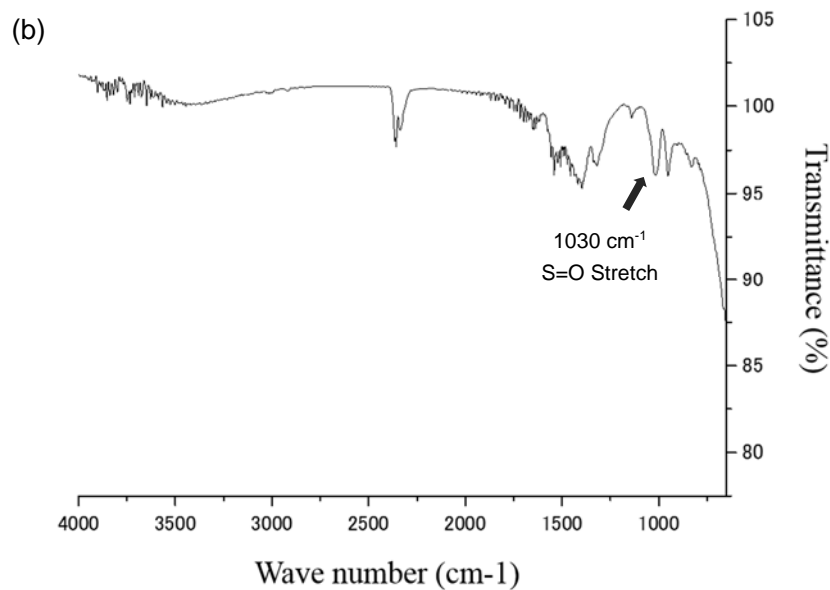


Figure 4.6 FT-IR spectra of (a) fresh Pd(OH)₂/CeO₂, and (b) Pd(OH)₂/CeO₂ treated with DMSO at 80 °C for 24 h.

The chemical state of Pd after reaction was confirmed by XAFS, and the results are shown in Figure 4.7. As we have confirmed that the chemical state of Pd in fresh Pd(OH)₂/CeO₂ was Pd^{II}. The chemical state of Pd after the reaction was also identified as Pd^{II} from XANES spectra (Figure 4.7a). The interaction of Pd–Pd was observed in RSF in both samples (Figure 4.7b).

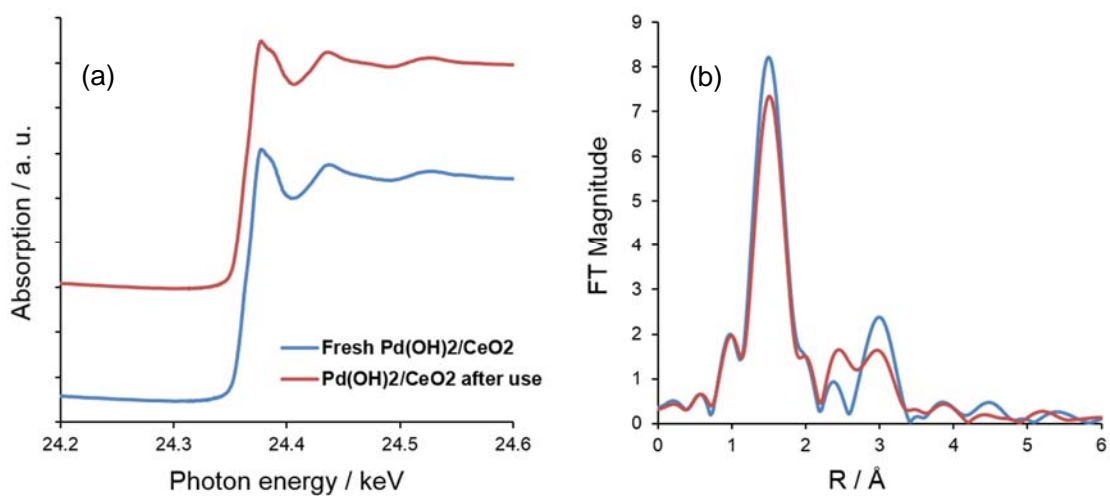


Figure 4.7 XAFS results of Pd(OH)₂/CeO₂ after use (red) and fresh Pd(OH)₂/CeO₂ (blue); (a) XANES spectra, and (b) radial structure functions.

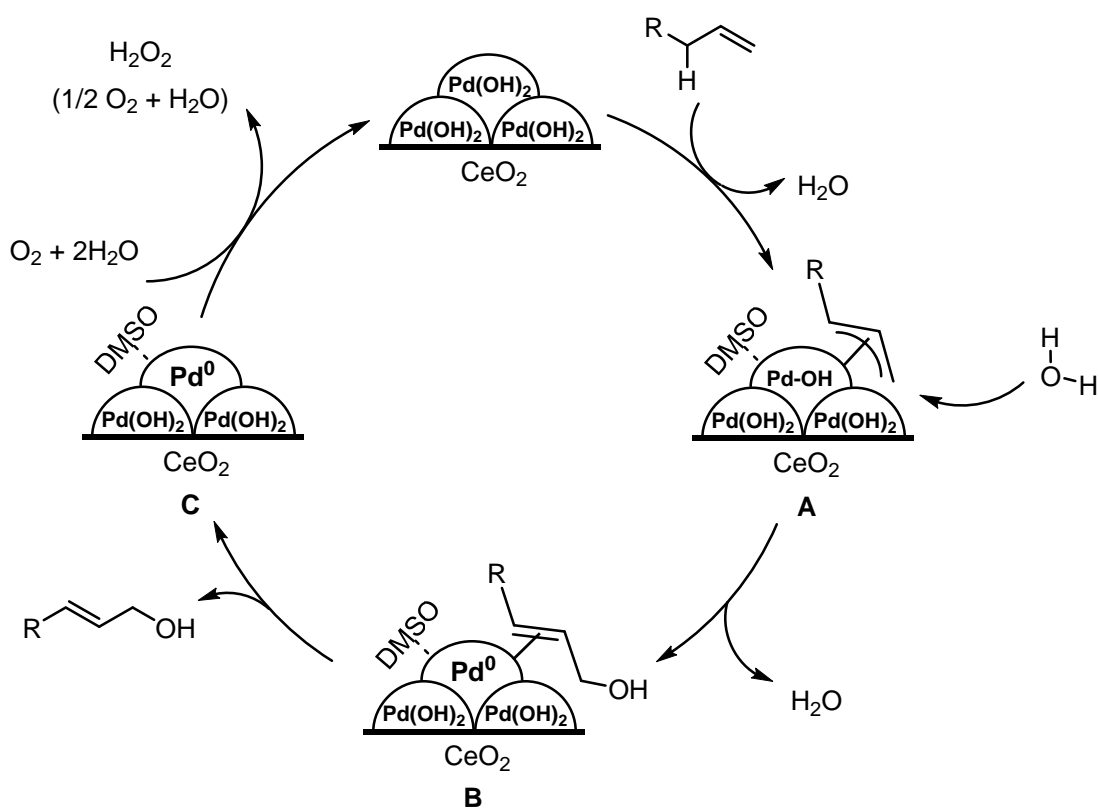


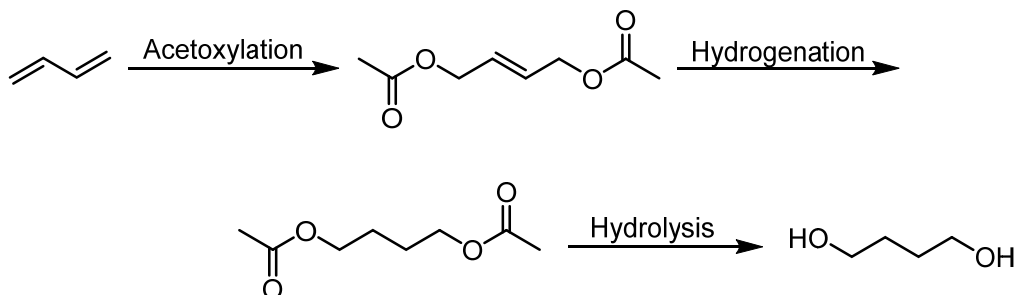
Figure 4.8 Possible reaction pathway for transformation of allylbenzene into cinnamyl alcohol.

Consequently, the reaction pathway is speculated in Figure 4.8. Allylic C–H bond is initially activated by supported Pd(OH)₂. Pd(OH)₂ serves as a basic component and reacts with substrate to form H₂O and π-allyl Pd^{II} intermediate (A). DMSO coordinate with Pd to provide a more stable structure. H₂O works as a nucleophile to attack the terminal position of π-allyl Pd^{II} intermediate, and form the intermediate (B). Pd⁰ species leave the substrate and are stabilized by DMSO. Simultaneously, primary allylic alcohol is formed. Pd⁰–DMSO is re-oxidized by O₂ and H₂O to re-generate the Pd(OH)₂.

4.2.6 Synthesis of *trans*-2-butene-1,4-diol from 1,3-butadiene

Transformation of terminal alkenes into primary alcohols also represent a long-standing challenge in chemical industry. For example, 1,4-butanediol, which is produced on an enormous scale (about 1 million metric tons annually), is an important industrial material as organic solvents and intermediate for polymers, paints, and pharmaceutical products.²⁶ In industrial process, 1,4-butanediol is produced by three steps including acetoxylation, hydrogenation, and hydrolysis. (Scheme 4.12).²⁷ These steps consumed large amount of energy and organic solvents for separation and purification of

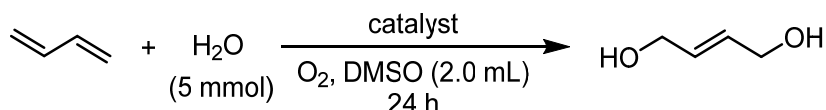
the products. Therefore, a straightforward oxidative hydration 1,3-butadiene to produce 1,4-butanediol is quite meaningful.



Scheme 4.12 Industrial process for production of 1,4-butanediol from 1,3-butadiene.

The oxidative hydration of 1,3-butadiene was also evaluated over supported Pd(OH)₂ catalysts. Due to the fact that the boiling point of 1,3-butadiene was lower than room temperature, 1,3-butadiene was introduced into the autoclave by cooling with liquid nitrogen. Since the amount of 1,3-butadiene was difficult to control, product yields were calculated based on the amount of H₂O added. After reaction, *trans*-2-butene-1,4-diol was detected as the product (Table 4.10). ZrO₂ supported Pd(OH)₂ promoted the reaction to give *trans*-2-butene-1,4-diol in 15% yield (Table 4.10, entries 1 and 2). CeO₂ supported Pd(OH)₂ was also screened. When CeO₂ with 15 m²/g surface area was used as a support, the catalytic activity was enhanced, and yield was improved to 24% (Table 4.10, entry 4). Pd(OH)₂/CeO₂ (CeO₂: 58 m²/g) gave *trans*-2-butene-1,4-diol in 31% yield under the optimized reaction conditions (Table 4.10, entry 7). In entry 8, when DMF was used as a solvent, the reaction was completely inhibited. Commercially available Pd/C and Pd(OH)₂/C were also tested, but, no product was formed (Table 4.10, entries 9 and 10).

Table 4.10 Transformation of 1,3-butadiene into *trans*-2-butene-1,4-diol.^a



Entry	Catalyst (Pd mmol)	Specific surface area of support (m ² /g)	1,3-butadiene (mmol) ^b	O ₂ (MPa)	Temp. (°C)	Yield (%) ^c
1	Pd(OH) ₂ /ZrO ₂ (0.015)	91	16	0.25	70	6
2	Pd(OH) ₂ /ZrO ₂ (0.04)	91	19	0.5	55	15

3	Pd(OH) ₂ /CeO ₂ (0.025)	15	11	2.0	60	13
4	Pd(OH) ₂ / CeO ₂ (0.04)	15	23	2.0	55	24
5 ^d	Pd(OH) ₂ / CeO ₂ (0.025)	58	27	0.1	55	3
6 ^e	Pd(OH) ₂ / CeO ₂ (0.025)	58	19	2.0	55	8
7	Pd(OH) ₂ / CeO ₂ (0.025)	58	21	2.0	55	31
8 ^f	Pd(OH) ₂ / CeO ₂ (0.025)	58	15	2.0	55	0
9	Pd/C (0.025)	--	31	2.0	55	0
10	Pd(OH) ₂ /C (0.025)	--	15	2.0	55	0

^a Reaction conditions: 1,3-butadiene, catalyst, H₂O (5 mmol), DMSO (2.0 mL), O₂.

^b Amount of 1,3-butadiene was estimated through subtraction of the bottle before and after addition.

^c Calculated on the basis of GC analysis using tridecane as an internal standard.

^d H₂O (10 mmol).

^e Reacted for 18 h.

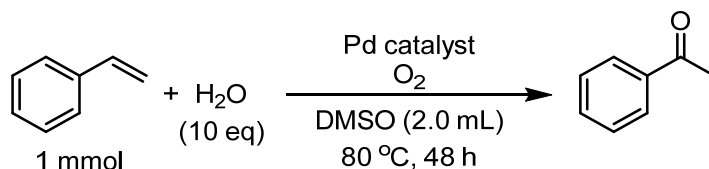
^f DMF was used as the solvent.

4.2.7 Wacker oxidation over supported Pd(OH)₂ catalysts

During optimization of reaction conditions, phenylacetone was observed as a side product, suggesting that Wacker oxidation occurred to form the ketone.²⁸ Wacker oxidation has wide applications in organic synthesis and chemical industry, such as, synthesis of acetaldehyde from ethene. However, acid, such as HCl, was required to achieve a favorable re-oxidation of Pd⁰ with co-catalyst, and to prevent aggregation of transient atomic Pd⁰ species to inactive Pd precipitates. PdCl₂, PdBr₂, and Pd(OAc)₂ are usually utilized as the catalyst for Wacker oxidations.^{28a-c} Although Kaneda and co-workers have reported a heterogeneous Pd catalyzed Wacker oxidation under acid-free conditions, CuCl₂ was still required as a co-catalyst.¹¹ In this work, CeO₂ supported Pd(OH)₂ catalyst, which is regarded as a basic component, facilitating Wacker oxidation in absence of other co-catalyst. The reaction conditions were further discussed with other substrates which are difficult to be oxidized on the allylic site, such as styrene and 1-octene, and the results are displayed in table 4.11 and 4.12, respectively. Pd(OH)₂/C was initially tested for Wacker oxidation of styrene in the presence of 10 equivalent of H₂O in DMSO, and acetophenone was obtained in 7% yield (Table 4.11, entry 1). The reaction proceeded over Pd/ZrO₂, but the product yield was low (Table 4.11, entry 2). Metal oxide supported Pd(OH)₂ catalysts markedly improved the product yield (Table 4.11, entries 3–5). After optimization of reaction conditions, 48% yield of acetophenone was obtained over Pd(OH)₂/ZrO₂

(Table 4.11, entry 5). Then, 1-octene was used as a substrate. The amount of catalyst and reaction temperature were optimized (Table 4.12, entries 1–5). However, the reactivity of 1-octene was lower than styrene.

Table 4.11 Wacker oxidation of styrene.^a



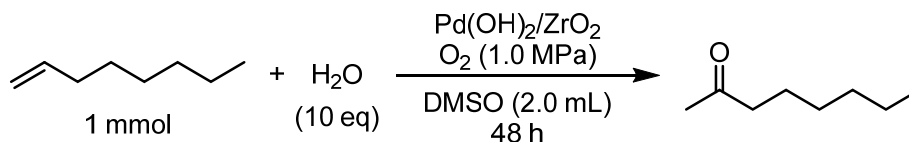
Entry	Catalyst (mol%)	O ₂ (MPa)	Conv. (%) ^b	Yield (%) ^b
1	Pd(OH) ₂ /C (1.5)	0.5	85	7
2	Pd/ZrO ₂ (1.5)	0.5	37	5
3 ^c	Pd(OH) ₂ /Al ₂ O ₃ (1.5)	1.0	91	33
4	Pd(OH) ₂ /ZrO ₂ (1.5)	1.0	66	41
5	Pd(OH) ₂ /ZrO ₂ (2.5)	2.0	75	48

^a Reaction conditions: styrene (1 mmol), H₂O (10 mmol), catalyst, H₂O (10 mmol), DMSO (2.0 mL), O₂, 80 °C, 48 h.

^b Calculated on the basis of GC analysis using tridecane as an internal standard.

^c Reacted at 24 h.

Table 4.12 Wacker oxidation of 1-octene.^a



Entry	Pd (mol%)	Temp. (°C)	Conv. (%) ^b	Yield (%) ^b
1	1.5	80	51	9
2	2.5	80	59	8
3	1.5	100	87	13
4	1.5	120	100	7
5	1.5	140	100	0

^a Reaction conditions: 1-octene (1 mmol), H₂O (10 mmol), Pd(OH)₂/ZrO₂, H₂O (10 mmol), DMSO (2.0 mL), O₂ (1.0 MPa), 80 °C, 48 h.

^b Calculated on the basis of GC analysis using tridecane as an internal standard.

4.3 Conclusion

In conclusion, allylic oxidation of allylbenzene into cinnamyl alcohol over supported Pd(OH)₂ catalysts was developed using O₂ as the sole oxidant. CeO₂ (58 m²/g) supported Pd(OH)₂ displayed the highest catalytic activity, and cinnamyl alcohol was obtained in 65%. The addition of 20 mol% of 2,5-*t*Bu₂-BQ as the oxidant improved the yield of cinnamyl alcohol to 74%. In contrast to the previous report in which stoichiometric amount of BQ was used,¹⁴ this work has superiority in terms of atom economy. Cinnamaldehyde and phenylacetone were formed as the byproducts. Cinnamaldehyde was probably formed by the over-oxidation of cinnamyl alcohol. Phenylacetone might be formed through Wacker oxidation. Moreover, styrene and 1-octene were selected as the substrates to test the catalytic activity of supported Pd(OH)₂ for Wacker oxidation. In this work, the heterogeneous catalytic system for the oxidative hydration of 1,3-butadiene to *trans*-2-butene-1,4-diol was first established. In the reaction mechanism, Pd(OH)₂ was suggested to activate the allylic C–H bond of terminal alkenes, and DMSO was coordinated with Pd to provide a stable π-allyl Pd^{II} intermediate. Oxygen worked to re-oxidize the Pd⁰ species to Pd^{II}.

4.4 Experimental section

4.4.1 Materials

Palladium chloride (PdCl₂), aqueous solution of palladium nitrate (Pd(NO₃)₂), and chloroauric acid (HAuCl₄ • 4H₂O) were purchased from Tanaka Kikinzoku Kogyo Co., Ltd.. Iridium trichloride hydrate (IrCl₃ • 3H₂O) was purchased from Wako Pure Chemical Industries, Ltd.. Ruthenium chloride trihydrate (RuCl₃ • 3H₂O) was purchased from Araya Special Metal Co., Ltd.. Palladium on carbon (5 wt% Pd/C) and palladium hydroxide on carbon (20 wt% Pd(OH)₂/C) were purchased from Sigma-Aldrich Co. LLC.. All these commercial reagents were used as received.

ZrO₂ (JRC-ZRO-4, 30 m²/g), ZrO₂ (RC-100, 91 m²/g), ZrO₂ (JRC-ZRO-3, 94 m²/g), ZrO₂ (JRC-ZRO-5, 194 m²/g), ZrO₂ (JRC-ZRO-6, 280 m²/g), CeO₂ (DKE-R9, 15 m²/g), CeO₂ (JRC-CEO-4, 65 m²/g), CeO₂ (JRC-CEO-3, 81 m²/g), CeO₂ (JRC-CEO-2, 123 m²/g), CeO₂ (JRC-CEO-1, 156 m²/g), and CeO₂ (CEO-HS, 173 m²/g) were Japan Reference Catalysts which were supplied from Catalysts Society of Japan. CeO₂ (CEO, 58 m²/g) was purchased from Kojundo Chemical Laboratory Co., Ltd.. Al₂O₃ (179 m²/g) was purchased from Mizusawa Chemicals Ltd.. TiO₂ (ST-111) was purchased from Titan Kogyo. Co., Ltd.. MgO (JRC-MGO-3, 14 m²/g) was supplied by UBE Industries,

Ltd.. CuO, NiO, La₂O₃, and ZnO were purchased from Wako Pure Chemical Industries, Ltd.. All these commercial reagents were used as received.

4.4.2 Instruments

Conversions and product yields for oxidative hydration of allylbenzene, oxidative hydration of phenylpropyne, Wacker oxidation of styrene, and Wacker oxidation of 1-octene, were analyzed by gas chromatography (GC) using Agilent GC 6850 Series II equipped with FID and a J&W HP-1 column (0.25 μm thickness, 0.25 mm I.D., 30 m) using tridecane as an internal standard. Conversions and product yields for oxidative hydration of 1,3-butadiene to *trans*-2-butene-1,4-diol were analyzed by gas chromatography (GC) using Agilent GC 6850 Series II equipped with FID and a J&W HP-INNOWAX column (0.25 μm thickness, 0.32 mm I.D., 30 m) using tridecane as an internal standard. Gas chromatography mass spectrometer (GC-MS) analysis was performed with Thermo Fisher Scientific Polaris Q equipped with a J&W HP-1 column (0.25 μm thickness, 0.25 mm I.D., 30 m). ¹H and ¹³C NMR spectra were recorded on a JEOL JNM-ECS400 spectrometer at 400 and 100 MHz, respectively. ¹H assignment abbreviations are the following; singlet (s), doublet (d), triplet (t), quintet (quin), double of doublet (dd), double of triplet (dt), multiplet (m) and broad peak (br). Analytical thin-layer chromatography (TLC) was performed with Merck, TLC silica gel 60 F₂₅₄ plates. Column chromatography was performed on silica gel (Kanto Chemicals, Silica gel 60N, spherical, neutral, particle size 40–100 μm).

Fourier transform infrared (FT-IR) spectra were obtained by JASCO FT-IR 6100 with an attenuated total reflection (ATR) accessory equipped with a single reflection ZnSe.

HAADF-STEM and XAFS measurements were performed using the same method as chapter 2.^{29,30} MP-AES tests were performed using the same method as chapter 3.

4.4.3 Preparation of catalysts

Deposition precipitation (DP) method:

Metal oxide-supported Pd(OH)₂ catalysts (Pd(OH)₂/MO_x) were prepared according to the literature with minor modifications.¹⁹ As for 5 wt% Pd(OH)₂/CeO₂, PdCl₂ (88 mg) was dissolved in an aqueous solution of conc. HCl (10 mL) and distilled water (400 mL). Alternatively, Pd(NO₃)₂ aqueous solution (Pd 5 wt%) and distilled water (400 mL) was used. The solution was warmed to 70 °C, and the pH of the solution was adjusted to 8.0 by adding 0.1 M NaOH aqueous solution. Then,

the support (1.0 g) was added to the solution, and the suspension was stirred at 70 °C for 1 h. The solid was filtered, washed with water, and then dried in air at 70 °C overnight. Pd/CeO₂ was prepared by the reduction of Pd(OH)₂/CeO₂ in a flow of pure H₂ (40 mL/min) at 200 °C for 2 h.

Al₂O₃ supported M(OH)₃ catalysts (Ir(OH)₃/Al₂O₃, Ru(OH)₃/Al₂O₃, and Au(OH)₃/Al₂O₃) were also prepared by DP method. As for 5 wt% Ir(OH)₃/Al₂O₃, IrCl₃ • 3H₂O (48 mg) was dissolved in distilled water (188 mL). The solution was warmed to 70 °C, and the pH of the solution was adjusted to 8.0 by adding 0.1 M NaOH aqueous solution. Then, Al₂O₃ (0.5 g) was added to the solution, and the suspension was stirred at 70 °C for 1 h. The solid was filtered, washed with water, and then dried in air at 70 °C overnight.

Impregnation (IMP) method:

Pd/ZrO₂ (Table 4.2, entry 4) was prepared by an impregnation method.²⁰ Pd(NO₃)₂ aqueous solution (Pd 5 wt%) was dissolved in distilled water (10 mL). To the aqueous solution was added supports (1.0 g) and the suspension was stirred at room temperature for 30 min. After impregnation, H₂O was removed by vacuum-freeze drying. The obtained catalyst was calcined at 300 °C for 4 h and treated in a flow of pure H₂ (40 mL/min) at 200 °C for 2h.

4.4.4 Catalytic reactions

A typical experiment for catalytic reactions:

To an autoclave was charged with allylbenzene (1 mmol), 5 wt% Pd catalyst (30 mg, Pd 1.5 mol%), solvent (1.5 mL), distilled water (10 mmol), and a magnetic stirring bar. The autoclave was purged and filled with O₂ until the pressure reached 0.25 MPa, and then, filled with CO₂ until the pressure reached 4.0 MPa. The reaction mixture was stirred at 80 °C for 24 h. After the reaction, the mixture was filtered, and the filtrate was analyzed by GC using tridecane as an internal standard.

A typical experiment for Scheme 4.9:

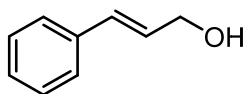
To an autoclave was charged with allylbenzene (1 mmol), 5 wt% Pd(OH)₂/CeO₂ (50 mg, Pd 2.5 mol%), DMSO (2.0 mL), distilled water (15 mmol), and a magnetic stirring bar. The autoclave was purged and filled with O₂ until the pressure reached 2.0 MPa. The reaction mixture was stirred at 80 °C

for 48 h. Then, the autoclave was cooled to room temperature and filled with pure H₂ until the pressure reached 0.5 MPa. The reaction mixture was stirred at 60 °C for 12 h. After the reaction, the mixture was filtered, and the filtrate was analyzed by GC using tridecane as an internal standard.

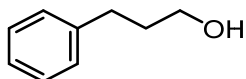
A typical experiment for Table 4.11:

To an autoclave was charged with 5 wt% Pd(OH)₂ catalyst (50 mg, Pd 2.5 mol%), DMSO (2.0 mL), distilled water (5 mmol), and a magnetic stirring bar. The autoclave was placed in liquid nitrogen bath to decrease the temperature below 0 °C, and 1,3-butadiene was introduced. Then, the autoclave was purged and filled with O₂ until the pressure reached 2.0 MPa. The reaction mixture was stirred at 55 °C for 24 h. After the reaction, the mixture was filtered, and the filtrate was analyzed by GC using tridecane as an internal standard.

4.4.5 Characterization of the isolated compounds

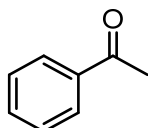


Cinnamyl alcohol: The mixture of allylbenzene (133 μL, 1.0 mmol), 5 wt% Pd(OH)₂/CeO₂ (50 mg, Pd 2.5 mol%), H₂O (270 μL, 15 mmol), in DMSO (2.0 mL) was stirred under pressurized O₂ (2.0 MPa) at 80 °C for 48 h. After the reaction, the catalyst was filtered off and the filtrate was washed by distilled H₂O. The organic layer was extracted with ethyl acetate, and then dried over Na₂SO₄. The organic solvents were removed and the crude product was purified by silica-gel column chromatography (hexane:ethyl acetate = 10:1) to give cinnamyl alcohol (67 mg, 0.50 mmol, 50%) as a white solid. (GC yield: 67%). ¹H NMR (400 MHz, CDCl₃): δ 7.38 (dd, *J* = 8.8, 7.2 Hz, 2H), 7.31 (dt, *J* = 6.8, 7.2 Hz, 2H), 7.26–7.22 (m, 1H), 6.60 (d, *J* = 15.6 Hz, 1H), 6.39–6.32 (m, 1H), 4.21 (dd, *J* = 5.2, 5.6 Hz, 2H), 1.88 (s, 1H); ¹³C NMR (100 MHz, CDCl₃): δ 136.75, 131.20, 128.71, 128.59, 127.80, 126.57, 63.79.



3-Phenylpropanol: The mixture of allylbenzene (133 μL, 1.0 mmol), 5 wt% Pd(OH)₂/CeO₂ (50 mg, Pd 2.5 mol%), H₂O (270 μL, 15 mmol), in DMSO (2.0 mL) was stirred under pressurized O₂ (2.0 MPa) at 80 °C for 48 h. Then, the mixture was stirred under pressurized H₂ (0.5 MPa) at 60 °C for 12 h. After the reaction, the catalyst was filtered off and the filtrate was washed by distilled H₂O. The

organic solvents were removed and the crude product was purified by silica-gel column chromatography (hexane:ethyl acetate = 10:1) to give 3-phenylpropanol (73 mg, 0.54 mmol, 54%) as a colorless liquid. (GC yield: 80%). ¹H NMR (400 MHz, CDCl₃): δ 7.31 (m, 2H), 7.22 (m, 3H), 3.66 (t, *J* = 6.4 Hz, 2H), 2.72 (t, *J* = 7.2 Hz, 2H), 2.23 (brs, 1H), 1.90 (quin, *J* = 8.0 Hz, 2H); ¹³C NMR (100 MHz, CDCl₃): δ 141.99, 128.57, 128.53, 125.98, 62.24, 34.33, 32.20.



Acetophenone: The mixture of styrene (115 μL, 1.0 mmol), 5 wt% Pd(OH)₂/ZrO₂ (50 mg, Pd 2.5 mol%), H₂O (180 μL, 10 mmol), in DMSO (2.0 mL) was stirred under pressurized O₂ (1.0 MPa) at 80 °C for 48 h. After the reaction, the catalyst was filtered off and the filtrate was washed by distilled H₂O. The organic layer was extracted with ethyl acetate, and then dried over Na₂SO₄. The organic solvents were removed and the crude product was purified by silica-gel column chromatography (hexane:ethyl acetate = 10:1) to give acetophenone (39 mg, 0.33 mmol, 33%) as a colorless liquid. (GC yield: 48%). ¹H NMR (400 MHz, CDCl₃): δ 7.94 (dt, *J* = 8.0, 8.4 Hz, 2H), 7.54 (t, *J* = 8.8 Hz, 1H), 7.44 (dt, *J* = 7.6 Hz, 6.0 Hz, 2H), 2.58 (s, 3H); ¹³C NMR (100 MHz, CDCl₃): δ 198.3, 137.2, 133.2, 128.7, 128.4, 26.7.

Characterization of cinnamaldehyde, *trans*-2-butene-1,4-diol, and 2-octanone were performed by GC and GC-MS by the comparison of authentic sample which was purchased from Wako Pure Chemical Industries, Ltd., Sigma-Aldrich Co. LLC., Kanto Chemical Industry Co., Inc., respectively.

4.5 References

- [1] H. A. Wittcoff, B. G. Reuben, J. S. Plotkin, *Industrial Organic Chemistry, –2nd Ed.*, John Wiley & Sons: New Jersey, **2004**.
- [2] (a) M. B. Smith, J. March, *March's advanced organic chemistry*, John Wiley & Sons: New Jersey, 2001. (b) M. Beller, J. Seayad, A. Tillack, H. Jiao, *Angew. Chem. Int. Ed.*, **2004**, 43, 3368–3398. (c) R. I. McDonald, G. Liu, S. S. Stahl. *Chem. Rev.*, **2011**, 111, 2981–3019. (d) J. J. Dong, W. R. Browne, B. L. Feringa, *Angew. Chem. Int. Ed.*, **2014**, 52, 2–13. (e) L. Zhang, Z. Zuo, X. Leng, Z. Huang, *Angew. Chem. Int. Ed.*, **2014**, 53, 2696–2700. (f) J. Guo, P. Teo, *Dalton Trans.*, **2014**, 43, 6952–6964.

- [3] Haggin J., *Chem. Eng. News*, **1993**, 71, 23–27.
- [4] K. Takahashi, M. Yamashita, T. Ichihara, K. Nakano, K. Nozaki, *Angew. Chem. Int. Ed.*, **2010**, 49, 4488–4490.
- [5] G. Dong, P. Teo, Z. K. Wickens, R. H. Grubbs, *Science*, **2011**, 16, 1609–1612.
- [6] (a) T. T. Wenzel, *J. Chem. Soc. Chem. Commun.*, **1993**, 862–864. (b) B. L. Feringa, *J. Chem. Soc. Chem. Commun.*, **1986**, 909–910. (c) T. Ogura, R. Kamikawa, A. Shiga, T. Hosokawa, *Bull. Chem. Soc. Jpn.*, **2005**, 78, 1555–1557. (d) P. Teo, Z. K. Wickens, G. Dong, R. H. Grubbs, *Org. Lett.*, **2012**, 14, 3237–3239.
- [7] (a) M. S. Chen, M. C. White, *J. Am. Chem. Soc.*, **2004**, 126, 1346–1347. (b) W. H. Henderson, C. T. Check, N. Proust, J. P. Stambuli, *Org. Lett.*, **2010**, 12, 824–827.
- [8] (a) K. J. Fraunhofer, M. C. White, *J. Am. Chem. Soc.*, **2007**, 129, 7274–7276. (b) S. A. Reed, M. C. White, *J. Am. Chem. Soc.*, **2008**, 130, 3316–3318.
- [9] (a) M. S. Chen, N. Prabakaran, N. A. Labenz, M. C. White, *J. Am. Chem. Soc.*, **2007**, 127, 6970–6971. (b) A. J. Young, M. C. White, *J. Am. Chem. Soc.*, **2008**, 130, 14090–14091.
- [10] A. N. Campbell, P. B. White, L. A. Guzei, S. S. Stahl, *J. Am. Chem. Soc.*, **2010**, 132, 15116–15119.
- [11] T. Mitsudome, T. Umetani, N. Nosaka, K. Mori, T. Mizugaki, K. Ebitani, K. Kaneda, *Angew. Chem. Int. Ed.*, **2006**, 45, 481–485.
- [12] J. Tsuji, *Synthesis*, **1990**, 739–749.
- [13] K. E. Atkins, W. E. Walker, R. M. Manyik, *J. Chem. Soc. D.*, **1971**, 330–330.
- [14] R. Tomita, K. Mantani, A. Hamasaki, T. Ishida, M. Tokunaga, *Chem. Eur. J.*, **2014**, 20, 9914–9917.
- [15] I. Schnapperelle, W. Hummel, H. Gröger, *Chem. Eur. J.*, **2012**, 18, 1073–1076.
- [16] J. R. Zbieg, E. Yamaguchi, E. L. McInturff, M. J. Krische, *Science*, **2012**, 336, 324–327.
- [17] T. Ishida, R. Tsunoda, Z. Zhang, A. Hamasaki, T. Honma, H. Ohashi, T. Yokoyama, M. Tokunaga, *Appl. Catal. B: Environ.*, **2014**, 150–151, 523–531.
- [18] Z. Zhang, T. Hashiguchi, T. Ishida, A. Hamasaki, T. Honma, H. Ohashi, T. Yokoyama, M. Tokunaga, *Org. Chem. Front.*, **2015**, in press.
- [19] S. S. Soomro, F. L. Ansari, K. Chatziapostolou, K. Köhler, *J. Catal.*, **2010**, 273, 138–146.
- [20] N. Iwasa, T. Mayanagi, W. Nomura, M. Arai, N. Takezawa, *Appl. Catal. A: General.*, **2003**, 248, 153–160.

- [21] J. Piera, J. E. Bäckvall, *Angew. Chem. Int. Ed.*, **2008**, 47, 3506–3523.
- [22] G. Busca, *Phys. Chem. Chem. Phys.*, **1999**, 1, 723–736.
- [23] (a) J. E. Bäckvall, A. Gogoll, *Tetrahedron Lett.*, **1998**, 29, 2243–2246. (b) K. J. Sazbó, *Organometallics*, **1998**, 17, 1677–1686. (c) B. L. Lin, J. A. Labinger, J. E. Bercaw, *Can. J. Chem.*, **2009**, 87, 264–271. (d) H. Grennberg, A. Gogoll, J. E. Bäckvall, *Organometallics*, **1993**, 12, 1790–1793.
- [24] (a) B. A. Steinhoff, S. R. Fix, S. S. Stahl, *J. Am. Chem. Soc.*, **2002**, 124, 766–767. (b) W. Zierkiewicz, T. Privalov, *Organometallics*, **2005**, 24, 6019–6028. (c) T. Diao, S. S. Stahl, *J. Am. Chem. Soc.*, **2011**, 133, 14566–14596. (d) Z. Lu, S. S. Stahl, *Org. Lett.*, **2012**, 14, 1234–1237.
- [25] G. Socrates, *Infrared and Raman characteristic group frequencies, –3rd Ed.*, John Wiley & Sons: England, **2001**.
- [26] “Commercial-scale production of bio-based BDO announced”, *Chemical Engineering*, 2013-2-21.
- [27] (a) R. D. Ashford, *Ashford’s dictionary of industrial chemicals, –3rd Ed.*, Wavelength: London, **2011**. (b) Mitsubishi Kasei Corporation, *CHEMTECH*, **1988**, 759.
- [28] (a) W. Ren, Y. Xia, S. J. Ji, Y. Zhang, X. Wan, J. Zhao, *Org. Lett.*, **2009**, 11, 1841–1844. (b) Z. Zhang, J. Tang, Z. Wang, *Org. Lett.*, **2008**, 10, 173–175. (c) P. Teo, Z. K. Wickens, G. Dong, R. H. Grubbs, *Org. Lett.*, **2012**, 14, 3237–3239. (d) T. Mitsudome, T. Umetani, K. Mori, T. Mizugaki, K. Ebitani, K. Kaneda, *Tetrahedron Lett.*, **2006**, 47, 1425–1428. (e) X. Wang, N. S. Venkataramanan, H. Kawanami, Y. Ikushima, *Green. Chem.*, **2007**, 9, 1352–1355.
- [29] (a) T. Honma, H. Oji, S. Hirayama, Y. Taniguchi, H. Ofuchi, M. Takagaki, *AIP Conf. Proc.*, **2010**, 1234, 13–16; (b) H. Oji, Y. Taniguchi, S. Hirayama, H. Ofuchi, M. Takagaki, T. Honma, *J. Synchrotron Rad.*, **2012**, 19, 54–59.
- [30] B. Ravel, M. Newville, *J. Synchrotron Rad.*, **2005**, 12, 537–541.

Chapter 5. Conclusion

In this thesis, several oxidative reactions were developed over supported Pd catalysts in the presence of molecular oxygen as the sole oxidant.

The intramolecular oxidative coupling reaction was performed using diphenyl ether as the substrate. After optimization of reaction conditions, ZrO₂ supported Pd(OH)₂ was selected as a suitable catalyst to promote the reaction in good yield with a broad substrate scope. The chemical state of Pd in the Pd(OH)₂/ZrO₂ was confirmed as Pd^{II} by XANES spectra. In contrast with standard samples of Pd(OH)₂ and PdO, Pd(OH)₂ might exist as one of the components in catalysts, although the formation of Pd(OH)₂ cannot be fully asserted by XAFS.

Then, an aerobic oxidation process of cyclohexanone was developed using Pd(OH)₂/ZrO₂ and Pd/ZrO₂ as catalysts. Cyclic enone and phenol were formed as products. However, the selectivity to cyclic enones was difficult to control, because further oxidation of cyclohexanone to phenol could not be avoided. Phenol was obtained in excellent yields over Pd/ZrO₂ catalyst, and this catalyst was characterized by XAFS, XRD, and HAADF-STEM. The results suggested that Pd particles might be dissolved into the solution from ZrO₂ support, and promote the reaction via quasi-homogeneous catalysis. However, MP-AES test for the used catalyst demonstrated that most of Pd could be recovered after the reaction as supported catalysts. Additionally, Pd/ZrO₂ showed good recyclability for synthesis of phenol.

Aryl ethers were also synthesized from cyclohexanone in the presence of orthoesters such as TMOF, TEOF, and TIPOF. The reaction of cyclohexanones and alcohols was performed using TIPOF as a dehydrating reagent to synthesize the corresponding aryl ethers. The substrate scope, recyclability of catalyst, and reaction pathway were also studied.

In the third section, I focused on the transformation of terminal alkenes to primary allylic alcohols over supported Pd catalysts. Synthesis of cinnamyl alcohol from allylbenzene was selected as a model reaction. After optimization of reaction conditions, cinnamyl alcohol could be obtained in 65% yield in the presence of O₂ over Pd(OH)₂/CeO₂. Cinnamaldehyde and phenyl acetone were formed as by-products. In addition, styrene and 1-octene were tested to discuss the conversion of terminal alkenes to ketones via Wacker oxidation process. Finally, the synthesis of 2-butene-1,4-diol from 1,3-butadiene was explored. 2-Butene-1,4-diol is an intermediate for the synthesis of 1,4-butanediol which is an important material for chemical industry. In this work, Pd(OH)₂/CeO₂ catalyzed oxidative hydration of 1,3-butadiene gave 2-buten-1,4-diol in 31% yield (calculated based on H₂O). Although

the yield was still low, this work opens a new environmentally friendly method for the production of 1,4-butanediol from 1,3-butadiene.

As described above, supported Pd catalysts displayed good catalytic activity for several oxidative reactions. The reactivity and product selectivity were affected by a number of factors, such as preparation method, metal particle size, and different properties of support. The demonstrated supported Pd catalytic systems prevail in existing homogeneous systems with a number of advantages. This work is expected to be a good initiation to enlarge the applications of supported transition metal catalysts in aerobic oxidation reactions and further applications in industrial process.

Acknowledgement

I would like to express my deepest appreciation to all those who helped me to complete this thesis. A special gratitude I give to my supervisors, Prof. Makoto Tokunaga and Project Prof. Tamao Ishida, who provided me the chance to study in Kyushu University and supported me for living in Japan. Particularly, I appreciate that they taught me the professional knowledge and gave me much valuable suggestions on my research work. I would like to acknowledge Assistant Prof. Akiyuki Hamasaki for the advices he have given to me during this three years. My thanks and appreciations also go to every member and graduated students in Tokunaga group. Especially, I would like to thank my team members, Mr. Ryosuke Tsunoda, Mr. Qixun Wu, Mr. Kohei Mantani, and Mr. Taishin Hashiguchi. It was a great pleasure to work together with them.

I would like to thank Dr. Tetsuo Honma, Assistant Prof. Hironori Ohashi, and Prof. Takushi Yokoyama for their guidance about XAFS measurements and result analysis. I would like to thank Ultramicroscopy Research Center at Kyushu University for HAADF-STEM observations.

Finally, I would like to express my gratitude towards my family members and my friends for their kind encouragement and support.

List of publications

Research papers:

1. Supported palladium hydroxide-catalyzed intramolecular double C–H bond functionalization for synthesis of carbazoles and dibenzofurans

Tamao Ishida, Ryosuke Tsunoda, Zhenzhong Zhang, Akiyuki Hamasaki, Tetsuo Honma, Hironori Ohashi, Takushi Yokoyama, Makoto Tokunaga

Appl. Catal. B: Environ., **2014**, 150–151, 523–531.

2. Aerobic oxidation of cyclohexanones to phenols and aryl ethers over supported palladium catalysts
Zhenzhong Zhang, Taishin Hashiguchi, Tamao Ishida, Akiyuki Hamasaki, Tetsuo Honma, Hironori Ohashi, Takushi Yokoyama, Makoto Tokunaga

Org. Chem. Front., **2015**, *Accepted*. (Invited research article for celebrating the 80th birthday of professor Ei-ichi Negishi)

3. Supported palladium catalyzed allylic C–H acetoxylation for synthesis of allyl acetates from terminal alkenes

Zhenzhong Zhang, Qixun Wu, Taishin Hashiguchi, Tamao Ishida, Akiyuki Hamasaki, Tetsuo Honma, Hironori Ohashi, Takushi Yokoyama, Makoto Tokunaga

In preparation.

4. Transformation of terminal alkenes to primary allylic alcohols over supported palladium hydroxide catalysts

Zhenzhong Zhang, Tamao Ishida, Akiyuki Hamasaki, Tetsuo Honma, Hironori Ohashi, Takushi Yokoyama, Makoto Tokunaga

In preparation.

Patents:

1. パラジウム水酸化物担持固体触媒及びその製造方法、並びに縮合環化合物の製造方法
(石田玉青、角田亮介、張振中、濱崎昭行、徳永信共著)

特開 2013-212499、平成 25 年 10 月 17 日公開。

2. アリルアルコール類の製造方法

(徳永信、石田玉青、張振中、井澤雄輔共著)

出願番号 2015-025722、平成 27 年 2 月 12 日出願。